

# Stabilizing the Splits through Minimax Decision Trees

Zhenyuan Zhang\*      Hengrui Luo†

## Abstract

By revisiting the end-cut preference (ECP) phenomenon associated with a single CART (Breiman et al. (1984)), we introduce MinimaxSplit decision trees, a robust alternative to CART that selects splits by minimizing the worst-case child risk rather than the average risk. For regression, we minimize the maximum within-child squared error; for classification, we minimize the maximum child entropy, yielding a C4.5-compatible criterion. We also study a cyclic variant that deterministically cycles coordinates, leading to our main method of cyclic MinimaxSplit decision trees.

We prove oracle inequalities that cover both regression and classification, under mild marginal non-atomicity conditions. The bounds control the tree's global excess risk by local worst-case impurities and yield fast convergence rates compared to CART. We extend the analysis to ensembles that subsample coordinates per node.

Empirically, (cyclic) MinimaxSplit trees and their forests improve on structured heterogeneity data such as EEG amplitude regression over fixed time horizons, seasonal air quality forecasting, and image denoising framed as non-parametric regression on spatial coordinates.

*Keywords:* CART; convergence rates; decision tree models; non-parametric regression

## Contents

<b>1</b>	<b>Introduction</b>	<b>2</b>
<b>2</b>	<b>Minimax decision trees for regression</b>	<b>3</b>
2.1	Algorithm formulation	3
2.2	Risk bound	7
2.3	Empirical risk bound for cyclic MinimaxSplit	13
2.4	Why cyclic MinimaxSplit outperforms MinimaxSplit	14
<b>3</b>	<b>Ensemble models</b>	<b>15</b>
3.1	MinimaxSplit random forests	15
3.2	Empirical risk bound for MinimaxSplit random-dimension random forests	16
<b>4</b>	<b>Minimax decision trees for classification</b>	<b>16</b>

\*Department of Mathematics, Stanford University. Email: zzy@stanford.edu

†Corresponding Author. Department of Statistics, Rice University; Computational Research Division, Lawrence Berkeley National Laboratory. Email: hrluo@rice.edu

<b>5 Numerical experiments and applications</b>	<b>18</b>
5.1 Avoiding end-cut preference for stable cuts	18
5.2 Fixed-horizon EEG amplitude regression	20
5.3 Image denoising with ensembles	22
<b>6 Conclusion</b>	<b>23</b>
<b>A On partition-based martingale approximations</b>	<b>27</b>
A.1 Basic concepts	27
A.2 Uniform convergence rates	29
A.3 Non-uniform convergence rates	31
A.4 Proof of Theorem 16	33
<b>B Proofs of main results</b>	<b>39</b>
B.1 Proofs of results in Section 2	39
B.2 Proofs of results in Section 3	44
B.3 Proofs of results in Section 4	48
<b>C Additional example for anti-symmetry-breaking preference</b>	<b>51</b>
<b>D Further numerics</b>	<b>53</b>
D.1 Performance metrics	53
D.2 Higher-dimensional input domain	54
<b>E Pseudocode for algorithms</b>	<b>56</b>

## 1 Introduction

Tree-based predictors are classical non-parametric learners, from early systems such as THAID to the CART formalization (Morgan and Messenger, 1973; Breiman et al., 1984), with surveys charting both breadth and limitations (Gordon and Olshen, 1984; Loh, 2014) and recent work revisiting large-scale aspects (Klusowski and Tian, 2024). A persistent and practically important pathology of single-tree greedy splitting is the *end-cut preference* (ECP): standard impurity/variance criteria favor splits near node boundaries, especially under weak or no signal. ECP has long been observed empirically (Morgan and Messenger, 1973; Torgo, 2001; Su et al., 2024; Wang, 2025) and is now rigorously characterized in simple settings, where noisy directions drive splits toward extremes (Breiman et al., 1984; Cattaneo et al., 2022).

For a *single* deep tree, ECP can be harmful: aggressive boundary splits create highly unbalanced children, amplify estimation noise, and can stall meaningful refinement along informative coordinates. However, Ishwaran (2015) argues that the same tendency can be *beneficial* in *deep random forests*: when a candidate split falls on a noise variable, an end-cut keeps one child large, preserving downstream sample size so later splits (possibly on strong variables) can recover the signal; even along strong variables, ECP-like behavior can be adaptive in regions with little local signal. Thus, while ECP degrades a single tree’s stability, it may aid an ensemble by lowering tree correlation and enabling recovery via aggregation. At the same time, the forest setting introduces its own costs: ECP interacts with candidate-set multiplicity and variable-usage bias, skewing split frequencies and importance metrics, and further reducing model interpretability. Existing

methods to mitigate ECP include the delta splitting rule (Morgan and Messenger, 1973), regularization of node size (Torgo, 2001), and the Smooth Sigmoid Surrogate (Su et al., 2024). We refer to Wang (2025) for a more comprehensive review of the ECP.

As illustrated in Figure 1, ECP arises from the greedy split search itself. At each node, the algorithm scans many thresholds and chooses the one with the largest impurity decay. Thresholds near the boundary isolate very few points; the sample mean of such a tiny child has a high variance, so even pure noise can create a large difference between child means and an inflated impurity reduction. Taking the maximum over many candidate cut-off points amplifies this selection bias—extremal thresholds are disproportionately likely to ‘win’.

Our focus is on *explicitly mitigating ECP at the algorithmic level* for trees, while retaining the transparency that makes single decision trees interpretable. Beyond prediction, this design goal is interpretability: balanced, nondegenerate splits yield partitions whose geometry is easier to understand and communicate than the heterogeneous, boundary-driven partitions that arise under ECP in deep trees and ensembles.

In this paper, we revisit ECP empirically and theoretically, clarifying the cases in which standard CART-style criteria drift toward extreme cut-off points and how this differs between single trees and forests (Breiman et al., 1984; Morgan and Messenger, 1973; Torgo, 2001; Su et al., 2024; Ishwaran, 2015; Wang, 2025; Cattaneo et al., 2022). Then, we introduce a Minimax splitting rule with a cyclic coordinate schedule that systematically discourages degenerate child nodes, thereby mitigating ECP while preserving interpretability. As a consequence, our splitting rule admits a faster convergence guarantee compared to standard CART—we establish exponential error decay under mild conditions and relate our guarantees to existing theory (Chi et al., 2022; Syrgkanis and Zampetakis, 2020; Mazumder and Wang, 2024; Cattaneo et al., 2024). Conceptually, the analysis connects to partition-based martingale approximations (Simons, 1970; Zhang et al., 2024) and complements asymptotic and inferential developments for trees/forests (Klusowski and Tian, 2024; Chi et al., 2022; Syrgkanis and Zampetakis, 2020; Mazumder and Wang, 2024; Cattaneo et al., 2024), as well as recent scalable partitioning frameworks (Liu et al., 2023; Luo and Pratola, 2023; Luo et al., 2024) and complexity-theoretic perspectives on hierarchical splits (Blanc et al., 2020; O’Donnell et al., 2005).

## 2 Minimax decision trees for regression

The goal of this section is to construct MinimaxSplit decision tree algorithms that avoid ECP and attain exponential convergence. We first focus on the regression setting and we discuss the classification setting in Section 4. In CART-style regression, a decision tree greedily splits in order to minimize the *sum* of variances over the responses of the child nodes (Liu et al., 2023; Breiman et al., 1984); instead, we propose to greedily minimize the *maximum* variance among the child nodes. In Section 2.1, we rigorously introduce the algorithms (summarized in Figure 2). We study exponential rates for marginally atomless joint distributions (that may not arise from empirical measures  $\mathbb{P}_N$ ) in Section 2.2. Section 2.3 builds upon this case, covering more generally the non-marginally atomless setting and, in particular, the empirical risk bounds. All proofs can be found in Appendix B.1. Throughout, we use the notation  $[d] = \{1, 2, \dots, d\}$  for  $d \in \mathbb{N}$ . All splits we consider in this paper will be binary.

### 2.1 Algorithm formulation

We begin by recapping the greedy splitting regime in the VarianceSplit algorithm to construct an efficient decision tree. We need the following notion of a splittable set. A similar notion is also introduced by Definition

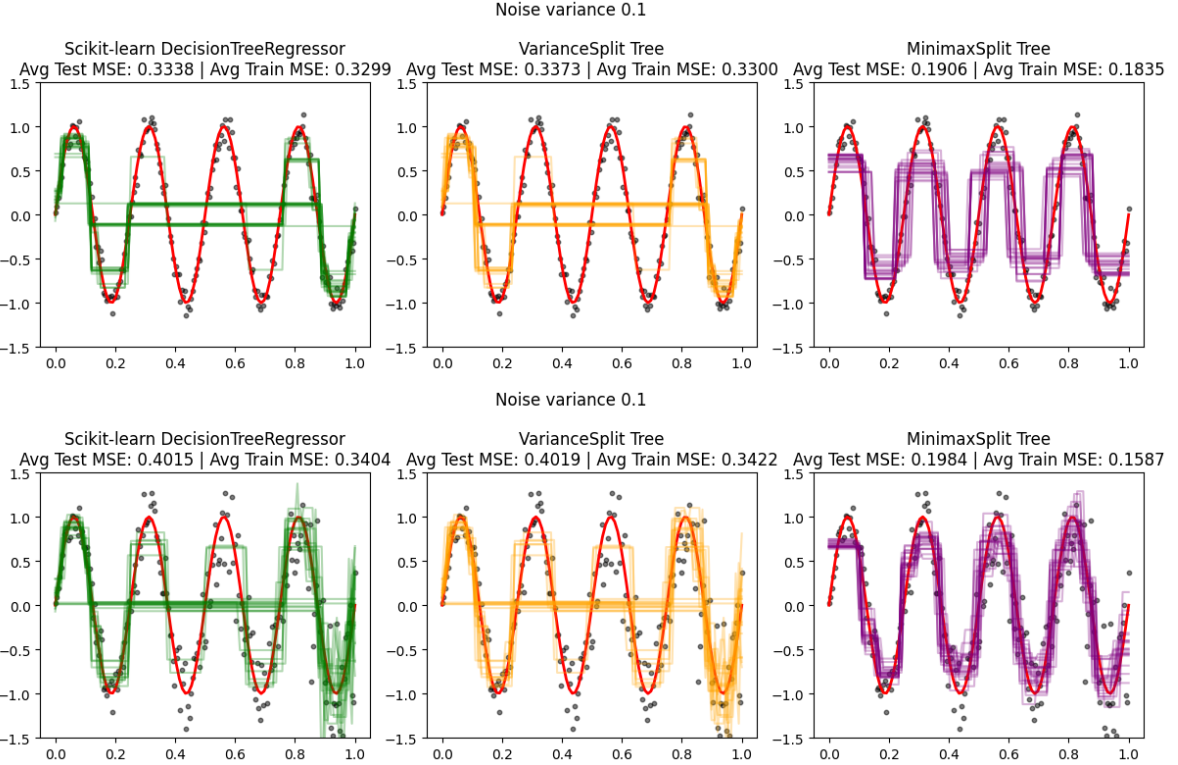


Figure 1: The comparison of the scikit-learn DecisionTreeRegressor, our MinimaxSplit tree, and VarianceSplit tree on a sinusoidal target function (in red)  $Y = f(X) + \varepsilon = \sin(4\pi X) + \varepsilon$ ,  $X \stackrel{\text{law}}{\sim} \text{Unif}(0,1)$ , and  $\varepsilon \stackrel{\text{law}}{\sim} \mathcal{N}(0,0.1)$ , with maximum depth 4 (top row) and 5 (bottom row). We display 10 different model fits based on 10 different batches of training sets of size 100, and the average mean squared error (MSE) evaluated on a different training set across 10 batches.

3.1 of [Klusowski and Tian \(2024\)](#).

**Definition 2.1.** Consider a joint distribution  $(\mathbf{X}, Y)$  on  $\mathbb{R}^{d+1}$ . We say a set  $A \subseteq \mathbb{R}^d$  is  $(\mathbf{X}, Y)$ -unsplittable, or unsplittable, if any of the following occurs:

- $\mathbb{P}(\mathbf{X} \in A) = 0$ ;
- $\mathbb{P}(\mathbf{X} \in A) > 0$  and  $Y \mid \mathbf{X} \in A$  is a constant;
- $\mathbb{P}(\mathbf{X} \in A) > 0$  and  $\mathbf{X} \mid \mathbf{X} \in A$  is a constant.

Otherwise, we say that  $A$  is  $(\mathbf{X}, Y)$ -splittable, or splittable.

The greedy VarianceSplit construction (Section 8.4 of [Breiman et al. \(1984\)](#)) proceeds by introducing nested partitions  $\{\pi_k\}_{k \geq 0}$  of  $\mathbb{R}^d$  with axis-aligned borders, in a way that sequentially and greedily minimizes the total risk  $\mathbb{E}[(Y - M_k)^2]$  at each step  $k$  (or depth  $k$ , while splitting from the fixed partition  $\pi_{k-1}$ ), where  $M_k$  is taken as the conditional mean of  $Y$  given the  $\sigma$ -algebra generated by the collection  $\mathbb{1}_{\{\mathbf{X} \in A\}}$ ,  $A \in \pi_k$ . So, the partitions  $\{\pi_k\}_{k \geq 0}$  of the input space  $\mathbb{R}^d$  are nested and we require that each  $\pi_k$  consists of sets that split each splittable element  $A \in \pi_{k-1}$  into two hyper-rectangles with axis-aligned borders.

Formally, suppose that a hyper-rectangle  $A = [a_1, b_1] \times \dots \times [a_d, b_d]$  belongs to the partition  $\pi_{k-1}$  and is splittable (if  $A$  is unsplittable, we do not split  $A$  and  $A \in \pi_\ell$  for every  $\ell \geq k$ ). In particular,

$M_{k-1}(\omega) = \mathbb{E}[Y \mid \mathbf{X} \in A]$  if  $\mathbf{X}(\omega) \in A$ . To find a split of  $A$  at depth  $k$ , the VarianceSplit algorithm looks for a dimension  $j \in [d]$  and covariate  $x_j \in [a_j, b_j]$  such that the remaining risk is the smallest after splitting  $A$  at  $x_j$  in covariate  $j$ . In other words, one seeks for

$$\begin{aligned}
(j, \hat{x}_j) &= \arg \min_{\substack{j \in [d] \\ x_j \in [a_j, b_j]}} \left( \mathbb{P}(\mathbf{X} \in A, X_j < x_j) \text{Var}(Y \mid \mathbf{X} \in A, X_j < x_j) \right. \\
&\quad \left. + \mathbb{P}(\mathbf{X} \in A, X_j \geq x_j) \text{Var}(Y \mid \mathbf{X} \in A, X_j \geq x_j) \right) \\
&= \arg \min_{\substack{j \in [d] \\ x_j \in [a_j, b_j]}} \left( \mathbb{E}[(Y - \mathbb{E}[Y \mid \mathbf{X} \in A, X_j < x_j])^2 \mathbb{1}_{\{\mathbf{X} \in A, X_j < x_j\}}] \right. \\
&\quad \left. + \mathbb{E}[(Y - \mathbb{E}[Y \mid \mathbf{X} \in A, X_j \geq x_j])^2 \mathbb{1}_{\{\mathbf{X} \in A, X_j \geq x_j\}}] \right) \\
&=: \arg \min_{\substack{j \in [d] \\ x_j \in [a_j, b_j]}} (V_{\text{left}}(j) + V_{\text{right}}(j)),
\end{aligned} \tag{1}$$

where we break ties arbitrarily.<sup>1</sup> Consequently, the splittable set  $A$  splits into the sets  $A_L := [a_1, b_1] \times \cdots \times [a_j, \hat{x}_j] \times \cdots \times [a_d, b_d]$  and  $A_R := [a_1, b_1] \times \cdots \times [\hat{x}_j, b_j] \times \cdots \times [a_d, b_d]$  to form its two descendants in the set  $\pi_k$ , and define

$$M_k(\omega) = \begin{cases} \mathbb{E}[Y \mid \mathbf{X} \in A, X_j < x_j] & \text{if } \mathbf{X}(\omega) \in A_L; \\ \mathbb{E}[Y \mid \mathbf{X} \in A, X_j \geq x_j] & \text{if } \mathbf{X}(\omega) \in A_R. \end{cases} \tag{2}$$

In other words, at depth  $k \geq 0$  and after constructing the partition  $\pi_k$ , define  $M_k$  by

$$M_k(\omega) = \mathbb{E}[Y \mid \mathbf{X} \in A], \quad \text{if } \mathbf{X}(\omega) \in A, \quad \text{for } A \in \pi_k. \tag{3}$$

This leads to an associated process  $\{M_k\}_{k \geq 0}$  to the joint distribution  $(\mathbf{X}, Y)$ .<sup>2</sup> To connect  $M_k$  with the estimator  $\hat{m}_k$  of the regression function at step  $k$ , we note that for any  $\mathbf{x} \in \mathbb{R}^d$ , there exists a unique  $A_{\mathbf{x}} \in \pi_k$  containing  $\mathbf{x}$ , then  $\hat{m}_k(\mathbf{x}) = \mathbb{E}[Y \mid \mathbf{X} \in A_{\mathbf{x}}]$ .

**The MinimaxSplit algorithm.** We now introduce the MinimaxSplit algorithm. A common feature of the MinimaxSplit and VarianceSplit algorithms is that they both start from a nested sequence of partitions  $\{\pi_k\}_{k \geq 0}$  of  $\mathbb{R}^d$  consisting of (at-most) binary splits into hyper-rectangles with axis-aligned borders. The two algorithms differ in the way the partition is constructed: in the MinimaxSplit setting, the split is chosen to minimize the maximum variance among the two descendants. Formally, for a splittable set  $A =$

<sup>1</sup>Strictly speaking, the  $\arg \min$  in (1) may not always be attained for general joint distributions  $(\mathbf{X}, Y)$ , unless we assume that  $\mathbf{X}$  is marginally either atomless or has a finite support, which will always be the case in our analysis (such as the atomicity condition in Theorem 6 below). However, in the general setting, if we allow splits in which atoms can be duplicated and assigned to both nodes (instead of only on the right node as in (1)),  $\arg \min$  can be attained. In this paper, we will implicitly assume that  $\arg \min$  is always attained unless otherwise stated.

<sup>2</sup>The process  $\{M_k\}_{k \geq 0}$  is a martingale, but we will not use this fact in the rest of the main text.

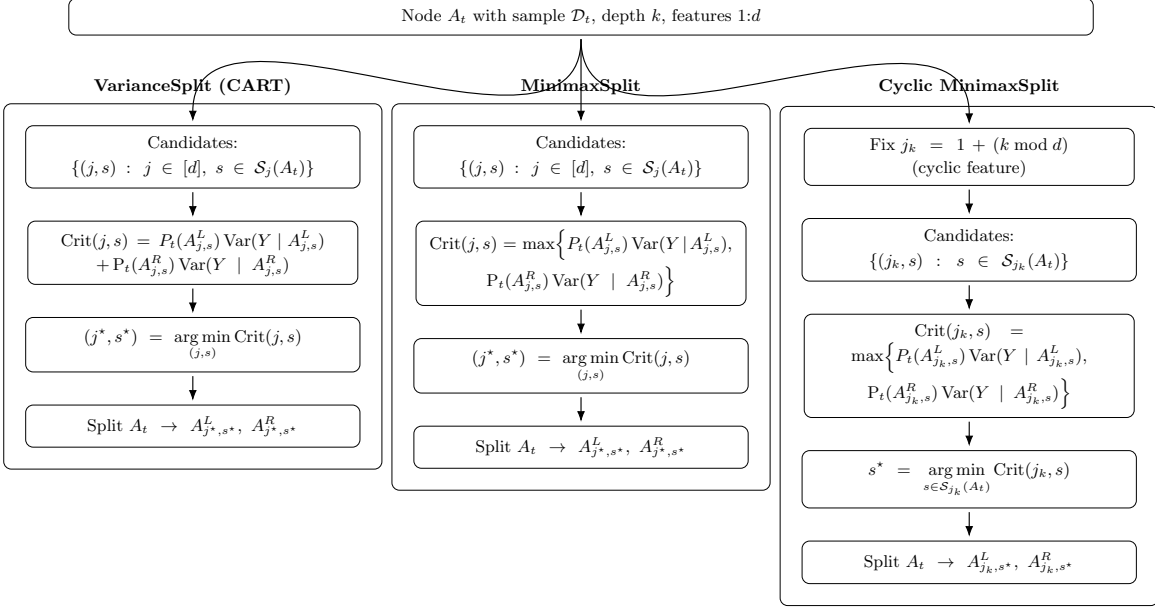


Figure 2: The comparison of the VarianceSplit, MinimaxSplit and cyclic MinimaxSplit trees. Here we use the notation:  $A_{j,s}^L = A_t \cap \{x_j < s\}$ ,  $A_{j,s}^R = A_t \cap \{x_j \geq s\}$ ;  $S_j(A_t)$  are candidate thresholds (e.g., midpoints of sorted  $x_j$  in  $A_t$ );  $P_t(B) = \mathbb{P}(\mathbf{X} \in B \mid \mathbf{X} \in A_t)$ .

$[a_1, b_1) \times \dots \times [a_d, b_d) \in \pi_{k-1}$ , define the split location as

$$\begin{aligned}
(j, \hat{x}_j) &= \arg \min_{\substack{j \in [d] \\ x_j \in [a_j, b_j]}} \max \left\{ \mathbb{E}[(Y - \mathbb{E}[Y \mid \mathbf{X} \in A, X_j < x_j])^2 \mathbb{1}_{\{\mathbf{X} \in A, X_j < x_j\}}], \right. \\
&\quad \left. \mathbb{E}[(Y - \mathbb{E}[Y \mid \mathbf{X} \in A, X_j \geq x_j])^2 \mathbb{1}_{\{\mathbf{X} \in A, X_j \geq x_j\}}] \right\} \\
&= \arg \min_{\substack{j \in [d] \\ x_j \in [a_j, b_j]}} \max \left\{ \mathbb{P}(\mathbf{X} \in A, X_j < x_j) \text{Var}(Y \mid \mathbf{X} \in A, X_j < x_j), \right. \\
&\quad \left. \mathbb{P}(\mathbf{X} \in A, X_j \geq x_j) \text{Var}(Y \mid \mathbf{X} \in A, X_j \geq x_j) \right\}, \tag{4} \\
&= \arg \min_{\substack{j \in [d] \\ x_j \in [a_j, b_j]}} \max \left\{ V_{\text{left}}(j), V_{\text{right}}(j) \right\},
\end{aligned}$$

where we break ties arbitrarily. We call this the *MinimaxSplit rule*. After obtaining the partition  $\pi_k$ , define  $M_k$  through (3).

**The cyclic MinimaxSplit algorithm.** The cyclic MinimaxSplit algorithm is a variation of the MinimaxSplit algorithm. Instead of optimizing over all covariates  $j \in [d]$  in (4), we cycle through the  $d$  covariates as the tree grows. That is, for  $k \geq 0$ , let  $j = j_k = 1 + (k \text{ mod } d)$ . For all splittable sets  $A \in \pi_k$ , we split  $A$

in the  $j$ -th coordinate to form its two descendants at depth  $k + 1$ . The split location is then defined as

$$\begin{aligned}
\hat{x}_j &= \arg \min_{x_j \in [a_j, b_j]} \max \left\{ \mathbb{E}[(Y - \mathbb{E}[Y \mid \mathbf{X} \in A, X_j < x_j])^2 \mathbb{1}_{\{\mathbf{X} \in A, X_j < x_j\}}], \right. \\
&\quad \left. \mathbb{E}[(Y - \mathbb{E}[Y \mid \mathbf{X} \in A, X_j \geq x_j])^2 \mathbb{1}_{\{\mathbf{X} \in A, X_j \geq x_j\}}] \right\} \\
&= \arg \min_{x_j \in [a_j, b_j]} \max \left\{ \mathbb{P}(\mathbf{X} \in A, X_j < x_j) \text{Var}(Y \mid \mathbf{X} \in A, X_j < x_j), \right. \\
&\quad \left. \mathbb{P}(\mathbf{X} \in A, X_j \geq x_j) \text{Var}(Y \mid \mathbf{X} \in A, X_j \geq x_j) \right\},
\end{aligned} \tag{5}$$

where we break ties arbitrarily. Define  $M_k$  by (3).

If  $d = 1$ , the cyclic MinimaxSplit algorithm coincides with the MinimaxSplit algorithm. If  $d > 1$ , compared to the MinimaxSplit algorithm, the cyclic MinimaxSplit algorithm is technically more tractable. Moreover, since all features are considered equally, the cyclic MinimaxSplit algorithm appears more robust in recovering the underlying geometry of the regression function, which we illustrate numerically in Section 5. On the other hand, the cyclic MinimaxSplit algorithm may be less effective in higher dimensions because the relevant dimensions may not be easily identified or reached in the first few splits, yet it avoids a pathological example in Section 2.4.

## 2.2 Risk bound

The goal of this section is to justify the exponential convergence under the cyclic MinimaxSplit rule. Assuming marginal non-atomicity, we show that up to universal constants and model mis-specification, the approximation error decays exponentially with rate  $r^k$  for some explicit  $r \in (0, 1)$  that depends only on dimension  $d$ .

We note here a crucial difference from the statistics literature that our analysis of the MinimaxSplit rule first focuses on *general joint distributions*  $(\mathbf{X}, Y)$  on  $\mathbb{R}^{d+1}$ , where  $\mathbf{X} \in \mathbb{R}^d$  and  $Y \in \mathbb{R}$ .<sup>3</sup> Empirical measures are a special case. The class of joint distributions we consider will satisfy the following marginally atomless property.

**Definition 2.2.** Let  $d \geq 1$  and  $\mathbf{X} = (X_1, \dots, X_d)$  be an  $\mathbb{R}^d$ -valued random vector. We say that  $\mathbf{X}$  (or its law) is marginally atomless if for any  $j \in [d]$  and  $x \in \mathbb{R}$ ,  $\mathbb{P}(X_j = x) = 0$ .

The reason for considering general joint distributions is twofold. First, we provide more general probabilistic results that may be of interest in other settings. Second, in our derivation of the empirical risk bounds, it would be more natural and technically convenient to first study the marginally atomless setting. Although the empirical measure is not marginally atomless, only minor changes will be required to take care of the atomic case (to be discussed in Section 2.3 below).

Let us start with some simple observations on the MinimaxSplit rule. The following lemma is a simple consequence of the total variance formula and will be proved in Appendix B.1.

**Lemma 2.1.** Suppose that  $\mathbf{X}$  is marginally atomless and  $j \in [d]$ . Then the function

$$\varphi_L : x_j \mapsto \mathbb{P}(\mathbf{X} \in A, X_j < x_j) \text{Var}(Y \mid \mathbf{X} \in A, X_j < x_j) \tag{6}$$

---

<sup>3</sup>This can be intuitively regarded as empirical measures with infinitely many samples.

is non-decreasing and continuous. Similarly,

$$\varphi_R : x_j \mapsto \mathbb{P}(\mathbf{X} \in A, X_j \geq x_j) \text{Var}(Y \mid \mathbf{X} \in A, X_j \geq x_j)$$

is non-increasing and continuous.

Choose an arbitrary element  $\hat{x}_j \in \arg \min_{x_j} \max\{\varphi_L(x_j), \varphi_R(x_j)\}$ . Let us first assume that  $\varphi_L(\hat{x}_j) \leq \varphi_R(\hat{x}_j)$ . Define  $x_j^* := \min\{x_j : \varphi_L(x_j) = \varphi_R(x_j)\}$ . By the monotonicity of  $\varphi_L$  and  $\varphi_R$ , we have  $\hat{x}_j \leq x_j^*$ , and thus

$$\varphi_L(\hat{x}_j) \leq \varphi_L(x_j^*) = \varphi_R(x_j^*) \leq \varphi_R(\hat{x}_j). \quad (7)$$

Using (7) and the fact that  $\hat{x}_j \in \arg \min_{x_j} \max\{\varphi_L(x_j), \varphi_R(x_j)\}$ , we have

$$\varphi_L(x_j^*) = \varphi_R(x_j^*) = \varphi_R(\hat{x}_j). \quad (8)$$

Since the events  $A_L = \{\mathbf{X} \in A, X_j < x_j^*\}$  and  $A_R = \{\mathbf{X} \in A, X_j \geq x_j^*\}$  form a partition of  $\{\mathbf{X} \in A\}$ , we have by the total variance formula,

$$\varphi_L(\hat{x}_j) + \varphi_R(\hat{x}_j) \leq \varphi_L(x_j^*) + \varphi_R(x_j^*) \leq \mathbb{E}[(Y - \mathbb{E}[Y \mid \mathbf{X} \in A])^2 \mathbb{1}_{\{\mathbf{X} \in A\}}]. \quad (9)$$

Combining (8) and (9), we have

$$\max \left\{ \varphi_L(\hat{x}_j), \varphi_R(\hat{x}_j) \right\} = \varphi_R(\hat{x}_j) \leq \frac{1}{2} \mathbb{E}[(Y - \mathbb{E}[Y \mid \mathbf{X} \in A])^2 \mathbb{1}_{\{\mathbf{X} \in A\}}]. \quad (10)$$

The other case  $\varphi_L(\hat{x}_j) \geq \varphi_R(\hat{x}_j)$  is similar. In other words, the remaining risk on each descendant is at most half the risk on the parent node. Inductively, we gain a *uniform* exponential decay of the maximum risk among the nodes at depth  $k$ :

$$\max_{A \in \pi_k} \mathbb{P}(\mathbf{X} \in A) \text{Var}(Y \mid \mathbf{X} \in A) = \max_{A \in \pi_k} \mathbb{E}[(Y - \mathbb{E}[Y \mid \mathbf{X} \in A])^2 \mathbb{1}_{\{\mathbf{X} \in A\}}] \leq 2^{-k} \text{Var}(Y). \quad (11)$$

This is the key to controlling the ‘‘sizes of the nodes’’. In the case of the VarianceSplit construction, such uniform control is not possible—counterexamples exist due to ECP, which we explain in the next example.

**Example 1.** We revisit (a special case of) the location regression model analyzed in [Cattaneo et al. \(2022\)](#). Let  $(X, Y)$  be an empirical measure of  $\text{Unif}(0, 1) \times \mathcal{N}(0, 1)$  on  $[0, 1] \times \mathbb{R}$  with  $n$  samples.<sup>4</sup> Suppose that we perform VarianceSplit for one step. Theorem 4.1 of [Cattaneo et al. \(2022\)](#) implies that, for  $n$  large enough, the split lies between the first and  $\sqrt{n}$ -th order statistics with probability exceeding  $1/6$ . With high probability (meaning  $1 - o(1)$  as  $n \rightarrow \infty$ ), the right node has remaining risk at least  $(1 - o(1))n$  while the total risk at the parent node is at most  $(1 + o(1))n$ . By a union bound, we see that with an arbitrary  $\varepsilon > 0$ , for sufficiently large  $n$ ,

$$\mathbb{P} \left( \max_{A \in \pi_1} \mathbb{P}(X \in A) \text{Var}(Y \mid X \in A) \geq (1 - \varepsilon) \text{Var}(Y) \right) > \frac{1}{7}.$$

This example also explains why assumptions such as the sufficient impurity decay (SID) condition are

---

<sup>4</sup>  $X$  is not marginally atomless, but the example can always be modified by smoothing the data without affecting its validity.

favorable to ensure risk decay when using the splitting criterion (1) (Chi et al., 2022; Mazumder and Wang, 2024).

To see further intuition of ECP, we consider the event  $\{\mathbf{X} \in A\}$  and sub-events  $A_L = \{\mathbf{X} \in A, X_j < \hat{x}_j\}$  and  $A_R = \{\mathbf{X} \in A, X_j \geq \hat{x}_j\}$ . Without loss of generality, we may assume  $\mathbb{P}(\mathbf{X} \in A) = 1$  and apply the total variance formula to this partition, yielding

$$\begin{aligned}\mathbb{P}(\mathbf{X} \in A)\text{Var}(Y) &= \text{Var}(Y) = \mathbb{E}[\text{Var}(Y \mid \sigma(A_L))] + \text{Var}(\mathbb{E}[Y \mid \sigma(A_L)]) \\ &= \text{Var}(Y \mid A_L)\mathbb{P}(A_L) + \text{Var}(Y \mid A_R)\mathbb{P}(A_R) \\ &\quad + (\mathbb{E}[Y \mid A_L] - \mathbb{E}[Y \mid A_R])^2(1 - \mathbb{P}(A_L))\mathbb{P}(A_L).\end{aligned}\tag{12}$$

From this, we see that when ECP occurs,  $\mathbb{P}(A_L) \approx 1$  or 0, the improvement is dominated by the first two terms of (12):  $\text{Var}(Y \mid A_L)\mathbb{P}(A_L) + \text{Var}(Y \mid A_R)\mathbb{P}(A_R) = V_{\text{left}}(j) + V_{\text{right}}(j)$ . Therefore, when ECP occurs, the sum of variances does not necessarily decay fast enough for the VarianceSplit.

However, for (cyclic) MinimaxSplit,  $\max\{V_{\text{left}}(j), V_{\text{right}}(j)\}$  always displays exponential decay (11), hence “avoiding” the ECP phenomenon. In other words, the fast decay of the sum of variances is not easily guaranteed from the VarianceSplit construction due to ECP; but the exponential decay of the maximum variance can be assured by the MinimaxSplit construction, as we show in Theorem 2.

We consider the additive function class

$$\mathcal{G} := \{g(\mathbf{x}) := g_1(x_1) + \cdots + g_d(x_d)\},$$

where  $\mathbf{x} = (x_1, \dots, x_d)$ . For  $g \in \mathcal{G}$ , define  $\|g\|_{\text{TV}}$  as the infimum of  $\sum_{i=1}^d \|g_i\|_{\text{TV}}$  over all such additive representations of  $g$ , where  $\|\cdot\|_{\text{TV}}$  denotes the total variation of a univariate function of bounded variation.

**Theorem 2.** *Suppose that  $\mathbf{X}$  is marginally atomless. Let the associated  $\{M_k\}_{k \geq 0}$  be constructed from the cyclic MinimaxSplit algorithm. Then uniformly for any  $\delta > 0$  and  $k \geq 0$ ,*

$$\begin{aligned}\mathbb{E}[(Y - M_k)^2] &\leq \inf_{g \in \mathcal{G}} \left( \left( (1 + \delta) + \frac{2(1 + \delta)(1 + \delta^{-1})}{3 \cdot 2^{2\lfloor k/d \rfloor / 3}} \right) \mathbb{E}[(Y - g(\mathbf{X}))^2] \right. \\ &\quad \left. + (1 + \delta^{-1}) \left( \frac{1}{3} + \left( \frac{1 + \delta^{-1}}{4} \right)^{2/3} \right) 2^{-2\lfloor k/d \rfloor / 3} \|g\|_{\text{TV}}^2 \right).\end{aligned}\tag{13}$$

*Remark 3* (The MinimaxSplit analogue). Theorem 2 does not hold in general for  $d \geq 2$  if we replace the cyclic MinimaxSplit algorithm by the MinimaxSplit algorithm, a phenomenon we illustrate in Section 2.4 below. Nevertheless, the MinimaxSplit algorithm often achieves desirable risk decay in high-dimensional settings in which cyclic MinimaxSplit is inefficient; see Appendix D.2.

The first general result for the convergence rate of the VarianceSplit algorithm without the variance decay assumption was obtained by Klusowski and Tian (2024). In a similar vein, Cattaneo et al. (2024) studied the convergence rates of the *oblique* CART and obtained a  $1/k$  upper bound for MSE in the general setting (Theorem 1 therein) as well as an  $r^k$  upper bound under further assumptions such as node sizes (Theorem 4 therein). The unconditional rate guarantee of  $1/k$  appears significantly slower than the exponential decay rates under variance decay assumptions. (A continuous version of) Theorem 4.2 of Klusowski and Tian (2024) states that if the associated  $\{M_k\}_{k \geq 0}$  is constructed from the VarianceSplit algorithm, then for each

$k \geq 1$ ,

$$\mathbb{E}[(Y - M_k)^2] \leq \inf_{g \in \mathcal{G}} \left( \mathbb{E}[(Y - g(\mathbf{X}))^2] + \frac{\|g\|_{\text{TV}}^2}{k+3} \right). \quad (14)$$

Let us compare the rates between (14) and (13). Consider  $Y = g(\mathbf{X})$  with  $g \in \mathcal{G}$  and  $\varepsilon > 0$ . The following table summarizes the convergence rates of the VarianceSplit and MinimaxSplit algorithms. Note that Theorem 2 exhibits the curse of dimensionality, which cannot be circumvented in the current setting to the best of our knowledge (Cattaneo et al., 2022; Tan et al., 2022).

Splitting rule	Risk decay guarantee	Max level required to guarantee $\text{MSE} \leq \varepsilon$
VarianceSplit (1)	(14)	$O(1/\varepsilon)$
MinimaxSplit (4)	N/A	does not exist in general for $d \geq 2$
Cyclic MinimaxSplit (5)	Theorem 2	$O(d \log(1/\varepsilon))$

Since the bound (13) is uniform over  $\delta, k, d$ , one can further optimize over  $\delta$  for fixed  $k, d$ . For example, taking  $\delta = 2^{-\lfloor k/d \rfloor / 10}$ , the right-hand side of (13) then has the more explicit (but cruder) upper bound

$$\inf_{g \in \mathcal{G}} \left( 5\mathbb{E}[(Y - g(\mathbf{X}))^2] + 2^{1-\lfloor k/d \rfloor / 2} \|g\|_{\text{TV}}^2 \right).$$

*Remark 4.* In the case where  $\|g\|_{\text{TV}}$  is much larger than the range  $\Delta g := \sup g - \inf g$ , (13) can be further improved to

$$\begin{aligned} \mathbb{E}[(Y - M_k)^2] &\leq \inf_{g \in \mathcal{G}} \left( (1 + \delta) \mathbb{E}[(Y - g(\mathbf{X}))^2] + 2^{1/3} (1 + \delta^{-1}) 2^{-2\lfloor k/d \rfloor / 3} \|g\|_{\text{TV}}^{2/3} \mathbb{E}[(Y - g(\mathbf{X}))^2]^{2/3} \right. \\ &\quad \left. + 2^{-2/3} (1 + \delta^{-1}) 2^{-2\lfloor k/d \rfloor / 3} \|g\|_{\text{TV}}^{2/3} (\Delta g)^{4/3} \right). \end{aligned} \quad (15)$$

Theorems 6 and 7 below enjoy the same specialized bounds.

In the remainder of this section, we explain the ideas underlying the proof of Theorem 2, in the special case where  $d = 1$  and  $Y = g(\mathbf{X})$  for some  $g \in \mathcal{G}$ . In this case, (13) reduces to

$$\mathbb{E}[(Y - M_k)^2] \leq L 2^{-2k/3} \|g\|_{\text{TV}}^2 \quad (16)$$

for some  $L > 0$ , which we verify next.

We employ the following *binary subtree representation* to control  $\mathbb{E}[(M_k - M_{k+1})^2]$ . Let  $(\tilde{V}, \tilde{E})$  be a binary tree with root  $\emptyset$ . We call a subtree of a binary tree a *binary subtree*. Then, given an at-most-binary sequence of nested partitions  $\{\pi_k\}_{k \geq 0}$ , there exists a subtree  $(V, E)$  of  $(\tilde{V}, \tilde{E})$  such that each vertex  $v \in V_k$  can be identified as a set  $A \in \pi_k$ , where  $V_k$  is the set of all vertices in  $V$  with the graph distance from the root equal to  $k$ .<sup>5</sup> With each edge  $e = (A_k, A_{k+1}) \in E$  where  $A_k \in \pi_k$  and  $A_{k+1} \in \pi_{k+1}$ , we may associate a coefficient  $p_e := \mathbb{P}(\mathbf{X} \in A_{k+1}) \in [0, 1]$ . With each vertex  $v = A_k$ , we may associate a location  $\ell_v := \mathbb{E}[Y \mid \mathbf{X} \in A_k]$ . See Figure 3 for an illustration. It follows that  $M_k$  is supported on the discrete points

<sup>5</sup>The tree may not be a binary tree due to possible unsplittable sets.

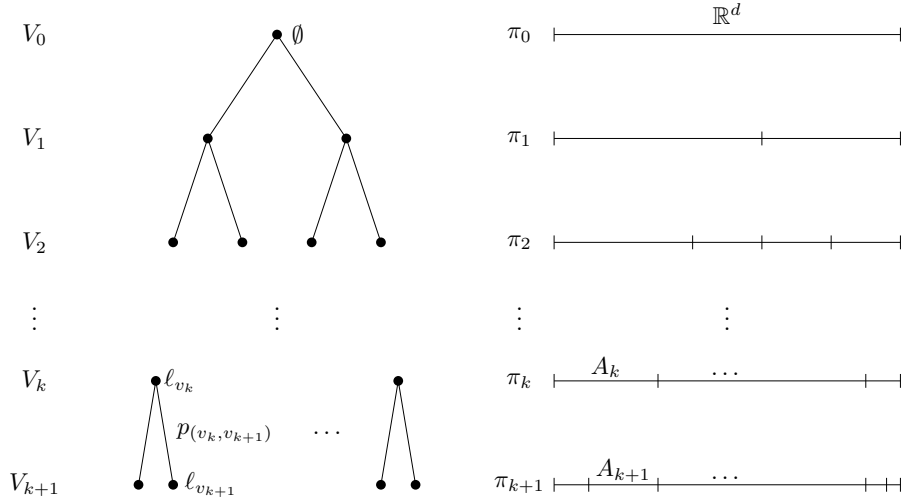


Figure 3: Visualizing the nested sequence of partitions  $\{\pi_k\}_{k \geq 0}$  and its associated binary subtree representation.

$\{\ell_v\}_{v \in V_k}$  and furthermore,

$$\mathbb{E}[(M_k - M_{k+1})^2] = \sum_{\substack{v_k \in V_k, v_{k+1} \in V_{k+1} \\ v_k \sim v_{k+1}}} p_{(v_k, v_{k+1})} (\ell_{v_k} - \ell_{v_{k+1}})^2, \quad (17)$$

where for two vertices  $v, w$ , we write  $v \sim w$  if they are connected. Let  $\mathcal{F}_k$  denote the  $\sigma$ -algebra generated by the collection  $\mathbb{1}_{\{\mathbf{X} \in A\}}$ ,  $A \in \pi_k$ . The nodewise predictor  $M_k = \mathbb{E}[Y | \mathcal{F}_k]$  is a Doob martingale in  $L^2$ , and its risk satisfies

$$\mathbb{E}[(Y - M_k)^2] = \sum_{i=k}^{\infty} \mathbb{E}[(M_{i+1} - M_i)^2] \quad \text{and} \quad \mathbb{E}[(M_k - M_{k+1})^2] = \sum_{A \in \pi_k} \sum_{\substack{A' \in \pi_{k+1} \\ A' \subset A}} \mathbb{P}(A') (\mu_{A'} - \mu_A)^2. \quad (18)$$

In other words, convergence rates reduce to controlling the one-step increments created by each split. The VarianceSplit rule provides no uniform control: under ECP, a child can have arbitrarily small mass, so large within-node fluctuations can be confined to microscopic slivers, and the increment need not contract at a fixed rate. Our MinimaxSplit instead minimizes  $\max\{\mathbb{P}(A_L)\text{Var}(Y | A_L), \mathbb{P}(A_R)\text{Var}(Y | A_R)\}$ , ensuring that at every refinement the worst child risk decreases by a constant factor. Summed along the tree, this yields an exponential contraction of  $\mathbb{E}[(M_{k+1} - M_k)^2]$  and hence of  $\mathbb{E}[(Y - M_k)^2]$ . The *cyclic* schedule strengthens this guarantee by forcing each coordinate to be refined regularly, preventing all contraction from being spent on a single axis and avoiding symmetry-breaking failures; see Section 2.4.

To put the above intuition into play, we apply Hölder's inequality and (11) to obtain

$$\begin{aligned}
\mathbb{E}[(M_k - M_{k+1})^2] &= \sum_{\substack{v_k \in V_k, v_{k+1} \in V_{k+1} \\ v_k \sim v_{k+1}}} p_{(v_k, v_{k+1})} (\ell_{v_k} - \ell_{v_{k+1}})^2 \\
&\leq \left( \sum_{\substack{v_k \in V_k, v_{k+1} \in V_{k+1} \\ v_k \sim v_{k+1}}} p_{(v_k, v_{k+1})} \right)^{1/3} \\
&\quad \times \left( \max_{\substack{v_k \in V_k, v_{k+1} \in V_{k+1} \\ v_k \sim v_{k+1}}} p_{(v_k, v_{k+1})} (\ell_{v_k} - \ell_{v_{k+1}})^2 \sum_{\substack{v_k \in V_k, v_{k+1} \in V_{k+1} \\ v_k \sim v_{k+1}}} |\ell_{v_k} - \ell_{v_{k+1}}| \right)^{2/3} \quad (19) \\
&\leq \text{Var}(Y)^{2/3} 2^{-2k/3} \left( \sum_{\substack{v_k \in V_k, v_{k+1} \in V_{k+1} \\ v_k \sim v_{k+1}}} |\ell_{v_k} - \ell_{v_{k+1}}| \right)^{2/3}.
\end{aligned}$$

Since each split introduces a difference term  $|\ell_{v_k} - \ell_{v_{k+1}}|$ , which is bounded by the values of  $Y$  conditioned on a partition in the covariate space, we have

$$\sum_{\substack{v_k \in V_k, v_{k+1} \in V_{k+1} \\ v_k \sim v_{k+1}}} |\ell_{v_k} - \ell_{v_{k+1}}| \leq \sum_{A \in \pi_{k+1}} \left( \sup_A g - \inf_A g \right) \leq \|g\|_{\text{TV}}. \quad (20)$$

On the other hand,  $\text{Var}(Y) = \text{Var}(g(X)) \leq \|g\|_{\text{TV}}^2$ . Inserting (20) into (19) and using (18), we obtain  $\mathbb{E}[(Y - M_k)^2] \leq L 2^{-2k/3} \|g\|_{\text{TV}}^2$  for some  $L > 0$ .

Our approach is fundamentally different from [Klusowski and Tian \(2024\)](#) in the following sense. On the one hand, the approach of [Klusowski and Tian \(2024\)](#) relies on aggregating one-step lower bounds on the impurity gain (or the decay of the risk). On the other hand, recall from (12) that the total risk decreases by the amount

$$(\mathbb{E}[Y | A_L] - \mathbb{E}[Y | A_R])^2 (1 - \mathbb{P}(A_L)) \mathbb{P}(A_L) \quad (21)$$

after  $A$  splits into  $A_L \cup A_R$ . The intuition is that although the gain (21) can be small at a certain step, it reveals information on the underlying joint distribution that guarantees that either it has already gone through significant risk decay in previous steps, or it is soon happening, or the total variation  $\|g\|_{\text{TV}}$  must be large. Let us illustrate the above intuition by a quick example.

**Example 5.** Consider the case where  $d = 1$ ,  $X \stackrel{\text{law}}{\sim} \text{Unif}(0, 1)$ , and  $Y = \sin(2\pi 2^p X)$ . Figure 4 below plots the remaining risk  $\mathbb{E}[(Y - M_k)^2]$ ,  $1 \leq k \leq K$  with power parameters  $p = 1, 2, 3, 4$  and maximum tree depth  $K = 12$ . Due to the symmetry of the sine function, the first few splits of the MinimaxSplit do not reduce the remaining risk, since the splitting points are points of symmetry. However, as soon as the splitting breaks through the symmetries, the remaining risk decays exponentially to zero. The VarianceSplit algorithm makes mild progress at every step, but is quickly surpassed by MinimaxSplit once the latter breaks through the symmetries. The reason is that due to ECP, the splitting points are near the boundary of the nodes, leading to unbalanced nodes. In other words, while the MinimaxSplit algorithm may not reduce the risk as steadily as VarianceSplit, the steps with little risk reduction often implicitly overcome certain hard constraints inherent to the regression problem (such as the symmetries of the sine function), paving the way for a much faster risk decay in later stages. Note that the occurrence of minimal risk deduction from the first few steps of MinimaxSplit does not contradict the risk bound from Theorem 2, because the upper bound

already incorporates the total variation of the signal function.

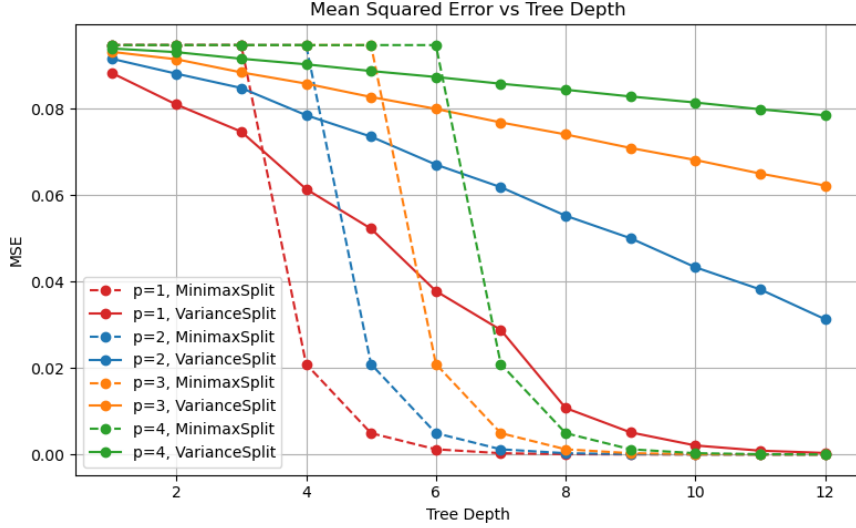


Figure 4: Comparison of the mean squared errors for the MinimaxSplit and VarianceSplit regimes, in the setting where  $X \stackrel{\text{law}}{\sim} \text{Unif}(0, 1)$  and  $Y = \sin(2\pi 2^p X)$  with  $p = 1, 2, 3, 4$  and maximum tree depth 12.

### 2.3 Empirical risk bound for cyclic MinimaxSplit

So far, we have discussed the cases where the joint distribution  $(\mathbf{X}, Y)$  is marginally atomless, which does not include the class of empirical measures. We now focus on the regression setting and derive finite-sample performance guarantees. Suppose that under the original law  $\mathbb{P}_*$ ,  $\mathbf{X}_*$  is marginally atomless and  $Y_* \mid \mathbf{X}_* = g_*(\mathbf{X}_*) + \varepsilon := \mathbb{E}[Y_* \mid \mathbf{X}_*] + \varepsilon$ , where the error  $\varepsilon = Y_* - g_*(\mathbf{X}_*)$  is sub-Gaussian, i.e., for some  $\sigma > 0$ ,  $\mathbb{P}_*(|\varepsilon| \geq u) \leq 2 \exp(-u^2/(2\sigma^2))$ ,  $u \geq 0$ . Also, we consider the empirical law of  $(\mathbf{X}, Y)$  of  $N$  samples from  $\mathbb{P}_*$ .

A limitation of Theorem 2 is that it applies only if the covariate  $\mathbf{X}$  is marginally atomless (for (10) to hold). Therefore, we need the following result that deals with measures whose marginals may contain atoms. For a random variable  $Y$ , denote by  $\text{supp } Y$  the support of  $Y$ .

**Theorem 6.** *Suppose that  $\mathbf{X}$  is purely atomic and for some  $N > 0$ ,*

$$\max_{j \in [d]} \max_{u \in \mathbb{R}} \mathbb{P}(X_j = u) \leq \frac{1}{N}. \quad (22)$$

Let  $\Delta Y := \sup \text{supp } Y - \inf \text{supp } Y$ , and let the associated  $\{M_k\}_{k \geq 0}$  be constructed from the cyclic MinimaxSplit algorithm. Then uniformly for any  $\delta > 0$  and  $k \geq 0$ ,

$$\begin{aligned} \mathbb{E}[(Y - M_k)^2] &\leq (1 + \delta^{-1}) 2^{-2\lfloor k/d \rfloor / 3} \frac{2^{k+2}(\Delta Y)^2}{3N} + \inf_{g \in \mathcal{G}} \left( \left( (1 + \delta) + \frac{2(1 + \delta)(1 + \delta^{-1})}{3 \cdot 2^{2\lfloor k/d \rfloor / 3}} \right) \mathbb{E}[(Y - g(\mathbf{X}))^2] \right. \\ &\quad \left. + (1 + \delta^{-1}) \left( \frac{2}{3} + \left( \frac{1 + \delta^{-1}}{4} \right)^{2/3} \right) 2^{-2\lfloor k/d \rfloor / 3} \|g\|_{\text{TV}}^2 \right). \end{aligned} \quad (23)$$

Our next key result is the following oracle inequality for decision trees under model mis-specification

(i.e., when  $g_*$  does not belong to  $\mathcal{G}$ ). Let  $g_k$  be the output of the cyclic MinimaxSplit construction (that is,  $M_k = g_k(\mathbf{X})$ ). Note that  $g_k$  is random under the law  $\mathbb{P}_*$ . We use  $\|\cdot\|$  to denote the  $L^2$  norm in  $\mathbb{P}_*$ , e.g.  $\|g_k - g_*\|^2 = \mathbb{E}[(g_k(\mathbf{X}_*) - g_*(\mathbf{X}_*))^2]$ , where the expectation is taken in  $\mathbb{P}_*$ .

**Theorem 7.** *Assume that  $\mathbf{X}_*$  is marginally atomless. We have for  $\delta \geq 2^{-2\lfloor k/d \rfloor/3}$ ,*

$$\begin{aligned} \mathbb{E}[\|g_k - g_*\|^2] &\leq \frac{C2^k(\log N)^2 \log(Nd)}{N} + 2 \inf_{g \in \mathcal{G}} \left( \left( (1 + \delta) + \frac{2(1 + \delta)(1 + \delta^{-1})}{3 \cdot 2^{2\lfloor k/d \rfloor/3}} \right) \|g - g_*\|^2 \right. \\ &\quad \left. + (1 + \delta^{-1}) \left( \frac{2}{3} + \left( \frac{1 + \delta^{-1}}{4} \right)^{2/3} \right) 2^{-2\lfloor k/d \rfloor/3} \|g\|_{\text{TV}}^2 \right), \end{aligned}$$

where  $C > 0$  is a constant depending only on  $\|g_*\|_\infty$  and  $\sigma^2$ .

For a fixed sample size  $N$ , if we assume that  $g_* \in \mathcal{G}$  and  $k = 3d \log_2 N / (3d+2)$  is a multiple of  $d$ , Theorem 7 has the further consequence that (under the same assumptions)

$$\mathbb{E}[\|g_k - g_*\|^2] \leq CN^{-\frac{2}{3d+2}} (\|g_*\|_{\text{TV}} + (\log N)^2 \log(Nd)). \quad (24)$$

The proof of Theorem 7 follows essentially the same path as Theorem 4.3 for CART of [Klusowski and Tian \(2024\)](#) while replacing Theorem 4.2 therein by our Theorem 6.

In addition to the performance and convergence rate guarantees, we briefly comment on the computational efficiency of MinimaxSplit compared to VarianceSplit. Typically, the time complexity consists of sorting and identifying the split dimension and location ([Louppe, 2014](#), Section 5). The time complexity for sorting does not depend on the splitting criteria. In terms of solving for the split dimension and location, our MinimaxSplit algorithm (4) (or its cyclic variant (5)) is advantageous over VarianceSplit (1), because of the monotonicity of the risk as a function of the split location, thus reducing the time complexity from linear in the node size to logarithmic in the node size.

## 2.4 Why cyclic MinimaxSplit outperforms MinimaxSplit

The key reason why the above risk bounds and the oracle inequality are only derived for the *cyclic* MinimaxSplit algorithm is that there is an *anti-symmetry-breaking preference* (ASBP) for MinimaxSplit, which we briefly explain in this section. The gist is that if the underlying model possesses different symmetry conditions across different dimensions, the MinimaxSplit algorithm is likely to always split over the asymmetric dimensions, thus leaving the symmetric dimensions untouched. This leads to an undesirable convergence rate, or even inconsistency in the large-sample regime. We start with a simple example in the marginally atomless case.

**Example 8.** Consider  $\mathbf{X} = (X_1, X_2)$  uniformly distributed on  $[-1, 1]^2$  and  $Y = X_1 + |X_2|$ . Clearly,  $Y = f(\mathbf{X})$  for some  $f \in \mathcal{G}$  with  $\|f\|_{\text{TV}} = 4$ . Recall (4) and consider a MinimaxSplit step applied to a splittable set  $A = [\alpha, \beta] \times [-1, 1]$  where  $-1 \leq \alpha < \beta \leq 1$ . Along the second dimension  $x_2$ , the split location of MinimaxSplit in (4) is always given by  $x_2 = 0$ , due to the symmetry of the law of  $(\mathbf{X}, Y)$  along  $x_2 = 0$  on the set  $A$ . However, there is no risk decay given by this split, again due to the above symmetry. On the other hand, along the first dimension  $x_1$ , the split location of MinimaxSplit in (4) is given by  $x_1 = (\alpha + \beta)/2$  and the risk decay is strictly positive. It follows that the arg min in (4) always satisfies  $j = 1$ . By induction, if we apply the MinimaxSplit algorithm to the joint distribution  $(\mathbf{X}, Y)$ , the split will always be along the first dimension  $x_1$ .

Therefore, if the associated  $\{M_k\}_{k \geq 0}$  is constructed from the MinimaxSplit algorithm, each  $M_k$  can be written as a function of  $X_1$  only, say  $M_k = h_k(X_1)$ . But then by the independence of  $X_1$  and  $X_2$ , for any  $k$ ,

$$\begin{aligned}
\mathbb{E}[(Y - M_k)^2] &= \mathbb{E}[(X_1 - h_k(X_1) + |X_2|)^2] \\
&= \mathbb{E}[(X_1 - h_k(X_1))^2] + \mathbb{E}[|X_2|^2] + 2\mathbb{E}[(X_1 - h_k(X_1))]\mathbb{E}[|X_2|] \\
&\geq \text{Var}(X_1 - h_k(X_1)) + \text{Var}(|X_2|) + (\mathbb{E}[X_1 - h_k(X_1)] + \mathbb{E}[|X_2|])^2 \\
&\geq \text{Var}(|X_2|) = \frac{1}{12},
\end{aligned} \tag{25}$$

and thus the MSE does not even decay to zero, meaning that the counterpart of (13) cannot hold.

Example 8 does not involve samples, but it is intuitively true that ASBP should still hold if one considers empirical measures of  $(\mathbf{X}, Y)$  with the goal of estimating  $f$ . This can be made rigorous using a Donsker class argument, which we discuss in Appendix C. Example 8 also generalizes to higher dimensions, such as using the function  $Y = f(\mathbf{X})$  where  $f(x_1, \dots, x_d) = x_1 + \dots + x_{d-1} + |x_d|$ .

This ASBP phenomenon has an important consequence of the inadmissibility of classic random forests in the context of MinimaxSplit. We follow the setting of Section 7 of [Klusowski and Tian \(2024\)](#), which is a slight adaptation of the Breiman's classic random forest ([Breiman, 2001](#)). A random forest consists of a collection of independent subsampled trees, where at each node, the split dimensions are optimized among a random pre-selected set  $\mathcal{S} \subseteq [d]$ . The set  $\mathcal{S}$  is independently randomly generated with a fixed size  $m_{\text{try}} \in [d]$  for each node. The notation  $m_{\text{try}}$  will be kept throughout this paper. Consider a random forest under the MinimaxSplit regime, with  $m_{\text{try}} \geq 2$  and  $g(\mathbf{x}) = x_1 + \dots + x_{d-1} + |x_d|$  on  $[-1, 1]^d$ . Then each  $\mathcal{S}$  must include a dimension in  $[d-1]$ , along which the split always reduces more risk than the  $d$ -th dimension. This implies that the  $d$ -th dimension is never reached and the risk is strictly bounded away from zero for any  $k$ , using an argument similar to (25). Therefore, the consistency of the random forest under the MinimaxSplit regime is not always guaranteed in the large-sample regime (even if the signal is noiseless), unless we pick  $m_{\text{try}} = 1$ . In the next section, we analyze the case  $m_{\text{try}} = 1$ , which we call a *random-dimension random forest*, and establish the corresponding consistency for the MinimaxSplit random forest. The empirical performance will be presented in Section 5.3.

### 3 Ensemble models

#### 3.1 MinimaxSplit random forests

Although a single decision tree can capture patterns in data through hierarchical partitioning, it often suffers from high variance in predictions, which makes it sensitive to small changes in the training dataset. To address these limitations, an ensemble approach can be utilized to combine multiple decision trees, leading to improved stability and predictive accuracy. In this section, we extend the MinimaxSplit and cyclic MinimaxSplit methods to an ensemble context.

The ensemble method we consider here is the original Breiman's random forest ([Breiman et al., 1984](#)), which aggregates multiple decision trees to improve the precision and robustness of the prediction. Each tree is grown to a fixed depth  $k$  according to some splitting rule, and the split dimension of each node is optimized among independent selections of random subsets of  $[d]$  with a fixed cardinality  $m_{\text{try}}$ . Each tree in the ensemble is trained on a bootstrap sample of the original dataset and predictions are made by averaging the output of individual trees, effectively reducing the overall variance of the model (see Algorithm

1 in Appendix E). We call the ensemble the *MinimaxSplit* (resp. *VarianceSplit*) *random forest*, if the base learners follow the MinimaxSplit (resp. VarianceSplit) algorithm.<sup>6</sup>

### 3.2 Empirical risk bound for MinimaxSplit random-dimension random forests

Our discussions in Section 2.4 indicate that the random forest approach for the MinimaxSplit algorithms is better performed with  $m_{\text{try}} = 1$  to guarantee consistency. In other words, we randomize the dimension at *every* node. As a consequence, applying the MinimaxSplit and the cyclic MinimaxSplit splitting rules yield the same ensemble in distribution. We call the resulting ensemble the *MinimaxSplit random-dimension random forest*.

Recall the regression setting from Section 2.3 and consider a random forest consisting of trees in which split dimensions at each node are i.i.d. sampled from  $[d]$ , independently of the data, similar to ExtraTrees (Geurts et al., 2006) but the randomness lies in choosing the dimension instead of the split location. Fix a depth  $k$  and the number of samples  $N$ . Denote by  $n$  the number of trees in the forest. Let  $\Sigma$  denote the law of the splitting dimensions and  $\mathbb{E}_n$  denote the expectation with respect to the empirical measure on  $n$  samples from  $\Sigma$ . Let  $g_k$  be the estimator constructed at depth  $k$  from the MinimaxSplit random-dimension random forest. Our goal is then to bound the  $L^2$  error  $\mathbb{E}[\|\mathbb{E}_n[g_k] - g^*\|^2]$ , where the outer expectation is taken in terms of randomness both from the empirical samples from  $(\mathbf{X}_*, Y_*)$  and from the empirical measure  $\mathbb{E}_n$ . We will provide empirical evidence of the effectiveness of such a randomised construction in Section 5.3.

**Theorem 9.** *Assume the same regression setting of Theorem 7, and the above random forest definition. We have*

$$\begin{aligned} \mathbb{E}[\|\mathbb{E}_n[g_k] - g^*\|^2] &\leq \frac{C2^k(\log N)^2 \log(Nd) + 2^k(\log N)dn^{-1/3}}{N} \\ &\quad + 2 \inf_{g \in \mathcal{G}} \left( 2\|g - g^*\|^2 + \frac{8}{3} \left( \|g - g^*\|^2 + \|g\|_{\text{TV}}^2 \right) \left( e^{-\frac{k}{6d}} + \frac{d}{n^{1/3}} \right) \right), \end{aligned} \quad (26)$$

where  $C > 0$  is a constant depending only on  $\|g^*\|_\infty$  and  $\sigma^2$ . In particular, if  $N/(2^k(\log N)^2 \log(Nd)) \rightarrow \infty$ ,  $k/d \rightarrow \infty$ , and  $n/d^3 \rightarrow \infty$ , then the MinimaxSplit random-dimension random forest is consistent.

Let us compare Theorem 9 with the empirical risk bound for a single tree given by Theorem 7. First, the exponent  $-k/(6d)$  now does not contain a floor function but has an asymptotically slower rate if  $k/d \rightarrow \infty$ . This is due to the non-cyclicity of the (random) selection of dimensions. Second, the formula (26) does not involve  $\delta$  for simplicity, although the same argument works for more general choices of  $\delta > 0$ .

## 4 Minimax decision trees for classification

Following the C4.5 generalization in Klusowski and Tian (2024), we also provide corresponding results when using MinimaxSplit for entropy loss. Throughout this section, we consider binary response  $Y \in \{\pm 1\}$  with covariates  $\mathbf{X} \in \mathbb{R}^d$  (so we consider  $(\mathbf{X}, Y)$  as a joint distribution), and  $\eta(\mathbf{x}) := \mathbb{P}(Y = 1 \mid \mathbf{X} = \mathbf{x})$  denotes the regression function. For any measurable cell  $A \subset \mathbb{R}^d$  we write

$$\eta_A := \mathbb{P}(Y = 1 \mid \mathbf{X} \in A), \quad w(A) := \mathbb{P}(\mathbf{X} \in A),$$

---

<sup>6</sup>Note that the cyclic MinimaxSplit case does not apply (unless  $m_{\text{try}} = 1$ ) due to the lack of an optimization procedure over the dimensions.

and we measure impurity on  $A$  with the Shannon entropy

$$H(Y \mid \mathbf{X} \in A) = h(\eta_A) := -\eta_A \log \eta_A - (1 - \eta_A) \log(1 - \eta_A). \quad (27)$$

Axis-aligned splits refine a cell  $A$  into left and right children  $A_L = \{\mathbf{x} \in A : x_j < z\}$  and  $A_R = A \setminus A_L$  for some  $j \in [d]$  and  $z \in \mathbb{R}$ . Standard C4.5 chooses  $(j, z)$  to minimize the weighted sum  $w(A_L)h(\eta_{A_L}) + w(A_R)h(\eta_{A_R})$ . In the *MinimaxSplit* version, we instead choose  $(j, z)$  to minimize  $\max\{w(A_L)h(\eta_{A_L}), w(A_R)h(\eta_{A_R})\}$ , which explicitly prevents one child from remaining both large and highly impure. As in the regression setting, when splitting at level  $k$ , the *cyclic MinimaxSplit* variant fixes the coordinate at level  $k$  to  $j_k = 1 + (k \pmod d)$  and optimizes only over the threshold  $z$ .

Given a split rule, we obtain a nested sequence of axis-aligned partitions  $\{\pi_k\}_{k \geq 0}$  by applying a single binary split per level. For any  $\omega$ , we let  $A_k(\omega) \in \pi_k$  be the unique cell containing  $\mathbf{X}(\omega)$ . The node statistic we track is the log-odds of the average class-probability in that cell,

$$M_k(\omega) := \log \left( \frac{\eta_{A_k(\omega)}}{1 - \eta_{A_k(\omega)}} \right). \quad (28)$$

Let  $g_k(\mathbf{x}) := \log(\eta_{A_k}/(1 - \eta_{A_k}))$  for  $\mathbf{x} \in A_k$ ,  $A_k \in \pi_k$ . The predictor associated with depth  $k$  is the plug-in classifier  $2\mathbb{1}_{\{g_k(\mathbf{x}) \geq 0\}} - 1$  (or equivalently,  $2\mathbb{1}_{\{\eta_{A_k} \geq 1/2\}} - 1$  for the unique  $A_k \in \pi_k$  that contains  $\mathbf{x}$ ) and the canonical convex surrogate is the conditional cross-entropy on the partition.

With this preparation, the results in this section follow the same logical arc as in the regression setting. Theorem 10 treats the marginally atomless case and shows that, under the cyclic MinimaxSplit schedule, the log-odds process  $\{M_k\}$  contracts in mean square at an exponential rate that depends only on the dimension and the coordinate range. Theorem 11 covers the complementary purely atomic setting. Here, we need a mild anti-concentration assumption on coordinate masses; the theorem then delivers an explicit upper bound for  $\mathbb{E}[(Y - M_k)^2]$  that reflects the discrete resolution  $N$  of the atoms. Finally, Theorem 12 translates these bounds into an oracle inequality for the excess classification risk of  $g_k$  under the 0-1 loss via standard calibration between cross-entropy and misclassification.

**Theorem 10.** *Suppose that  $\mathbf{X}$  is marginally atomless. Let the associated process  $\{M_k\}_{k \geq 0}$  be constructed from (28) using the cyclic MinimaxSplit algorithm. Then uniformly for any  $k \geq 0$ ,*

$$\mathbb{E}[(Y - M_k)^2] \leq \inf_{g \in \mathcal{G}} \left( \mathbb{E}[(Y - g(\mathbf{X}))^2] + \sqrt{\frac{\log 2}{4}} 2^{-\lfloor k/d \rfloor/2} \|g\|_{\text{TV}}^{1/2} \right). \quad (29)$$

**Theorem 11.** *Suppose that  $\mathbf{X}$  is purely atomic and for some  $N > 0$ ,*

$$\max_{j \in [d]} \max_{u \in \mathbb{R}} \mathbb{P}(X_j = u) \leq \frac{1}{N}. \quad (30)$$

*Let the associated process  $\{M_k\}_{k \geq 0}$  be constructed from (28) using the cyclic MinimaxSplit algorithm. Then uniformly for any  $k \geq 0$ ,*

$$\mathbb{E}[(Y - M_k)^2] \leq 2^{-\lfloor k/d \rfloor/2} \frac{2^k \log N}{N} + \inf_{g \in \mathcal{G}} \left( \mathbb{E}[(Y - g(\mathbf{X}))^2] + \sqrt{\frac{\log 2}{4}} 2^{-\lfloor k/d \rfloor/2} (\|g\|_{\text{TV}}^{1/2} + \frac{\|g\|_{\text{TV}}}{2}) \right). \quad (31)$$

The proofs of Theorems 10 and 11 follow essentially the same principles as in the regression setting, except that now  $\{M_k\}_{k \geq 0}$  no longer forms a martingale. The key is to apply the monotonicity of the map

$z \mapsto \mathbb{P}(\mathbf{X} \in A, X_j < z) h(\mathbb{P}(Y = 1 \mid \mathbf{X} \in A, X_j < z))$ , a fact that mirrors Lemma 2.1 and will be justified in Lemma B.3 below.

In the next result, we state the corresponding oracle inequality. Following [Klusowski and Tian \(2024\)](#), for a map  $g$  we consider the misclassification risk  $\text{Err}(g) := \mathbb{P}(Y \neq 2\mathbb{1}_{\{g(\mathbf{X}) \geq 0\}} - 1)$ . Further, we set  $g_*(\mathbf{x}) := \log(\mathbb{P}(Y = 1 \mid \mathbf{X} = \mathbf{x})/\mathbb{P}(Y = -1 \mid \mathbf{X} = \mathbf{x}))$ .

**Theorem 12.** *Assume that  $\mathbf{X}_*$  is marginally atomless. We have that under the cyclic MinimaxSplit construction,*

$$\begin{aligned} \mathbb{E}[\text{Err}(g_k)] - \text{Err}(g_*) &\leq L \left( \frac{2^k (\log N)^2 \log(Nd)}{N} \right)^{1/4} \\ &\quad + \inf_{g \in \mathcal{G}} \left( \|g - g_*\|^2 + \left( \frac{\log 2}{4} \right)^{1/4} 2^{1-\lfloor k/d \rfloor/4} (\|g\|_{\text{TV}}^{1/4} + \frac{\|g\|_{\text{TV}}^{1/2}}{\sqrt{2}}) \right), \end{aligned} \quad (32)$$

where  $L > 0$  is a positive universal constant.

*Remark 13.* The bound (32) can be relaxed to

$$\mathbb{E}[\text{Err}(g_k)] - \text{Err}(g_*) \leq L \left( \frac{2^k (\log N)^2 \log(Nd)}{N} \right)^{1/4} + \inf_{g \in \mathcal{G}} \left( \|g - g_*\|^2 + L 2^{-\lfloor k/d \rfloor/4} (\|g\|_{\text{TV}} + 1) \right)$$

for some large constant  $L > 0$ , using the rough inequality  $x \leq \min\{x^2 + 1, x^4 + 1\}$ . Compared to the oracle inequality of [Klusowski and Tian \(2024\)](#), we see that we have achieved exponential convergence rates and removed the factor  $\|g\|_\infty$ . The proof of Theorem 12 follows in exactly the same way as Theorem 4.3 of [Klusowski and Tian \(2024\)](#) in the C4.5 case, as the arguments therein do not depend on how the tree is constructed, as long as the splitting rule is axis-aligned.

## 5 Numerical experiments and applications

In this section, we provide experiments that verify the advantages of MinimaxSplit and cyclic MinimaxSplit methods in low-dimensional domains, as well as integrated ensemble methods applied to approximating a real-valued function and denoising images. Performance metrics are defined in Appendix D.1, and further numerical experiments (including those in high dimensions) are provided in Appendix D.

### 5.1 Avoiding end-cut preference for stable cuts

To show that the ECP is remedied in MinimaxSplit, we consider a special case of the location regression model in [\(Cattaneo et al., 2022\)](#), similar to the discussions in Example 1. In our experiment, we generate independent replicates with  $X \stackrel{\text{law}}{\sim} \text{Unif}(0, 1)$  and  $Y$  following the standard normal or Student's  $t(\cdot)$  distributions (pure noise), sort by  $X$ , and scan all possible splits in the experiments in Figure 5. We also provide two baselines: Uniform random cutting picks a split point entirely at random within the current predictor range, ensuring that there is no systematic bias yet, ignoring any data-driven signal. Sampling an observed value similarly randomizes split location among actual samples. Both serve as baseline benchmarks: they eliminate ECP, but do not offer an impurity-guided improvement mechanism.

For each replicate, we record  $\min(n_L, n_R)/n$ , the relative size of the smaller child, and we choose either VarianceSplit (the standard CART impurity reduction) or MinimaxSplit. As the tail of the noise becomes heavier, VarianceSplit becomes increasingly prone to end-cuts, isolating tiny child nodes almost every time

under Student's t with one degree of freedom. In contrast, the output of MinimaxSplit remains more tightly concentrated near perfectly balanced halves across all three distributions, especially for the light-tailed noise cases, thus preventing small-node failures. Random uniform and random observed-point cuts likewise avoid pathological end-cuts but do so at the cost of entirely unguided splits. Thus, if one requires a data-adaptive binary split that resists extreme outliers without surrendering balance, the MinimaxSplit criterion clearly outperforms VarianceSplit (or CART) and random baselines.

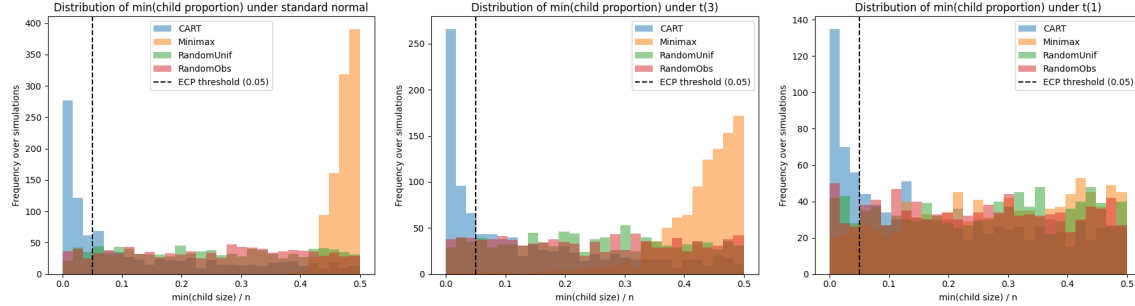


Figure 5: Empirical distributions of sample size  $n = 500$  over 1000 replicates of the smaller-child proportion  $\min(n_L, n_R)/n$  when splitting pure-noise data generated by standard normal (left),  $t(3)$  (middle), and  $t(1)$  (right) distributions. We also use dashed lines to denote the threshold 0.05.

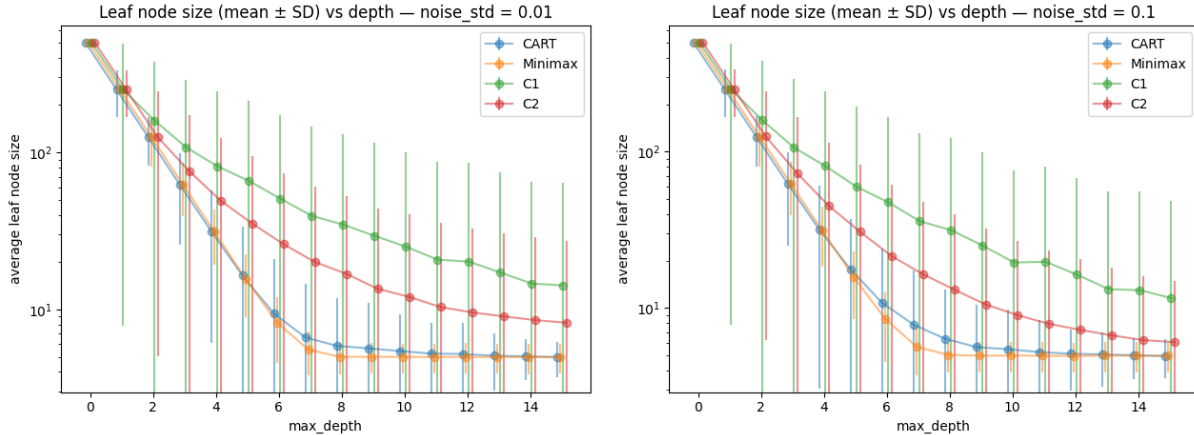


Figure 6: Average leaf size (mean number of samples per leaf) versus maximum tree depth for four splitting criteria (VarianceSplit (CART), MinimaxSplit, C1, C2), at two noise levels. Error bars show one standard deviation across repeated fits. The vertical axis is on a log scale to expose imbalance: small and collapsing leaf means with low variability (as for MinimaxSplit and, to a lesser extent, CART) indicate balanced partitioning, whereas the slower decay and large spread for C1/C2 reflect persistent ECP that peels off tiny fragments and leaves dominant branches. The signal function is given by (33). Increasing the centered Gaussian noise from  $\sigma = 0.01$  to  $\sigma = 0.1$  slightly attenuates rates but does not erase the structural contrast.

End-cut preference propagates imbalance down the tree: a tiny "peeled-off" child at one split creates a

cascade of uneven leaves. To quantify this, in the next experiment, for each fully grown tree we compute

$$\text{average leaf node size} = \frac{1}{L} \sum_{j=1}^L n_j,$$

$$\text{standard deviation of leaf node size} = \sqrt{\frac{1}{L} \sum_{j=1}^L (n_j - \text{avg of leaf node size})^2},$$

where  $L$  is the number of leaves and  $n_j$  is the size of leaf  $j$ . Small average leaf node sizes and collapsed error bars signal balanced partitions; large means with huge variance indicate persistent end-cuts leaving one dominant branch and tiny fragments. Our main methodological contribution, the MinimaxSplit algorithm can be used with ensembles and is applicable in real data, but also yields a theoretically stronger version of [Buja and Lee \(2001\)](#)'s formula C1 and C2, where they showed that the minimum variance (a.k.a., one-sided purity) approach can identify extreme subsets much better than traditional CART. Figure 6 records the leaf distributions as the maximum depth of the tree grows, with  $X \stackrel{\text{law}}{\sim} \text{Unif}(0, 1)$  and signal

$$f(x) = \begin{cases} \sin(x), & 0 \leq x < \frac{1}{3}; \\ -2x, & \frac{1}{3} \leq x < \frac{2}{3}; \\ 0, & \text{otherwise.} \end{cases} \quad (33)$$

MinimaxSplit quickly reduces average leaf size and variability, yielding balanced leaves. VarianceSplit (CART), C1, and C2 shrink mean leaf size slowly and retain a large spread: they repeatedly cut tiny end pieces while leaving a large branch, showing ECP.

## 5.2 Fixed-horizon EEG amplitude regression

We now examine whether the theoretical advantages of MinimaxSplit and cyclic MinimaxSplit carry over to a non-parametric time-series regression problem built from the Bonn electroencephalography (EEG) corpus ([Andrzejak et al., 2001](#)).<sup>7</sup> Each EEG record is a single-channel segment of length  $T \approx 23.6$  seconds sampled at 173.61 Hz. We formulate a scalar regression task: given time  $t \in [0, T]$  within a fixed horizon  $T$ , predict the standardized EEG amplitude  $y(t)$ . This time-only design isolates the splitting behavior along a single coordinate, precisely the regime in which ECP is the most consequential for greedy impurity splits and where our minimax approach is expected to stabilize partitions.

Our preprocessing follows two principles. First, we standardize the amplitudes within each segment to zero mean and unit variance. This removes irrelevant scale without obscuring the short-range temporal variability that the tree must fit. Second, we optionally downsample by an integer factor to control computational budget while preserving the temporal ordering. Both steps are label-free and therefore introduce no leakage. For evaluation, we fix a horizon  $T = 20$  s, draw train-test splits inside  $[0, T]$  by a random holdout, and keep the split fixed across methods and depths so that any performance difference reflects only the splitting rule. These choices echo our theoretical emphasis on how the split criterion shapes the geometry of the partition.

In Figure 7, we compare three trees with identical hyperparameters (maximum split size ( $= 2$ ) and stopping rules kept fixed): standard CART using squared-error reduction (with pruning), its variant Vari-

<sup>7</sup> as explained at <https://www.mathworks.com/help/wavelet/ug/time-frequency-convolutional-network-for-eeg-data-classification.html>

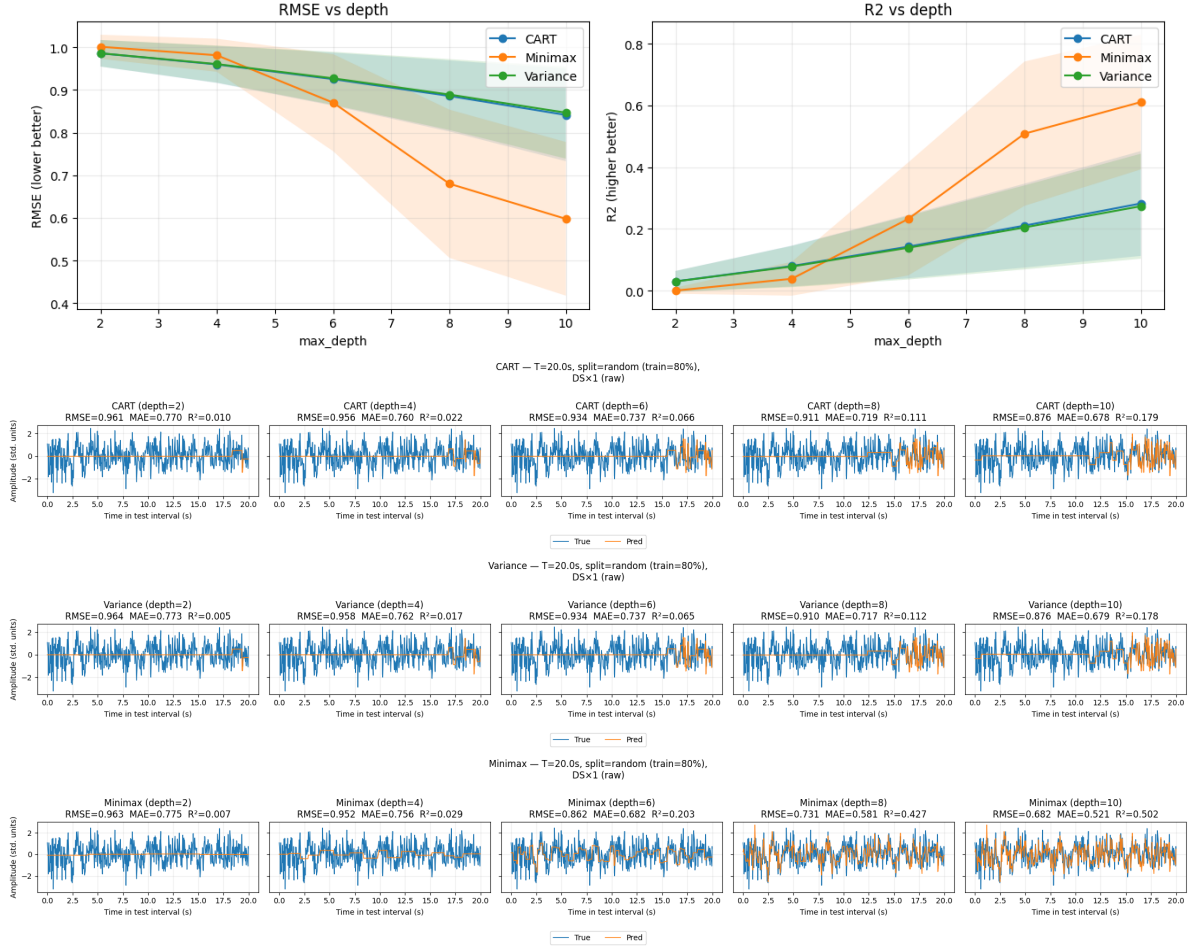


Figure 7: Fixed-horizon EEG amplitude regression with trees. The top row summarizes performance across Bonn EEG segments when predicting standardized amplitude  $y(t)$  from time only over a  $T = 20$  s window (random 80/20 split within the window; identical splits reused for all methods; no downsampling). Curves show mean RMSE (left; lower is better) and mean  $R^2$  (right; higher is better) versus tree depth, with shaded bands denoting  $\pm$ standard deviation across segments. The mosaics below plot, for one representative segment, the true (blue) and predicted (orange) test-interval traces for each method at depths  $k \in \{2, 4, 6, 8, 10\}$  along with the reported RMSE/MAE/ $R^2$ .

anceSplit, and our MinimaxSplit which minimizes the worst child variance. The experimental protocol is intentionally minimal so that the fitted functions reveal the partition geometry. Input features consist only of time  $t$  and targets are the standardized amplitudes  $y(t)$ . We train each tree on the training subset within  $[0, T]$  and report test RMSE, MAE, and the coefficient of determination  $R^2$  on the holdout portion, aggregating results across all available EEG segments. Because the same split is reused across methods, depth-wise comparisons are matched at the sample level. We also visualize the predicted curves against the ground truth on a representative segment to expose the qualitative effect of each split rule.

The results align with the theoretical expectations. As the tree depth increases, CART and the sum-of-variances baseline increasingly display end-cut behavior, producing piecewise constant fits that flatten toward the edges of the interval and degrade extrapolation between local extrema. MinimaxSplit, by contrast, maintains near-balanced children throughout the path, which yields visibly tighter fits to the oscillatory structure of the signal and systematically lower errors. In addition, MinimaxSplit reduces error and raises

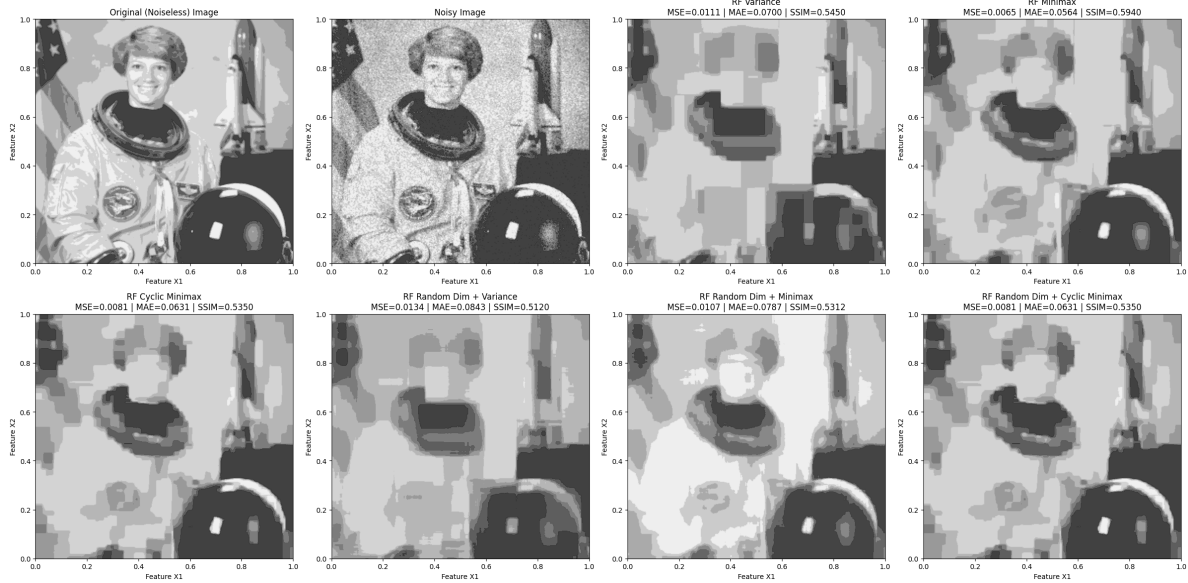


Figure 8: Comparative analysis of various random forest (depth  $K = 10$ , 50 estimators) approaches for image denoising using different splitting strategies. The experiment compares six random forest configurations on a noisy astronaut image: original noiseless image; noisy input; three greedily splitting methods ( $m_{\text{try}} = d$ ) using consistent splitting criteria across all weak learners (trees) — VarianceSplit, MinimaxSplit, and Cyclic MinimaxSplit; three random-dimension methods where feature selection is randomized at each node (i.e.,  $m_{\text{try}} = 1$ ) while location selection follows the three different criteria, as described in Section 3.2.

$R^2$  markedly as depth increases, while CART and the VarianceSplit baseline improve more slowly. The trend is most pronounced in the random holdout regime where interpolation dominates; here, the additional leaves available to deeper trees are useful only if the split rule does not collapse sample sizes, and the MinimaxSplit criterion preserves effective sample size by construction. This observation matches our finding that MinimaxSplit concentrates the smaller-child proportion away from zero and one across noise laws, thereby eliminating pathological small-node failures observed under impurity-based CART.

### 5.3 Image denoising with ensembles

Another notable experiment involves applying decision trees to denoise noisy images (Luo et al., 2024). We apply the different tree variants to predict pixel values based on their locations, effectively treating this as a regression problem. The experiments shown in Figures 8 and 9 compare decision tree and random forest regression methods for denoising the classic Astronaut (Van der Walt et al., 2014) grayscale image, which has been preprocessed to 256 by 256.

The goal is to recover a clean grayscale image  $f : [0, 1]^2 \rightarrow [0, 1]$  from noisy observations  $Y = f(\mathbf{X}) + \varepsilon$  at pixel centers  $\mathbf{X} = (X_1, X_2)$  laid out on a  $256 \times 256$  grid (equipped with the uniform distribution). We normalize intensities to  $[0, 1]$  and add i.i.d. Gaussian noise  $\varepsilon \stackrel{\text{law}}{\sim} \mathcal{N}(0, 0.1^2)$ . Each pixel becomes one regression sample, and we fit axis-aligned trees that approximate the unknown  $f$  as a piecewise constant function on a dyadic partition, which is precisely the regime covered by our analysis of axis-aligned trees and their ensembles.

We compare six random forest variants built from our splitting rules: VarianceSplit, MinimaxSplit, and cyclic MinimaxSplit, each with or without random feature subsampling at every node ( $m_{\text{try}} = 1$  feature per

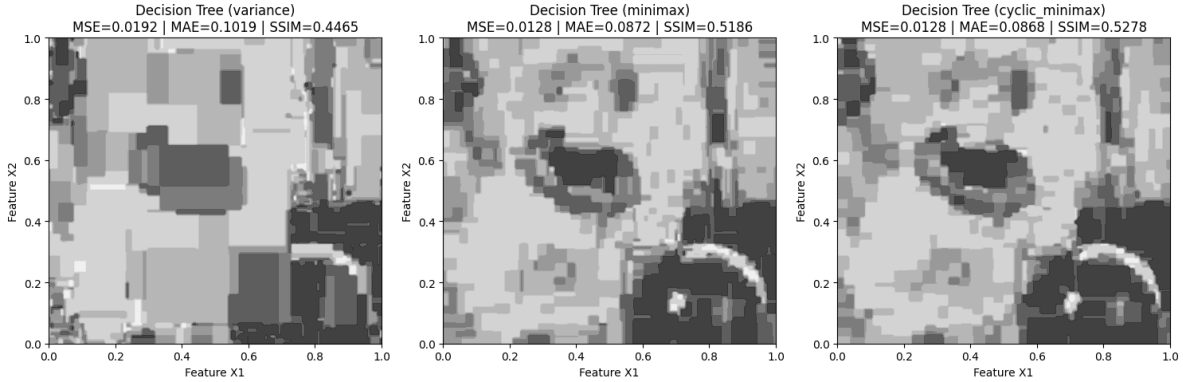


Figure 9: Comparison of decision tree regression methods (depth  $K = 10$ ) for image reconstruction using different splitting criteria — VarianceSplit, MinimaxSplit, and cyclic MinimaxSplit. Each method was trained on noisy astronaut image data with spatial coordinates as features and pixel intensities as targets.

split). All forests consist of 50 trees, each grown to depth  $K = 10$ ; trees are bootstrapped and predictions are averaged.

Figure 8 shows qualitative reconstructions for the six forests. The VarianceSplit forest leaves noticeable grain in flat regions and blurs edges at depth 10. In contrast, both Minimax ensembles suppress speckle while preserving high-contrast features such as facial contours and texture edges. Further, across all metrics, the MinimaxSplit forests outperforms the VarianceSplit forest, with the largest gains in SSIM, indicating better structural fidelity. The improvements are coherent with Theorem 9: the worst-child control given by the MinimaxSplit rule prevents high-variance children from persisting across levels. The single-tree performance is shown in Figure 9.

The experiments support two messages from the theory. First, enforcing a worst-child improvement at each split translates into visibly sharper reconstructions and uniformly better pixelwise metrics. Second, randomizing the split dimension ( $m_{\text{try}} = 1$ ) is not an arbitrary choice and ensures the consistency of Minimax forests and practical stability.

## 6 Conclusion

In this study, we reexamine the well-known phenomenon of ECP, which is associated with traditional CART decision trees Breiman et al. (1984). To remedy this undesirable behavior for single decision trees Ishwaran and Kogalur (2010), we introduce a novel decision tree splitting strategy, the MinimaxSplit algorithm, along with its multivariate variant, the cyclic MinimaxSplit algorithm. Unlike traditional VarianceSplit methods, which aim to reduce overall variance in the child nodes, our MinimaxSplit algorithm seeks to minimize the maximum variance within the split partitions, thereby reducing the risk of overly biased partitions. The cyclic MinimaxSplit algorithm further ensures that each dimension is used in a balanced manner throughout the tree construction process, avoiding dominance by a subset of features. We do not claim that this new method could outperform the classical CART-like splitting under all circumstances, yet we point out that our construction avoids ECP and attains a better convergence rate guarantee as the tree progresses deeper. The (non-cyclic) MinimaxSplit construction features the anti-symmetry-breaking preference—consistency is not guaranteed in certain symmetric cases, which can, however, be alleviated by using ensemble methods.

A key theoretical methodological development of this study is that the cyclic MinimaxSplit algorithm

achieves an exponential MSE decay rate given sufficient data samples, without requiring additional variance decay assumptions (Theorem 6) in regression and classification settings. Furthermore, we derive empirical risk bounds for this method, establishing its robustness in different settings (Theorem 7). Using the same powerful techniques used for trees, we prove novel results on the convergence rates of univariate partition-based martingale approximations as a by-product (see Appendix A), which are of their own interest.

In addition to single-tree regression analysis, we explore ensemble learning approaches, where we combine decision trees constructed using MinimaxSplit, cyclic MinimaxSplit, and VarianceSplit methods within a random forest framework. The results demonstrate that a hybrid approach leveraging different splitting techniques yields superior performance, particularly when dealing with non-uniform data distributions (Section 3). These findings suggest that the MinimaxSplit approach can provide more stable and adaptive decision trees compared to traditional methods, especially in low-dimensional settings.

## Acknowledgment

The authors thank Ruodu Wang for his valuable input. We provide our reproducible code at [github.com/hrluo](https://github.com/hrluo).

## References

Ralph G Andrzejak, Klaus Lehnertz, Florian Mormann, Christoph Rieke, Peter David, and Christian E Elger. Indications of nonlinear deterministic and finite-dimensional structures in time series of brain electrical activity: Dependence on recording region and brain state. *Physical Review E*, 64(6):061907, 2001.

Guy Blanc, Neha Gupta, Jane Lange, and Li-Yang Tan. Universal guarantees for decision tree induction via a higher-order splitting criterion. *Advances in Neural Information Processing Systems*, 33:9475–9484, 2020.

Yu V Borovskikh and VS Korolyuk. *Martingale Approximation*. Walter de Gruyter GmbH & Co KG, 1997.

Leo Breiman. Random forests. *Machine Learning*, 45(1):5–32, 2001.

Leo Breiman, Jerome Friedman, Richard Olshen, and Charles Stone. *Classification and Regression Trees*. Wadsworth, Inc., 1984.

Andreas Buja and Yung-Seop Lee. Data mining criteria for tree-based regression and classification. In *Proceedings of the seventh ACM SIGKDD international conference on Knowledge discovery and data mining*, pages 27–36, 2001.

Matias D Cattaneo, Jason M Klusowski, and Peter M Tian. On the pointwise behavior of recursive partitioning and its implications for heterogeneous causal effect estimation. *arXiv preprint arXiv:2211.10805*, 2022.

Matias D Cattaneo, Rajita Chandak, and Jason M Klusowski. Convergence rates of oblique regression trees for flexible function libraries. *The Annals of Statistics*, 52(2):466–490, 2024.

Chien-Ming Chi, Patrick Vossler, Yingying Fan, and Jinchi Lv. Asymptotic properties of high-dimensional random forests. *The Annals of Statistics*, 50(6):3415–3438, 2022.

Joseph L Doob. Regularity properties of certain families of chance variables. *Transactions of the American Mathematical Society*, 47(3):455–486, 1940.

Joseph L Doob. *Stochastic Processes*. John Wiley & Sons, New York, 1953.

Pierre Geurts, Damien Ernst, and Louis Wehenkel. Extremely randomized trees. *Machine learning*, 63(1):3–42, 2006.

Louis Gordon and Richard A Olshen. Almost surely consistent nonparametric regression from recursive partitioning schemes. *Journal of Multivariate Analysis*, 15(2):147–163, 1984.

Ion Grama, Ronan Lauvergnat, and Émile Le Page. Limit theorems for Markov walks conditioned to stay positive under a spectral gap assumption. *The Annals of Probability*, 46(4):1807–1877, 2018.

Peter Hall and Christopher C Heyde. *Martingale Limit Theory and Its Application*. Academic press, 2014.

Hemant Ishwaran. The effect of splitting on random forests. *Machine Learning*, 99:75–118, 2015.

Hemant Ishwaran and Udaya B Kogalur. Consistency of random survival forests. *Statistics & probability letters*, 80(13-14):1056–1064, 2010.

Aryan Jadon, Avinash Patil, and Shruti Jadon. A comprehensive survey of regression-based loss functions for time series forecasting. In *International Conference on Data Management, Analytics & Innovation*, pages 117–147. Springer, 2024.

Jason M Klusowski and Peter M Tian. Large scale prediction with decision trees. *Journal of the American Statistical Association*, 119(545):525–537, 2024.

Linxi Liu, Dangna Li, and Wing Hung Wong. Convergence rates of a class of multivariate density estimation methods based on adaptive partitioning. *Journal of Machine Learning Research*, 24(50):1–64, 2023.

Wei-Yin Loh. Fifty years of classification and regression trees. *International Statistical Review*, 82(3):329–348, 2014.

Gilles Louppe. *Understanding Random Forests: From Theory to Practice*. PhD thesis, University of Liège, Liège, Belgium, 2014. PhD thesis.

Hengrui Luo and Matthew T Pratola. Sharded Bayesian additive regression trees. *arXiv preprint arXiv:2306.00361*, 2023.

Hengrui Luo, Akira Horiguchi, and Li Ma. Efficient decision trees for tensor regressions. *arXiv preprint arXiv:2408.01926*, 2024.

Rahul Mazumder and Haoyue Wang. On the convergence of CART under sufficient impurity decrease condition. *Advances in Neural Information Processing Systems*, 36, 2024.

James N Morgan and Robert C Messenger. THAID, a sequential analysis program for the analysis of nominal scale dependent variables. Technical report, Ann Arbor: Institute for Social Research, University of Michigan, 1973.

Ryan O'Donnell, Michael Saks, Oded Schramm, and Rocco A Servedio. Every decision tree has an influential variable. In *46th Annual Symposium on Foundations of Computer Science (FOCS'05)*, pages 31–39. IEEE, 2005.

Aaditya Ramdas and Ruodu Wang. *Hypothesis Testing with E-values*. Foundations and Trends® in Statistics, 2025. Inaugural issue.

Ludger Rüschendorf. The Wasserstein distance and approximation theorems. *Probability Theory and Related Fields*, 70(1):117–129, 1985.

Gordon Simons. A martingale decomposition theorem. *The Annals of Mathematical Statistics*, 41(3):1102–1104, 1970.

Xiaogang Su, George Ekow Quaye, Yishu Wei, Joseph Kang, Lei Liu, Qiong Yang, Juanjuan Fan, and Richard A Levine. Smooth Sigmoid Surrogate (SSS): An alternative to greedy search in decision trees. *Mathematics*, 12(20):3190, 2024.

Vasilis Syrgkanis and Manolis Zampetakis. Estimation and inference with trees and forests in high dimensions. In *Conference on Learning Theory*, pages 3453–3454. PMLR, 2020.

Yan Shuo Tan, Abhineet Agarwal, and Bin Yu. A cautionary tale on fitting decision trees to data from additive models: generalization lower bounds. In *International Conference on Artificial Intelligence and Statistics*, pages 9663–9685. PMLR, 2022.

Luis Torgo. A study on end-cut preference in least squares regression trees. In *Portuguese Conference on Artificial Intelligence*, pages 104–115. Springer, 2001.

Aad van der Vaart and Jon Wellner. *Weak Convergence and Empirical Processes: With Applications to Statistics*. Springer Science & Business Media, 2013.

Stefan Van der Walt, Johannes L Schönberger, Juan Nunez-Iglesias, François Boulogne, Joshua D Warner, Neil Yager, Emmanuelle Gouillart, and Tony Yu. scikit-image: image processing in python. *PeerJ*, 2:e453, 2014.

Tianming Wang et al. Asymptotic expansions for inverse moments of binomial and negative binomial. *Statistics & Probability Letters*, 78(17):3018–3022, 2008.

Xiangya Wang. A study of end-cut preference in tree-based modeling. Master's thesis, The University of Texas at El Paso, 2025.

Zhou Wang, Alan C Bovik, Hamid R Sheikh, and Eero P Simoncelli. Image quality assessment: from error visibility to structural similarity. *IEEE transactions on image processing*, 13(4):600–612, 2004.

Wei Biao Wu and Michael Woodroffe. Martingale approximations for sums of stationary processes. *The Annals of Probability*, 32(2):1674–1690, 2004.

Zhenyuan Zhang, Aaditya Ramdas, and Ruodu Wang. On the existence of powerful p-values and e-values for composite hypotheses. *The Annals of Statistics*, 52(5):2241–2267, 2024.

Hang Zhao, Orazio Gallo, Iuri Frosio, and Jan Kautz. Loss functions for image restoration with neural networks. *IEEE Transactions on Computational Imaging*, 3(1):47–57, 2017.

Ou Zhao and Michael Woodroffe. On martingale approximations. *The Annals of Applied Probability*, 18(5): 1831–1847, 2008.

## A On partition-based martingale approximations

In this section, we develop the framework of partition-based martingale approximations and show that a number of constructions feature exponential convergence rates. These problems are of their own interest (see the end of Appendix A.1) and have implications in the regression tree setting. The main takeaway is that:

- The techniques developed in this work for analyzing convergence rates of the MinimaxSplit algorithm extend to many other settings, such as convergence rates for martingale approximations;
- Precise (asymptotic) convergence rates of martingale approximations depend on the initial law, but a uniform exponential rate is always guaranteed under mild conditions;
- Applying VarianceSplit to samples  $\{(\mathbf{X}_i, Y_i)\}_{1 \leq i \leq n}$  satisfying monotonicity in all  $d$  dimensions (meaning that for every  $j \in [d]$  and distinct  $i, i' \in [n]$ ,  $((\mathbf{X}_i)_j - (\mathbf{X}_{i'})_j)(Y_i - Y_{i'}) = \sigma_j$  where  $\sigma_j \in \{\pm 1\}$  depends only on  $j$ ) does not incur ECP.

### A.1 Basic concepts

Consider nested partitions  $\{\pi_k\}_{k \geq 0}$  of  $\mathbb{R}$  and a real-valued random variable  $U$  with a finite second moment. We use the abbreviation  $\sigma(\pi_k)$  to denote the  $\sigma$ -algebra generated by events of the form  $\{U \in A\}_{A \in \pi_k}$ . Define  $M_k := \mathbb{E}[U \mid \sigma(\pi_k)]$ . If  $\Pi := \{\pi_k\}_{k \geq 0}$  is a nested sequence of partitions,  $\{\sigma(\pi_k)\}_{k \geq 0}$  is a filtration generated by indicator functions of sets in  $\pi_k$ 's (Doob, 1953). It follows from the tower property of conditional expectations that the sequence  $\{M_k\}_{k \geq 0} = \{\mathbb{E}[U \mid \sigma(\pi_k)]\}_{k \geq 0}$  is a martingale (in fact, a Doob martingale (Doob, 1940, 1953)). We call this martingale the  $\Pi$ -based martingale approximation of the random variable  $U$ , or in general a *partition-based martingale approximation* that approximates the random variable  $U$  in  $L^2$ .

Unless  $U$  is a constant, there are different partition-based martingale approximations depending on the distribution of  $U$ . Our goal in this section is to identify a few partition-based martingale approximations that efficiently approximate  $U$ , where the construction algorithm is universal. The efficiency criterion is given by the decay of the MSE  $\mathbb{E}[(U - M_k)^2]$ . The MSE is non-increasing in  $k$  by the nested property of  $\{\pi_k\}_{k \geq 0}$  and the total variance formula.

Without loss of generality, we give our construction of a partition of a generic interval  $[a, b] \subset \mathbb{R}$ , where  $a, b \in \mathbb{R} \cup \{\pm\infty\}$ .<sup>8</sup> The sequence of partitions  $\Pi$  will be constructed recursively, where  $\pi_0 = \{\mathbb{R}\}$  and for every  $k \geq 0$ , each interval  $A \in \pi_k$  splits into two intervals, by following the same construction, forming the elements in  $\pi_{k+1}$ . In the following, we introduce four distinct splitting rules that define partition-based martingale approximations. For simplicity, we assume that  $U$  is atomless, so that the endpoints of the intervals do not matter and that no trivial split occurs. The general case with atoms can be analyzed in a similar way but with more technicality.

**Definition 14.** Suppose we are given an atomless law of  $U$  and a non-empty interval  $I = [a, b)$ , where  $a, b \in \mathbb{R} \cup \{\pm\infty\}$ .

---

<sup>8</sup>Here we slightly abuse notation that  $[a, b) = (-\infty, b)$  if  $a = -\infty$ .

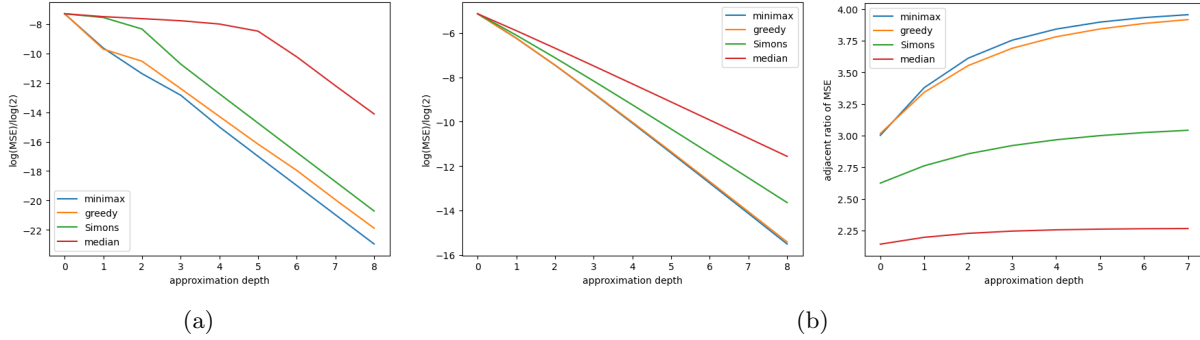


Figure 10: Plots of the log-MSE,  $\log_2(\mathbb{E}[(U - M_k)^2])$  versus the approximation depth  $k$  for four different methods, where the density of the law  $U$  is given: (a) by  $f(u) \propto \mathbb{1}_{[0,0.9]}(u) + (1 + 10^4(u - 0.9))\mathbb{1}_{[0.9,1]}(u)$  and (b) by  $f(u) \propto u^{10}\mathbb{1}_{[0,1]}(u)$ . The right panel of (b) shows the ratios  $\mathbb{E}[(U - M_{k+1})^2]/\mathbb{E}[(U - M_k)^2]$  for the four methods as a function of  $k$ .

(i) Define

$$u_{\text{var}} = \arg \min_{u \in I} (\mathbb{P}(U \in [a, u])\text{Var}(U \mid U \in [a, u]) + \mathbb{P}(U \in [u, b])\text{Var}(U \mid U \in [u, b])). \quad (34)$$

If the minimizer is not unique, we pick the largest minimizer. The *variance* splitting rule (corresponding to the VarianceSplit algorithm in Section 2.1) splits  $I$  into the two sets  $[a, u_{\text{var}})$  and  $[u_{\text{var}}, b)$ .

(ii) Define  $u_{\text{Simons}} = \mathbb{E}[U \mid U \in I]$ . The *Simons* splitting rule splits  $I$  into the two sets  $[a, u_{\text{Simons}})$  and  $[u_{\text{Simons}}, b)$ .

(iii) Define

$$u_{\text{minimax}} = \arg \min_{u \in I} \max \{ \mathbb{P}(U \in [a, u])\text{Var}(U \mid U \in [a, u]), \mathbb{P}(U \in [u, b])\text{Var}(U \mid U \in [u, b]) \}.$$

If the minimizer is not unique, we pick the largest minimizer. The *minimax* splitting rule (corresponding to the MinimaxSplit algorithm in Section 2.1) splits  $I$  into the two sets  $[a, u_{\text{minimax}})$  and  $[u_{\text{minimax}}, b)$ .

(iv) Define

$$u_{\text{median}} = \sup\{u \in I : \mathbb{P}(a \leq U < u) = \mathbb{P}(u \leq U < b)\}.$$

The *median* splitting rule splits  $I$  into two sets  $[a, u_{\text{median}})$  and  $[u_{\text{median}}, b)$ .

In turn, when applying recursively each splitting rule starting from  $\pi_0 = \{\mathbb{R}\}$ , we obtain a nested sequence of partitions  $\Pi = \{\pi_k\}_{k \geq 0}$  depending on the law of  $U$ . We call the resulting  $\Pi$ -based martingale approximation  $\{M_k\}_{k \geq 0} = \{\mathbb{E}[U \mid \sigma(\pi_k)]\}_{k \geq 0}$  the variance (resp. Simons, minimax, median) martingale (with respect to  $U$ ). See Figure 10 for examples of the four martingale approximations and their convergence rates.

**Example 15.** If  $U$  is uniformly distributed on a compact interval, all four martingales coincide. For example, if  $U \stackrel{\text{law}}{\sim} \text{Unif}(0, 1)$ , each of the four martingales from Definition 14 satisfy  $M_k = \mathbb{E}[U \mid \sigma(\pi_k)]$ , where  $\pi_k := \{[j/2^k, (j+1)/2^k] : 0 \leq j < 2^k\}$  and it follows that  $\mathbb{E}[(U - M_k)^2] = 4^{-k}/12$ .

The intuition for the minimax and median martingales is that at each splitting step, we balance the “sizes” of  $U\mathbb{1}_{\{U \in I\}}$  on the two sets. The “size” corresponds to the (unconditional) variance for the minimax

martingale and the total probability for the median martingale. Intending to minimize the MSE  $\mathbb{E}[(U - M_k)^2]$  at each step  $k$ , the variance martingale naturally arises as an algorithm that greedily reduces the remaining risk within  $U$  in each iteration through layers.

Motivated by a martingale embedding problem, [Simons \(1970\)](#) first introduced the Simons martingale and established the a.s. convergence  $M_k \rightarrow U$  (and hence also in  $L^2$ ), but did not analyze the convergence rate. A recent motivation for studying the convergence rate of the Simons martingale arises from the construction of powerful e-values in hypothesis testing ([Ramdas and Wang, 2025](#)). [Zhang et al. \(2024\)](#) (Lemma 5.6) proved that if  $U \in L^{2+\delta}$  for some  $\delta > 0$  and  $\{M_k\}$  is the Simons martingale, then there exist  $C > 0$  and  $r \in (0, 1)$  such that  $\mathbb{E}[(U - M_k)^2] \leq Cr^k$ , and  $r < 0.827$  is feasible if  $U$  is bounded. Our Theorem 16(ii) improves the rate to  $r = 1/2$  and hence provides a tighter theoretical bound. We also show by example that the rate  $r = 1/2$  is optimal.

The terminology *martingale approximation* has been used extensively in the probability literature with different meanings. In [Rüschendorf \(1985\)](#), it refers to the best approximation of a random vector by a (single) martingale based on ideas from optimal transport. In [Borovskikh and Korolyuk \(1997\)](#) and [Hall and Heyde \(2014\)](#), it refers to techniques from martingale theory (such as inequalities and CLT rates) with various applications in statistics. Similar techniques are also used in the study of stationary ergodic sequences ([Wu and Woodroffe, 2004](#); [Zhao and Woodroffe, 2008](#)) and Markovian walks ([Gramma et al., 2018](#)). Note that in our setting,  $Y$  is a sum of martingale differences, but whose variance is bounded, and hence one cannot apply the martingale CLT or its convergence rates.

In the next two sections, we discuss two types of results: *uniform* rates for bounded  $U$  (Appendix A.2) and *non-uniform* rates (Appendix A.3) where the asymptotic constant may depend on the possibly unbounded law of  $U$ .

## A.2 Uniform convergence rates

**Theorem 16.** *Let  $U$  be a  $[0, 1]$ -valued atomless random variable. The following statements hold.*

- (i) *If  $\{M_k\}_{k \geq 0}$  is the variance martingale,  $\mathbb{E}[(U - M_k)^2] \leq 2.71 \cdot 2^{-2k/3}$ .*
- (ii) *If  $\{M_k\}_{k \geq 0}$  is the Simons martingale,  $\mathbb{E}[(U - M_k)^2] \leq 2^{1-k}$ .*
- (iii) *If  $\{M_k\}_{k \geq 0}$  is the minimax martingale,  $\mathbb{E}[(U - M_k)^2] \leq 0.4 \cdot 2^{-2k/3}$ .*
- (iv) *If  $\{M_k\}_{k \geq 0}$  is the median martingale,  $\mathbb{E}[(U - M_k)^2] \leq 2^{-k}$ .*

The proof of Theorem 16 is lengthy and technical, which we defer to Appendix A.4.

The general case of a bounded  $U$  can be derived by a scaling argument, since the constructions in Definition 14 are scale-invariant. Finding the *optimal* rate  $r \in (0, 1)$  (where  $\mathbb{E}[(U - M_k)^2] \leq Lr^k$  for some universal constant  $L$ ) is also an intriguing question. Observe that one cannot have  $r < 1/4$  by Example 15 above. In Examples 17 and 18 below, we show that the rate  $r$  in Theorem 16 is indeed optimal for the Simons and median martingales.

**Example 17** (Rate  $r = 1/2$  is optimal for the Simons martingale). Fix an arbitrary  $s \in (1/2, 1)$  and let  $U$  satisfy  $\mathbb{P}(U = -1) = 1 - s$  and for  $J \geq 0$ ,

$$\mathbb{P}\left(U = \sum_{j=1}^J \left(\frac{1-s}{s}\right)^j\right) = s^{J+1}(1-s).$$

It follows that  $U$  is a bounded random variable. Next, we compute that

$$\begin{aligned}
\mathbb{E}\left[U \mid U \geq \sum_{j=1}^J \left(\frac{1-s}{s}\right)^j\right] &= \left(\sum_{\ell=J}^{\infty} s^{\ell+1}(1-s)\right)^{-1} \sum_{\ell=J}^{\infty} s^{\ell+1}(1-s) \sum_{j=1}^{\ell} \left(\frac{1-s}{s}\right)^j \\
&= s^{-(J+1)} \sum_{\ell=J}^{\infty} s^{\ell+1}(2s-1) \left(1 + \left(\frac{1-s}{s}\right)^{\ell}\right) \\
&= \frac{s^{-(J+1)}(2s-1)s^{J+1}}{1-s} + \frac{s^{-(J+1)}(2s-1)s}{1-(1-s)} \\
&= \sum_{j=1}^{J+1} \left(\frac{1-s}{s}\right)^j.
\end{aligned}$$

It is then straightforward to verify that in the Simons martingale  $\{M_k\}_{k \geq 0}$ , each  $M_{k+1} - M_k$  is supported on the set  $\{0, -((1-s)/s)^k, ((1-s)/s)^{k+1}\}$ , where  $\mathbb{P}(M_{k+1} - M_k = -((1-s)/s)^k) = (1-s)s^k$  and  $\mathbb{P}(M_{k+1} - M_k = ((1-s)/s)^{k+1}) = s^{k+1}$ . It follows that

$$\mathbb{E}[(M_{k+1} - M_k)^2] = (1-s)^{2k+1}s^{-(k+1)} \asymp \left(\frac{(1-s)^2}{s}\right)^k.$$

In other words, the rate  $r$  is given by  $r = (1-s)^2/s$ . If  $s$  is picked close to  $1/2$ ,  $r$  can be made close enough to  $1/2$ . Therefore,  $r = 1/2$  is the optimal rate parameter. This example is illustrated with an atomic distribution  $U$ , but a slight twist also leads to an example for an absolutely continuous law  $U$ .

**Example 18** (Rate  $r = 1/2$  is optimal for the median martingale). Let  $s \in (0, 1)$  and a bounded random variable  $U$  satisfy

$$\mathbb{P}\left(U = \sum_{j=1}^{k-1} s^{j-1} - s^{k-1}\right) = 2^{-k}, \quad k \geq 1.$$

Next, we compute that

$$\begin{aligned}
\mathbb{E}\left[U \mid U \geq \sum_{j=1}^k s^{j-1} - s^k\right] &= 2^k \sum_{\ell=k+1}^{\infty} 2^{-\ell} \left(\sum_{j=1}^{\ell-1} s^{j-1} - s^{\ell-1}\right) \\
&= 2^k \sum_{\ell=k+1}^{\infty} 2^{-\ell} \left(\frac{1}{1-s} - \frac{s^{\ell-1}(2-s)}{1-s}\right) \\
&= \frac{1}{1-s} - \frac{2-s}{s(1-s)} \frac{s^{k+1}/2}{1-s/2} \\
&= \sum_{j=1}^k s^{j-1}.
\end{aligned}$$

Note also that

$$\sum_{j=1}^k s^{j-1} - s^k < \sum_{j=1}^k s^{j-1} < \sum_{j=1}^{k+1} s^{j-1} - s^{k+1}.$$

It is then straightforward to verify that the law of  $M_{k+1} - M_k$  is supported on  $\{0, \pm s^k\}$  with  $\mathbb{P}(M_{k+1} - M_k =$

$s^k) = \mathbb{P}(M_{k+1} - M_k = -s^k) = 2^{-(k+1)}$ . We then obtain that

$$\mathbb{E}[(M_{k+1} - M_k)^2] = 2^{-k} s^{2k}.$$

In other words, the rate  $r = s^2/2$  has a limit  $1/2$  as  $s \rightarrow 1$  from below; hence, the optimal rate is  $1/2$ . Again, a simple twist yields similar examples, where the law of  $U$  is absolutely continuous.

### A.3 Non-uniform convergence rates

The above Theorem 16 requires that the support of  $U$  is bounded and the asymptotic constant depends only on  $\sup \text{supp } U - \inf \text{supp } U$ . We show in the next result that, without the bounded range assumption, non-uniform convergence rates can still be guaranteed.

**Theorem 19.** *Let  $U$  be an atomless random variable with a finite  $(2 + \varepsilon)$ -th moment for some  $\varepsilon > 0$ , and  $\{M_k\}_{k \geq 0}$  be one of the four partition-based martingale approximations given by Definition 14. Then there exists a constant  $r \in (0, 1)$  depending only on  $\varepsilon$  and another constant  $C > 0$  depending on the law of  $U$ , such that*

$$\mathbb{E}[(U - M_k)^2] \leq C r^k.$$

In particular,  $M_k \rightarrow U$  both a.s. and in  $L^2$ .

*Proof.* Let  $\text{supp } M_1 = \{x, y\}$  where  $x < y$ . Take  $M > \sup\{x, y\}$ . Let  $\tau_M^+$  be the first hitting time to  $\{x : x \geq M\}$ ,  $\tau_M^-$  be the first hitting time to  $\{x : x \leq -M\}$ , and  $\tau_M = \min\{\tau_M^+, \tau_M^-\}$ . It is straightforward to prove (see the proof of Lemma 5.6 of [Zhang et al. \(2024\)](#)) that for some  $r \in (0, 1)$  and  $C > 0$ ,

$$\mathbb{E}[(U - M_k)^2] \leq \mathbb{E}[\mathbb{1}_{\{\tau_M < \infty\}} U^2] + C M^2 r^k.$$

Since the supports of  $\{M_k\}_{k \geq 0}$  correspond to the means of  $U$  conditioned on nested partitions of  $\mathbb{R}$ , we have  $\tau_M^+ < \infty$  implies  $M_k \geq x$  for all  $k \geq 0$  and  $M_1 = y$ . Therefore, conditional on the event  $\tau_M^+ < \infty$ ,  $X$  is a martingale that is bounded from below by  $x$ . By Ville's inequality,

$$\begin{aligned} \mathbb{P}(\tau_M^+ < \infty) &\leq \mathbb{P}(\tau_M^+ < \infty \mid M_1 > x) \\ &= \mathbb{P}\left(\sup_{k \geq 0} M_k \geq M \mid M_1 > x\right) \leq \frac{\mathbb{E}[U \mid M_1 > x] - x}{M - x} = O(M^{-1}). \end{aligned}$$

Similarly, the same analysis holds for  $\tau_M^-$ . Hence, we conclude that  $\mathbb{P}(\tau_M < \infty) = O(M^{-1})$ . The rest follows line by line as in [Zhang et al. \(2024\)](#), which we sketch for completeness. By Hölder's inequality,  $\mathbb{E}[\mathbb{1}_{\{\tau_M < \infty\}} U^2] = O(M^{-\delta'})$  for some  $\delta' > 0$  depending only on  $\varepsilon$ . With the choices  $M = r^{-k/(2+\delta')}$  and  $q = r^{\delta'/(2+\delta')} \in (0, 1)$ , we have that for some  $C > 0$ ,

$$\mathbb{E}[(U - M_k)^2] \leq C(M^{-\delta'} + M^2 r^k) \leq C q^{-k}.$$

The final statement follows immediately from the martingale convergence theorem.  $\square$

If  $U$  is bounded, Theorem 19 is a special case of Theorem 16. The case of the Simons martingale has been established by [Zhang et al. \(2024\)](#), and our proof of Theorem 19 follows a similar route. Since the

asymptotic constant is allowed to depend on the law of  $U$ , the optimal non-uniform rate  $r$  might be smaller than the uniform ones (in Theorem 16).

Recall from Appendix A.2 that the rates obtained in Theorem 16 are asymptotically optimal for the Simons and median martingales (see Examples 17 and 18). For the variance and minimax martingales, we show in the next result that the rate  $r = 1/4$  is optimal under certain regularity conditions on the law of  $U$ .

**Theorem 20.** *Let  $\{M_k\}_{k \geq 0}$  be either the minimax or variance martingale converging to  $U$ . Suppose that  $U$  is bounded and has a bounded and continuous density  $f$  with  $\inf f > 0$  on  $\text{supp } U$ , which we assume is a connected interval. Then for any  $r > 1/4$ , there exists a constant  $C > 0$  (depending on  $r$  and the law of  $U$ ) such that*

$$\mathbb{E}[|U - M_k|^2] \leq Cr^k.$$

*Proof.* First, we claim that the split points for the nested partitions  $\{\pi_k\}$  are dense. Indeed, for both martingales, we have shown that the variances on each component in the partition  $\pi_k$  go to zero uniformly as  $k \rightarrow \infty$ . If the split points were not dense, some element in the partition would cover an interval of positive length, on which the variance of  $U$  cannot vanish since we assumed  $\inf f > 0$  and  $\sup f < \infty$ . Therefore, for any  $\varepsilon > 0$ , there exists  $k$  such that the  $k$ -th partition  $\pi_k$  is such that on each interval  $A \in \pi_k$ ,  $\sup_A f \leq (1 + \varepsilon) \inf_A f$ .

Since one-step variance is always better than one-step minimax, it remains to show that for an interval  $A$  with  $\sup_A f \leq (1 + \varepsilon) \inf_A f$ , there exists  $C(\varepsilon) \downarrow 1/4$  as  $\varepsilon > 0$  such that at each step the total variance reduces by a factor of  $C(\varepsilon)$  for the minimax martingale.

To see this, without loss of generality we start from  $U$  supported on  $[0, 1]$  (meaning that  $\mathbb{P}(U \in [0, 1]) = 1$ ) whose density takes values in  $[1, 1 + \varepsilon]$  (we may normalize afterwards to a probability measure, which we omit). Then for any interval  $[a, b] \subseteq [0, 1]$ ,

$$\mathbb{E}[U \mid U \in [a, b]] \in \left[ a + \frac{1}{2 + \varepsilon}(b - a), a + \frac{1 + \varepsilon}{2 + \varepsilon}(b - a) \right].$$

Therefore,

$$\begin{aligned} \mathbb{P}(U \in [a, b]) \text{Var}(U \mid U \in [a, b]) &\leq \sup_{m \in [a + \frac{1}{2 + \varepsilon}(b - a), a + \frac{1 + \varepsilon}{2 + \varepsilon}(b - a)]} \int_a^b (1 + \varepsilon)(x - m)^2 dx \\ &\leq \frac{2(1 + \varepsilon)^4}{3(2 + \varepsilon)^3} (b - a)^3. \end{aligned}$$

Similarly,

$$\mathbb{P}(U \in [a, b]) \text{Var}(U \mid U \in [a, b]) \geq \inf_{m \in [a + \frac{1}{2 + \varepsilon}(b - a), a + \frac{1 + \varepsilon}{2 + \varepsilon}(b - a)]} \int_a^b (x - m)^2 dx \geq \frac{1}{12} (b - a)^3.$$

It follows that the split point  $x_* \in [0, 1]$  must satisfy

$$\frac{1}{12} x_*^3 \leq \frac{2(1 + \varepsilon)^4}{3(2 + \varepsilon)^3} (1 - x_*)^3 \quad \text{and} \quad \frac{1}{12} (1 - x_*)^3 \geq \frac{2(1 + \varepsilon)^4}{3(2 + \varepsilon)^3} x_*^3.$$

Therefore, for some  $a_\varepsilon \rightarrow 0$ ,  $|x_* - 1/2| \leq a_\varepsilon$ .

A direct computation yields  $\text{Var}(U) \geq \frac{1}{12}$ . The total remaining variance  $\mathbb{E}[(U - M_1)^2]$  is bounded by

$$\mathbb{E}[(U - M_1)^2] \leq \frac{2(1 + \varepsilon)^4}{3(2 + \varepsilon)^3} (x_*^3 + (1 - x_*)^3) \leq \frac{4(1 + \varepsilon)^4}{3(2 + \varepsilon)^3} \left(\frac{1}{2} + a_\varepsilon\right)^3.$$

Hence, as  $\varepsilon \rightarrow 0$ , the ratio becomes

$$\frac{\mathbb{E}[(U - M_1)^2]}{\text{Var}(U)} \leq \frac{2(1 + \varepsilon)^4}{(2 + \varepsilon)^3} (1 + 2a_\varepsilon)^3 \rightarrow \frac{1}{4},$$

as desired.  $\square$

In other words, under the assumptions in Theorem 20, the MSE has an asymptotic convergence rate of “ $1/4 + \varepsilon$ ”. Unfortunately, we are unable to remove the assumptions for the density of  $U$  in Theorem 20 nor give counterexamples. We conjecture that the same conclusion of Theorem 20 holds without those assumptions.

## A.4 Proof of Theorem 16

### Variance

**Lemma A.1.** *Let  $U$  be an atomless random variable supported on  $I = [a, b]$ . Then there exists*

$$u_* \in \arg \min_{u \in I} (\mathbb{P}(U \in [a, u]) \text{Var}(U \mid U \in [a, u]) + \mathbb{P}(U \in [u, b]) \text{Var}(U \mid U \in [u, b]))$$

such that

$$2u_* = \mathbb{E}[U \mid U \leq u_*] + \mathbb{E}[U \mid U > u_*] \tag{35}$$

and moreover, splitting at  $u_*$  and at  $u_{\text{var}}$  defined through (34) have the same effect,<sup>9</sup> i.e.,  $\mathbb{P}(U \leq u_*) = \mathbb{P}(U \leq u_{\text{var}})$ .

*Proof.* Let  $Q$  be the quantile function of  $U$ . Since  $U$  is atomless, we have if  $u = Q(p)$ ,

$$\begin{aligned} & \mathbb{P}(U \in [a, u]) \text{Var}(U \mid U \in [a, u]) + \mathbb{P}(U \in [u, b]) \text{Var}(U \mid U \in [u, b]) \\ &= p \text{Var}(U \mid U \in [a, Q(p)]) + (1 - p) \text{Var}(U \mid U \in [Q(p), b]). \end{aligned}$$

Let  $u_{\text{var}}$  be defined through (34) and  $p_{\text{var}} = \mathbb{P}(U \leq u_{\text{var}})$ . Then with the short-hand notation  $m_a(p) = \mathbb{E}[U \mid U \in [a, Q(p)]]$  and  $m_b(p) = \mathbb{E}[U \mid U \in [Q(p), b]]$ , we have

$$\begin{aligned} p_{\text{var}} & \in \arg \min_{p \in [0, 1]} (p \text{Var}(U \mid U \in [a, Q(p)]) + (1 - p) \text{Var}(U \mid U \in [Q(p), b])) \\ &= \arg \max_{p \in [0, 1]} (p m_a(p)^2 + (1 - p) m_b(p)^2) =: \arg \max_{p \in [0, 1]} \Psi_U(p). \end{aligned}$$

Observe that for  $p \in (0, 1)$ ,

$$\frac{d}{dp} m_a(p) = \frac{Q(p) - m_a(p)}{p} \quad \text{and} \quad \frac{d}{dp} m_b(p) = \frac{m_b(p) - Q(p)}{1 - p}.$$

<sup>9</sup>Recall that we break ties in (34) by choosing the largest minimizer.

We then have

$$\begin{aligned}\frac{d}{dp}\Psi_U(p) &= m_a(p)^2 + 2m_a(p)(Q(p) - m_a(p)) - m_b(p)^2 + 2m_b(p)(m_b(p) - Q(p)) \\ &= (m_b(p) - m_a(p))(m_a(p) + m_b(p) - 2Q(p)).\end{aligned}$$

Since  $U$  is atomless, it is non-degenerate, and hence  $m_b(p_{\text{var}}) - m_a(p_{\text{var}}) > 0$  and  $p_{\text{var}} \in (0, 1)$ . Note that the functions  $m_a, m_b$  are differentiable and hence continuous;  $Q$  may have jumps but have limits on both sides at every point. Since  $p_{\text{var}} \in \arg \max_{p \in [0, 1]} \Psi_U(p)$ , there are two cases:

- $Q$  is continuous at  $p_{\text{var}}$ . Then  $\Psi'_U(p_{\text{var}}) = 0$ , so  $m_a(p_{\text{var}}) + m_b(p_{\text{var}}) = 2Q(p_{\text{var}})$ . In this case, we also have  $Q(p_{\text{var}}) = u_{\text{var}}$ . Therefore, taking  $u_* = u_{\text{var}}$  gives (35).
- $Q$  is discontinuous at  $p_{\text{var}}$ . Then we must have  $\Psi'_U(p_{\text{var}}^-) \geq 0$  and  $\Psi'_U(p_{\text{var}}^+) \leq 0$ , where for a generic function  $f$  defined on  $\mathbb{R}$  we use the notation  $f(x^-) = \lim_{y \rightarrow x^-} f(y)$  and  $f(x^+) = \lim_{y \rightarrow x^+} f(y)$ . Equivalently,

$$2Q(p_{\text{var}}^-) \leq m_a(p_{\text{var}}) + m_b(p_{\text{var}}) \leq 2Q(p_{\text{var}}^+). \quad (36)$$

Let  $u_1 = Q(p_{\text{var}}^-)$  and  $u_2 = Q(p_{\text{var}}^+)$ . Since  $Q$  is discontinuous at  $p_{\text{var}}$ , we have  $\mathbb{P}(u_1 \leq U \leq u_2) = 0$ . Therefore, the map  $u \mapsto \mathbb{P}(U \leq u)$  is constant on  $[u_1, u_2]$  and for each  $u \in [u_1, u_2]$ ,  $(\mathbb{E}[U \mid U \leq u], \mathbb{E}[U \mid U > u]) = (m_a(p_{\text{var}}), m_b(p_{\text{var}}))$ . It follows from (36) that (35) holds for some  $u_* \in [u_1, u_2]$ . Using the definition (34) and  $p_{\text{var}} = \mathbb{P}(U \leq u_{\text{var}})$ , we have  $u_{\text{var}} = \max_{u \in [u_1, u_2]} u = u_2$ , which implies that  $\mathbb{P}(U \leq u_*) = \mathbb{P}(U \leq u_{\text{var}})$ .

Therefore, in both cases, the desired claim is verified.  $\square$

*Remark 21.* If the support of  $U$  is a connected interval, Lemma A.1 is a special case of Theorem 1 of [Ishwaran \(2015\)](#) applied with  $f$  monotone and  $X \stackrel{\text{law}}{\sim} \text{Unif}(0, 1)$ .

*Proof for the variance martingale.* Recall the binary subtree representation (17). Since  $U$  is atomless, the binary subtree is in fact always a binary tree. At level  $k$ ,  $\mathbb{E}[(M_{k-1} - M_k)^2]$  is a sum of  $2^k$  terms, which we may rewrite as  $\sum_j p_j d_j^2$  using a change of variable. This corresponds to the  $2^k$  edges (indexed by  $j \in [2^k]$ ) in the binary tree between levels  $k-1$  and  $k$ , and  $p_j$  represents the probabilities of the edge  $j$  and  $d_j$  is the location difference between the end vertices of the edge, or the *length* of the edge. Our goal is to bound from above

$$\mathbb{E}[(M_{k-1} - M_k)^2] = \sum_{j=1}^{2^k} p_j d_j^2.$$

The key is first to bound the quantity

$$\max_{1 \leq j \leq 2^{k-1}} (p_{2j-1} d_{2j-1}^2 + p_{2j} d_{2j}^2).$$

That is, the variance increases by splitting the  $j$ -th mass at level  $k-1$  (which is the common ancestor of the  $(2j-1)$ -th and  $(2j)$ -th masses). By the martingale property,

$$p_{2j-1} d_{2j-1} = p_{2j} d_{2j}.$$

It follows that

$$p_{2j-1}d_{2j-1}^2 + p_{2j}d_{2j}^2 = (p_{2j-1} + p_{2j})d_{2j-1}d_{2j}. \quad (37)$$

The general strategy to analyze the quantity (37) is to start from an arbitrary mass/node  $\mathbf{M}$  at level  $k-1$ , trace back its ancestors, bound from above the probability of the mass (which is  $p_{2j-1} + p_{2j}$  in the above expression), and establish upper bounds for the length of the edges (which is  $d_{2j-1}, d_{2j}$ ).

The path leading to a mass  $\mathbf{M}$  at level  $k-1$  in the binary tree representation (17) consists of  $k$  nodes:  $\emptyset = \mathbf{N}_0, \mathbf{N}_1, \dots, \mathbf{N}_{k-1} = \mathbf{M}$ , where  $\mathbf{N}_j \in V_j$ . We denote the lengths of the edges connecting the node  $\mathbf{N}_{j-1}$  to its two descendants on level  $j$  by  $a_j, b_j$ ,  $j \in [k-1]$ , where  $b_j = |\ell_{\mathbf{N}_{j-1}} - \ell_{\mathbf{N}_j}|$ . It follows by the martingale property that the mass  $\mathbf{M}$  has probability

$$\prod_{j=1}^{k-1} q_j := \prod_{j=1}^{k-1} \frac{a_j}{a_j + b_j}. \quad (38)$$

The lengths of the edges of  $\mathbf{M}$  are the mean distances of its children, which are bounded by the distances from  $\sum_{j=1}^{k-1} b_j$  (the location of  $\mathbf{M}$ ) to the endpoints of the interval that  $\mathbf{M}$  carries in the splitting process. Therefore, it is natural to update these two distances as we trace the path from the root of the tree down to the node  $\mathbf{M}$ .

Let  $a_0 = b_0 = 1 \geq \sup U - \inf U$ . We consider the following algorithm, which starts from the tuple  $(a_0, b_0, a_1, b_1, q_1)$  and updates it  $k-1$  times for each  $j \in [k-1]$  when we trace the path down to  $\mathbf{M}$ . At step  $j$ , the tuple represents the two pairs  $(a_k, b_k), (a_j, b_j)$  that govern the maximum length of the edges of the  $j$ -th node (that is, the distance from its location to the boundaries of the intervals this node represents) for a certain  $j \in [k-1]$ , as well as the probability weight  $q_j$  multiplied at this step. In a generic setting, suppose that we have  $(a_k, b_k, a_j, b_j, q_j)$  updated at the node  $\mathbf{N}_j \in V_j$ . This means that the edges forming  $a_{k+1}, \dots, a_j$  are all on one side of the path since only the last one of these contributes to the bound. Now when updating the node at level  $j+1$  there are two cases:

- (i)  $a_{j+1}$  and  $a_j$  are on the same side. We update  $(a_k, b_k, a_j, b_j, q_j)$  with  $(a_k, b_k, a_{j+1}, b_{j+1}, q_{j+1})$ , where  $a_{j+1} \leq (a_j + b_j)/2$  and  $b_{j+1} \leq (a_k + b_k)/2$  (they are the two edges) and  $q_{j+1} = a_{j+1}/(a_{j+1} + b_{j+1})$ ;
- (ii)  $a_{j+1}$  and  $a_j$  are on distinct sides. We update  $(a_k, b_k, a_j, b_j, q_j)$  with  $(a_j, b_j, a_{j+1}, b_{j+1}, q_{j+1})$ , where  $b_{j+1} \leq (a_j + b_j)/2$ ,  $a_{j+1} \leq (a_k + b_k)/2$ , and  $q_{j+1} = a_{j+1}/(a_{j+1} + b_{j+1})$ .

Here, we have used (38) and Lemma A.1.

Let  $(a, b, a', b', q)$  be generic entries of the tuple and  $(\hat{a}, \hat{b}, \hat{a}', \hat{b}', \hat{q})$  be the updated tuple, where we recall  $\hat{q} = \hat{a}'/(\hat{a}' + \hat{b}')$ . We claim that

$$\frac{(\hat{a} + \hat{b})(\hat{a}' + \hat{b}')}{(a + b)(a' + b')} \leq \frac{1}{2\hat{q}}. \quad (39)$$

To see this, we separately consider the two cases above.

- In case (i),  $\hat{a} = a$  and  $\hat{b} = b$ , and

$$\hat{a}' + \hat{b}' = a_{j+1} + b_{j+1} = \frac{a_{j+1}}{\hat{q}} \leq \frac{a_j + b_j}{2\hat{q}} = \frac{a' + b'}{2\hat{q}}.$$

- In case (ii),  $\hat{a} = a'$  and  $\hat{b} = b'$ , and

$$\hat{a}' + \hat{b}' = a_{j+1} + b_{j+1} = \frac{a_{j+1}}{\hat{q}} \leq \frac{a_k + b_k}{2\hat{q}} = \frac{a + b}{2\hat{q}}.$$

This proves (39).

Recall that our goal is to bound (37). The probability of the mass at each step is multiplied by  $q$ , and the edge lengths are bounded by  $(a + b)/2$  and  $(a' + b')/2$ . By (39), their product multiplies by at most  $1/2$  each time we update the tuple. We have thus shown that

$$\max_{1 \leq j \leq 2^{k-1}} (p_{2j-1} d_{2j-1}^2 + p_{2j} d_{2j}^2) \leq 2^{1-k}. \quad (40)$$

Observe also that  $\sum_j p_j = 1$  and  $\sum_j d_j \leq \sup U - \inf U \leq 1$  (because the edges at a single level cannot intersect each other since they represent the conditional means of  $U$  in disjoint intervals). By Hölder's inequality,

$$\begin{aligned} \mathbb{E}[(M_{k-1} - M_k)^2] &= \sum_{j=1}^{2^k} p_j d_j^2 \leq \left( \sum_{j=1}^{2^k} p_j d_j^3 \right)^{2/3} \left( \sum_{j=1}^{2^k} p_j \right)^{1/3} \\ &\leq \left( \max_{j \in [2^k]} (p_j d_j^2) \sum_{j=1}^{2^k} d_j \right)^{2/3} \leq \max_{j \in [2^k]} (p_j d_j^2)^{2/3} \leq 2^{-2(k-1)/3}. \end{aligned} \quad (41)$$

By the martingale property, we then have

$$\mathbb{E}[(U - M_k)^2] = \sum_{j=k}^{\infty} \mathbb{E}[(M_j - M_{j+1})^2] \leq \sum_{j=k}^{\infty} 2^{-2j/3} \leq \frac{2^{-2k/3}}{1 - 2^{-2/3}} \leq 2.71 \cdot 2^{-2k/3},$$

as desired.  $\square$

## Simons

*Proof for the Simons martingale.* It is noted in [Zhang et al. \(2024\)](#) that the Simons martingale satisfies the separated tree condition (i.e., the branches of the tree representation from all different levels, when projected onto the real line as intervals, are either disjoint or have a containment relationship), which is a consequence of the construction. We follow a similar argument to the variance martingale. Consider a node  $\mathbf{M}$  at level  $k-1$  and a path  $(\emptyset = \mathbf{N}_0, \dots, \mathbf{N}_{k-1} = \mathbf{M})$  leading to  $\mathbf{M}$ , where  $\emptyset$  denotes the root of a binary tree. We provide an algorithm that recursively defines the tuples  $(A_j, B_j, q_j)$ ,  $0 \leq j \leq k-1$  for each node  $\mathbf{N}_j$ ,  $0 \leq j \leq k-1$  on that path, from the root to  $\mathbf{M}$ . The quantities  $A_j$  and  $B_j$  represent the maximum possible lengths of the two edges emanating from a node  $\mathbf{N}_j$ , and  $q$  represents the one-step splitting probability leading to  $\mathbf{N}_j$ , based on the constraints from the separated tree property.

We start from  $(A_1, B_1, q_1) = (1, 1, 1)$ . Again, denote the lengths of the edges connecting the node  $\mathbf{N}_{j-1}$  to its two descendants at level  $j$  by  $a_j, b_j$ ,  $j \in [k-1]$ , where  $b_j = |\ell_{\mathbf{N}_{j-1}} - \ell_{\mathbf{N}_j}|$ . Consider the node  $\mathbf{N}_j$  at level  $j$ . Then  $(A_j, B_j, q_j)$  must be of the form (while not distinguishing the order of  $A_j$  and  $B_j$ )

$$(A_j, B_j, q_j) = \left( b_i - \sum_{\ell=i+1}^j b_{\ell}, b_j, \frac{a_j}{a_j + b_j} \right)$$

for some  $i \leq j-1$ . This happens when the edges  $a_{i+1}, \dots, a_j$  lie on the same side of the path  $(\mathbf{N}_1, \dots, \mathbf{N}_k)$ . For the descendant  $\mathbf{N}_{j+1}$  of  $\mathbf{N}_j$ , there are two possibilities:

(i) if  $a_{j+1}$  is on the same side of the path as  $a_j$ , we define

$$(A_{j+1}, B_{j+1}, q_{j+1}) = \left( b_i - \sum_{\ell=i+1}^{j+1} b_\ell, b_{j+1}, \frac{a_{j+1}}{a_{j+1} + b_{j+1}} \right),$$

where  $a_{j+1} \leq b_j$ ;

(ii) otherwise, we define

$$(A_{j+1}, B_{j+1}, q_{j+1}) = \left( b_j - b_{j+1}, b_{j+1}, \frac{a_{j+1}}{a_{j+1} + b_{j+1}} \right),$$

where  $a_{j+1} \leq b_i - \sum_{\ell=i+1}^j b_\ell$ .

The choice of  $(A_{j+1}, B_{j+1}, q_{j+1})$  is justified by the separated tree property.

Let  $q_{j+1} = a_{j+1}/(a_{j+1} + b_{j+1})$ . We next express the ratio  $A_{j+1}B_{j+1}/(A_jB_j)$  after the update in step  $j+1$  using  $q_{j+1}$ . We have in case (i) that

$$\frac{\left( b_i - \sum_{\ell=i+1}^{j+1} b_\ell \right) b_{j+1}}{\left( b_i - \sum_{\ell=i+1}^j b_\ell \right) b_j} \leq \frac{b_{j+1}}{b_j} \leq \frac{b_{j+1}}{a_{j+1}} = \frac{1}{q_{j+1}} - 1,$$

and in case (ii),

$$\frac{(b_j - b_{j+1}) b_{j+1}}{\left( b_i - \sum_{\ell=i+1}^j b_\ell \right) b_j} \leq \frac{b_{j+1}}{b_i - \sum_{\ell=i+1}^j b_\ell} \leq \frac{b_{j+1}}{a_{j+1}} = \frac{1}{q_{j+1}} - 1.$$

In both cases,  $A_{j+1}B_{j+1}/(A_jB_j) \leq 1/q_{j+1} - 1$ . In other words, the contribution of the two edges of  $\mathbf{M}$  is upper bounded by

$$A_k B_k \prod_{\ell=1}^{k-1} q_\ell = \prod_{\ell=1}^{k-1} \frac{A_\ell B_\ell}{A_{\ell-1} B_{\ell-1}} \prod_{\ell=1}^{k-1} q_\ell \leq \prod_{\ell=1}^{k-1} \left( \frac{1}{q_\ell} - 1 \right) q_\ell = \prod_{\ell=1}^{k-1} (1 - q_\ell),$$

where we recall that  $\{q_\ell\}_{1 \leq \ell \leq k-1}$  are the one-step probabilities leading to  $\mathbf{M}$ . On the other hand, we also know that the probability that an edge of  $\mathbf{M}$  carries must be bounded by  $\prod_{\ell=1}^{k-1} q_\ell$ . Therefore, we conclude that, with the decomposition

$$\mathbb{E}[(M_{k-1} - M_k)^2] = \sum_{j=1}^{2^k} p_j d_j^2,$$

it holds that for each  $j \in [2^k]$ , there exist  $\{q_\ell\}_{1 \leq \ell \leq k-1}$  such that

$$p_j d_j^2 \leq \prod_{\ell=1}^{k-1} (1 - q_\ell) \quad \text{and} \quad p_j \leq \prod_{\ell=1}^{k-1} q_\ell.$$

Multiplying the two inequalities leads to

$$p_j d_j \leq \sqrt{\prod_{\ell=1}^{k-1} q_\ell (1-q_\ell)} \leq 2^{1-k}.$$

Since this holds uniformly in  $j$ , we conclude that

$$\mathbb{E}[(M_{k-1} - M_k)^2] = \sum_{j=1}^{2^k} p_j d_j^2 \leq \max_{j \in [2^k]} (p_j d_j) \sum_{j=1}^{2^k} d_j \leq 2^{1-k}.$$

By the martingale property,

$$\mathbb{E}[(M_k - U)^2] = \sum_{j=k}^{\infty} \mathbb{E}[(M_j - M_{j+1})^2] \leq \sum_{j=k}^{\infty} 2^{-j} \leq 2^{1-k}.$$

This completes the proof.  $\square$

### Minimax

*Proof for the minimax martingale.* At level  $k$ , there are  $2^k$  vertices (denoted by  $j \in [2^k]$ ) in the binary tree representation of the partition-based martingale approximation. Denote the probabilities of the vertices by  $p_j$  (which correspond to  $\mathbb{P}(U \in A_j)$ ,  $A_j \in \pi_k$ ) and the locations by  $\ell_j$ . It follows that

$$\mathbb{E}[(U - M_k)^2] = \sum_{j=1}^{2^k} p_j \mathbb{E}[(U - \ell_j)^2 \mid U \in A_j] =: \sum_{j=1}^{2^k} p_j d_j^2.$$

Note that  $\sum_j p_j = 1$  and  $\sum_j d_j \leq \sup U - \inf U \leq 1$ . It follows analogously as the Hölder's inequality argument in (41) that

$$\mathbb{E}[(U - M_k)^2] \leq \max_{j \in [2^k]} (p_j d_j^2)^{2/3}.$$

Let  $\phi(u) = \mathbb{P}(U < u) \text{Var}(U \mid U < u)$  and  $\psi(u) = \mathbb{P}(U \geq u) \text{Var}(U \mid U \geq u)$ . Note that  $\phi$  is increasing and  $\psi$  is decreasing in  $u$ , and both functions are continuous if we assume that  $U$  is atomless. Recall by the minimax property that at each step we pick  $u \in \mathbb{R}$  such that  $\max\{\phi(u), \psi(u)\}$  is minimized. This means that  $\phi(u) = \psi(u)$ . Since  $\text{Var}(U) \geq \phi(u) + \psi(u)$ , we have both  $\phi(u) \leq \text{Var}(U)/2$  and  $\psi(u) \leq \text{Var}(U)/2$ . Inductively, we have for any  $k$ ,  $\max(p_j d_j^2) \leq 2^{-k} \text{Var}(U) \leq 2^{-2-k}$ . Combining the above, we arrive at

$$\mathbb{E}[(U - M_k)^2] \leq \max_{j \in [2^k]} (p_j d_j^2)^{2/3} \leq 2^{-4/3} 2^{-2k/3} \leq 0.4 \cdot 2^{-2k/3},$$

as desired.  $\square$

### Median

*Proof for the median martingale.* In the same setting as in the minimax case, we write

$$\mathbb{E}[(U - M_k)^2] = \sum_{j=1}^{2^k} p_j d_j^2,$$

where  $\sum_j p_j = 1$  and  $\sum_j d_j \leq 1$ . We further know that  $\max_j p_j = 2^{-k}$  by the median splitting construction. Therefore,

$$\mathbb{E}[(U - M_k)^2] = \sum_{j=1}^{2^k} p_j d_j^2 \leq 2^{-k} \sum_{j=1}^{2^k} d_j^2 \leq 2^{-k},$$

as desired.  $\square$

## B Proofs of main results

### B.1 Proofs of results in Section 2

*Proof of Lemma 2.1.* We take arbitrary  $a < b$  and define events  $E = E_1 \cup E_2$ , where  $E_1 = \{\mathbf{X} \in A, X_j < a\}$  and  $E_2 = E \setminus E_1 = \{\mathbf{X} \in A, a \leq X_j < b\}$ . By the total variance formula,

$$\begin{aligned} \text{Var}(Y \mid E) &= \mathbb{E}[\text{Var}(Y \mid \sigma(E_1, E_2)) \mid E] + \text{Var}(\mathbb{E}[Y \mid \sigma(E_1, E_2)] \mid E) \\ &\geq \mathbb{E}[\text{Var}(Y \mid \sigma(E_1, E_2)) \mid E] \geq \mathbb{P}(E_1 \mid E) \text{Var}(Y \mid E_1). \end{aligned} \tag{42}$$

Observe that  $\text{Var}(Y \mid E) = \text{Var}(Y \mid \mathbf{X} \in A, X_j < b)$  and  $\text{Var}(Y \mid E_1) = \text{Var}(Y \mid \mathbf{X} \in A, X_j < a)$ . Inserting these two expressions back into (42), we obtain

$$\text{Var}(Y \mid \mathbf{X} \in A, X_j < b) \geq \frac{\mathbb{P}(\mathbf{X} \in A, X_j < a)}{\mathbb{P}(\mathbf{X} \in A, X_j < b)} \text{Var}(Y \mid \mathbf{X} \in A, X_j < a).$$

Rearranging gives

$$\mathbb{P}(\mathbf{X} \in A, X_j < a) \text{Var}(Y \mid \mathbf{X} \in A, X_j < a) \leq \mathbb{P}(\mathbf{X} \in A, X_j < b) \text{Var}(Y \mid \mathbf{X} \in A, X_j < b)$$

and therefore  $\varphi_L$  is non-decreasing; and similarly  $\varphi_R$  is non-increasing. The continuity of  $\varphi_L$  and  $\varphi_R$  follows from the marginally atomless condition.  $\square$

We also need the following risk decomposition lemma.

**Lemma B.1.** *Let  $\delta > 0$ . Then for any joint distribution  $(X, Y)$  with  $X \geq \mathbb{E}[Y]$ , it holds that*

$$\text{Var}(Y) \leq (1 + \delta) \mathbb{E}[(X - Y)^2] + \frac{(1 + \delta)^3}{\delta^3} (\sup \text{supp } X - \inf \text{supp } X)^2. \tag{43}$$

*Proof.* Let  $C = (1 + \delta)^3 / \delta^3$ . Without loss of generality, we assume that  $\mathbb{E}[Y] = 0$ . Equivalent to (43) is

$$(1 + \delta) \mathbb{E}[X^2] - 2(1 + \delta) \mathbb{E}[XY] + \delta \mathbb{E}[Y^2] + C(\sup \text{supp } X - \inf \text{supp } X)^2 \geq 0.$$

After completing the square, it remains to show

$$\mathbb{E}\left[(\sqrt{\delta}Y - \frac{1+\delta}{\sqrt{\delta}}X)^2\right] + \left(C(\sup \text{supp } X - \inf \text{supp } X)^2 - \frac{1+\delta}{\delta}\mathbb{E}[X^2]\right) \geq 0. \quad (44)$$

If  $\inf \text{supp } X = 0$  or  $\sup \text{supp } X / \inf \text{supp } X \geq (1 - \sqrt{(1+\delta)/(C\delta)})^{-1}$ , the second term is always non-negative and hence (44) holds. Otherwise, since  $C = (1+\delta)^3/\delta^3$ ,

$$(1+\delta)(\inf \text{supp } X)^2 \geq (1+\delta)(1 - \sqrt{(1+\delta)/(C\delta)})(\sup \text{supp } X)^2 = (\sup \text{supp } X)^2.$$

It follows that

$$\begin{aligned} \mathbb{E}\left[(\sqrt{\delta}Y - \frac{1+\delta}{\sqrt{\delta}}X)^2\right] &\geq \mathbb{E}\left[\sqrt{\delta}Y - \frac{1+\delta}{\sqrt{\delta}}X\right]^2 \\ &= \frac{(1+\delta)^2}{\delta}\mathbb{E}[X]^2 \geq \frac{(1+\delta)^2}{\delta}(\inf \text{supp } X)^2 \geq \frac{(1+\delta)}{\delta}(\sup \text{supp } X)^2 \geq \frac{1+\delta}{\delta}\mathbb{E}[X^2]. \end{aligned}$$

This shows (44) and thus proves (43).  $\square$

*Proof of Theorem 2.* We divide the proof into three steps.

**Step I: reducing to an inequality involving  $\text{Var}(Y)$ .** We claim that it suffices to prove

$$\mathbb{E}[(Y - M_k)^2] \leq \inf_{g \in \mathcal{G}} \left( (1+\delta)\mathbb{E}[(Y - g(\mathbf{X}))^2] + (1+\delta^{-1})2^{-2\lfloor k/d \rfloor/3}(\|g\|_{\text{TV}} \text{Var}(Y))^{2/3} \right). \quad (45)$$

To this end, we need an upper bound of  $\text{Var}(Y)$ . Fix  $g \in \mathcal{G}$  and let  $g_* := (\sup g + \inf g)/2$ . By Minkowski's inequality,

$$\begin{aligned} \text{Var}(Y)^{1/2} &= \min_{y \in \mathbb{R}} \mathbb{E}[(Y - y)^2]^{1/2} \leq \mathbb{E}[(Y - g_*)^2]^{1/2} \leq \mathbb{E}[(Y - g(\mathbf{X}))^2]^{1/2} + \mathbb{E}[(g(\mathbf{X}) - g_*)^2]^{1/2} \\ &\leq \mathbb{E}[(Y - g(\mathbf{X}))^2]^{1/2} + \frac{1}{2}\|g\|_{\text{TV}}. \end{aligned} \quad (46)$$

Squaring both sides yields that for any  $\delta > 0$ ,

$$\text{Var}(Y) \leq (1+\delta)\mathbb{E}[(Y - g(\mathbf{X}))^2] + \frac{1+\delta^{-1}}{4}\|g\|_{\text{TV}}^2,$$

where we have used  $(a+b)^2 \leq (1+\delta)a^2 + (1+\delta^{-1})b^2$ . It follows that

$$\begin{aligned} \|g\|_{\text{TV}}^{2/3} \text{Var}(Y)^{2/3} &\leq \|g\|_{\text{TV}}^{2/3} \left( (1+\delta)^{2/3}\mathbb{E}[(Y - g(\mathbf{X}))^2]^{2/3} + \left(\frac{1+\delta^{-1}}{4}\right)^{2/3}\|g\|_{\text{TV}}^{4/3} \right) \\ &\leq \frac{2(1+\delta)}{3}\mathbb{E}[(Y - g(\mathbf{X}))^2] + \left(\frac{1}{3} + \left(\frac{1+\delta^{-1}}{4}\right)^{2/3}\right)\|g\|_{\text{TV}}^2, \end{aligned} \quad (47)$$

where we have used the inequality  $x^{1/3}y^{2/3} \leq x/3 + 2y/3$ , which follows from the concavity of logarithm and Jensen's inequality. Inserting (47) into (45) yields (13).

**Step II: decomposition of the risk.** It remains to establish (45). Denote by  $\pi_k = \{I_j\}_{j \in J_k}$  the partition of  $\mathbb{R}^d$  formed at level  $k$  by the cyclic minimax construction. Note that by construction,  $\#J_k \leq 2^k$  and  $M_k | \mathbf{X} \in I_j$  is a piecewise constant random variable, which takes a constant value  $y_{k,j}$  inside the box  $I_j$ , so  $M_k \mathbb{1}_{\{\mathbf{X} \in I_j\}} = y_{k,j} \mathbb{1}_{\{\mathbf{X} \in I_j\}}$ . By definition,  $y_{k,j} = \mathbb{E}[Y | \mathbf{X} \in I_j]$ . Define  $g_j = g|_{I_j}$ , so that  $\|g\|_{\text{TV}} = \sum_j \|g_j\|_{\text{TV}}$ . Define  $\text{Ran}(g_j) = [\inf g_j, \sup g_j]$  and recall that  $\Delta g_j = \sup g_j - \inf g_j \leq \|g_j\|_{\text{TV}}$ .

The key step is to decompose the local mean squared error  $\mathbb{E}[(Y - M_k)^2 \mathbb{1}_{\{\mathbf{X} \in I_j\}}]$  into two parts for each  $j$ , with the help of Lemma B.1. Next, we claim that

$$\mathbb{E}[(Y - M_k)^2 \mathbb{1}_{\{\mathbf{X} \in I_j\}}] = \mathbb{E}[(Y - y_{k,j})^2 \mathbb{1}_{\{\mathbf{X} \in I_j\}}] \leq U_j + V_j, \quad (48)$$

where  $U_j, V_j$  are defined in the following. We divide into two separate cases depending on the location of  $y_{k,j}$ :

(i)  $y_{k,j} \in \text{Ran}(g_j)$ . Define  $U_j = (1 + \delta) \mathbb{E}[(Y - g(\mathbf{X}))^2 \mathbb{1}_{\{\mathbf{X} \in I_j\}}]$  and

$$V_j = \min \left\{ (1 + \delta^{-1}) \mathbb{E}[(g(\mathbf{X}) - y_{k,j})^2 \mathbb{1}_{\{\mathbf{X} \in I_j\}}], \mathbb{E}[(Y - M_k)^2 \mathbb{1}_{\{\mathbf{X} \in I_j\}}] \right\}.$$

(ii)  $y_{k,j} \notin \text{Ran}(g_j)$ . Define  $U_j = (1 + \delta) \mathbb{E}[(Y - g(\mathbf{X}))^2 \mathbb{1}_{\{\mathbf{X} \in I_j\}}]$  and

$$V_j = \min \left\{ \frac{(1 + \delta)^3}{\delta^3} p_j (\Delta g_j)^2, \mathbb{E}[(Y - M_k)^2 \mathbb{1}_{\{\mathbf{X} \in I_j\}}] \right\}.$$

In case (i), (48) follows immediately from the polarization identity  $(a + b)^2 \leq (1 + \delta)a^2 + (1 + \delta^{-1})b^2$ . On the other hand, for case (ii), (48) follows by applying Lemma B.1 to the joint distribution  $(g(\mathbf{X}), Y) | \mathbf{X} \in I_j$  and using that  $y_{k,j} = \mathbb{E}[Y | \mathbf{X} \in I_j]$ . This completes the proof of (48).

**Step III: controlling  $\sum_j U_j$  and  $\sum_j V_j$ .** We have by construction and (48) that

$$\mathbb{E}[(Y - M_k)^2] = \sum_{j \in J_k} \mathbb{E}[(Y - M_k)^2 \mathbb{1}_{\{\mathbf{X} \in I_j\}}] \leq \sum_{j \in J_k} U_j + \sum_{j \in J_k} V_j. \quad (49)$$

The first term is easy to control by definition:

$$\sum_{j \in J_k} U_j = \sum_{j \in J_k} (1 + \delta) \mathbb{E}[(Y - g(\mathbf{X}))^2 \mathbb{1}_{\{\mathbf{X} \in I_j\}}] = (1 + \delta) \mathbb{E}[(Y - g(\mathbf{X}))^2]. \quad (50)$$

To control  $\sum_j V_j$ , we apply Hölder's inequality. We have

$$\begin{aligned} \sum_{j \in J_k} V_j &\leq \left( \sum_{j \in J_k} p_j \left( \frac{V_j}{p_j} \right)^{3/2} \right)^{2/3} \left( \sum_{j \in J_k} p_j \right)^{1/3} \\ &\leq \left( \left( \max_{j \in J_k} V_j \right) \sum_{j \in J_k} \sqrt{\frac{V_j}{p_j}} \right)^{2/3} \leq \left( \left( \max_{j \in J_k} \mathbb{E}[(Y - M_k)^2 \mathbb{1}_{\{\mathbf{X} \in I_j\}}] \right) \sum_{j \in J_k} \sqrt{\frac{V_j}{p_j}} \right)^{2/3}. \end{aligned} \quad (51)$$

To further bound the right-hand side of (51), we first recall from (11) that as a consequence of the marginally atomless property,

$$\max_{j \in J_k} \mathbb{E}[(Y - M_k)^2 \mathbb{1}_{\{\mathbf{X} \in I_j\}}] \leq 2^{-k} \text{Var}(Y). \quad (52)$$

Next, we claim that

$$\sqrt{\frac{V_j}{p_j}} \leq (1 + \delta^{-1})^{3/2} \Delta g_j. \quad (53)$$

This is immediate for case (ii) above (when  $y_{k,j} \notin \text{Ran}(g_j)$ ). By definition, we have for case (i) above (when  $y_{k,j} \in \text{Ran}(g_j)$ ),

$$V_j \leq (1 + \delta^{-1})p_j(\Delta g_j)^2 < p_j(1 + \delta^{-1})^3(\Delta g_j)^2,$$

as desired. On the other hand, suppose that  $k = dq + r$  for some integer  $q$  and  $0 \leq r < d$ , and denote by  $\pi_k$  the resulting partition of  $\mathbb{R}^d$ . Observe (by induction on  $q, r$ , and elementary geometry) that

$$\sum_{A \in \pi_k} \left( \sup_{\mathbf{x} \in A} g(\mathbf{x}) - \inf_{\mathbf{x} \in A} g(\mathbf{x}) \right) \leq 2^{q(d-1)+r} \|g\|_{\text{TV}}.$$

In other words, we have that for  $k \in \mathbb{N}$ ,

$$\sum_{j \in J_k} \Delta g_j = \sum_{A \in \pi_k} \left( \sup_{\mathbf{x} \in A} g(\mathbf{x}) - \inf_{\mathbf{x} \in A} g(\mathbf{x}) \right) \leq 2^{k - \lfloor k/d \rfloor} \|g\|_{\text{TV}}, \quad (54)$$

where  $\lfloor \cdot \rfloor$  is the floor function. Combined with (53), we arrive at

$$\sum_{j \in J_k} \sqrt{\frac{V_j}{p_j}} \leq (1 + \delta^{-1})^{3/2} 2^{k - \lfloor k/d \rfloor} \|g\|_{\text{TV}}.$$

Inserting into (51) gives

$$\sum_{j \in J_k} V_j \leq ((1 + \delta^{-1})^{3/2} 2^{k - \lfloor k/d \rfloor} \|g\|_{\text{TV}} 2^{-k} \text{Var}(Y))^{2/3} \leq (1 + \delta^{-1}) 2^{-2\lfloor k/d \rfloor/3} (\|g\|_{\text{TV}} \text{Var}(Y))^{2/3}. \quad (55)$$

Finally, inserting (50) and (55) into (49) yields

$$\mathbb{E}[(Y - M_k)^2] \leq (1 + \delta) \mathbb{E}[(Y - g(\mathbf{X}))^2] + (1 + \delta^{-1}) 2^{-2\lfloor k/d \rfloor/3} (\|g\|_{\text{TV}} \text{Var}(Y))^{2/3}.$$

This proves (45) and hence concludes the proof.  $\square$

*Proof of Remark 4.* In the proof of Theorem 2, the bound (46) can be improved to

$$\text{Var}(Y)^{1/2} \leq \mathbb{E}[(Y - g(\mathbf{X}))^2]^{1/2} + \frac{1}{2} \Delta g.$$

Inserting the following inequality (which follows from  $(a + b)^p \leq 2^{p-1}(a^p + b^p)$  for  $a, b \geq 0$  and  $p \geq 1$ )

$$\text{Var}(Y)^{2/3} \leq 2^{1/3} \mathbb{E}[(Y - g(\mathbf{X}))^2]^{2/3} + 2^{-2/3} (\Delta g)^{4/3}$$

into (45) yields (15).  $\square$

*Proof of Theorem 6.* Recall that  $\Delta Y := \sup \text{supp } Y - \inf \text{supp } Y$ . The only difference from the proof of Theorem 2 is (52), since for non-marginally atomless measures (10) and (11) may not hold. Instead, by our

assumptions, (10) is be replaced by

$$\max \left\{ \varphi_L(\hat{x}_j), \varphi_R(\hat{x}_j) \right\} \leq \frac{1}{2} \mathbb{E}[(Y - \mathbb{E}[Y \mid \mathbf{X} \in A])^2 \mathbb{1}_{\{\mathbf{X} \in A\}}] + \frac{(\Delta Y)^2}{N},$$

because adding an atom of weight  $\leq 1/N$  to a node increases the risk by at most  $(\Delta Y)^2/N$ . As a consequence, if we denote by

$$u_k := \max_{A \in \pi_k} \mathbb{E}[(Y - \mathbb{E}[Y \mid \mathbf{X} \in A])^2 \mathbb{1}_{\{\mathbf{X} \in A\}}],$$

then  $u_k$  satisfies the recursive inequalities

$$u_{k+1} \leq \frac{u_k}{2} + \frac{(\Delta Y)^2}{N}, \quad k \geq 0; \quad u_0 = \text{Var}(Y).$$

To solve this, let  $v_k := u_k - 2(\Delta Y)^2/N$ . Suppose that  $u_0 \geq 2(\Delta Y)^2/N$ . Then  $v_k$  satisfies  $v_{k+1} \leq v_k/2$  and  $v_0 \leq \text{Var}(Y)$ . It follows that  $v_k \leq 2^{-k} \text{Var}(Y)$  for all  $k \geq 0$ , and hence the maximum risk among the nodes at level  $k$  is

$$\max_{A \in \pi_k} \mathbb{E}[(Y - \mathbb{E}[Y \mid \mathbf{X} \in A])^2 \mathbb{1}_{\{\mathbf{X} \in A\}}] = u_k \leq 2^{-k} \text{Var}(Y) + \frac{2(\Delta Y)^2}{N}. \quad (56)$$

It is also easy to check that (56) is also satisfied for the case  $u_0 < 2(\Delta Y)^2/N$ , that is, (56) holds in general. Replacing (52) by (56) leads to

$$\mathbb{E}[(Y - M_k)^2] \leq \inf_{g \in \mathcal{G}} \left( (1 + \delta) \mathbb{E}[(Y - g(\mathbf{X}))^2] + (1 + \delta^{-1}) 2^{-2\lfloor k/d \rfloor / 3} \left( \|g\|_{\text{TV}} (\text{Var}(Y) + 2^{k+1} \frac{(\Delta Y)^2}{N}) \right)^{2/3} \right).$$

Applying concavity of the function  $x \mapsto x^{2/3}$  for  $x > 0$ , (47), and that

$$\|g\|_{\text{TV}}^{2/3} \left( 2^{k+1} \frac{(\Delta Y)^2}{N} \right)^{2/3} \leq \frac{\|g\|_{\text{TV}}^2}{3} + \frac{2^{k+2}}{3} \frac{(\Delta Y)^2}{N},$$

we obtain (23).  $\square$

*Proof of Theorem 7.* Note that if  $\mathbf{X}_*$  is marginally atomless, the assumption (22) for the joint distribution  $(\mathbf{X}, Y)$  in Theorem 6 holds  $\mathbb{P}_*$ -almost surely. Consequently, the proof is almost verbatim compared to Theorem 4.3 of [Klusowski and Tian \(2024\)](#), by applying our Theorem 6 instead of Theorem 4.2 therein. The only difference here is the extra term

$$(1 + \delta^{-1}) 2^{-2\lfloor k/d \rfloor / 3} \frac{2^{k+2} (\Delta Y)^2}{3N}$$

appearing in (23), where we remind the reader that  $\Delta Y = \sup \text{supp } Y - \inf \text{supp } Y$ . Nevertheless, since the proof of Theorem 4.3 of [Klusowski and Tian \(2024\)](#) deals first with the case with bounded data, we may simply replace  $\Delta Y$  by that bound. Specifically, the first part of the proof of Theorem 4.3 of [Klusowski and Tian \(2024\)](#) assumes  $\max_i |Y_i| \leq U$ . We may set  $\Delta Y = 2U$  and add the term

$$(1 + \delta^{-1}) 2^{-2\lfloor k/d \rfloor / 3} \frac{2^{k+2} (\Delta Y)^2}{3N} \leq \frac{2^{k+5} U^2}{3N}$$

in (B.28) therein (where we used  $\delta \geq 2^{-2\lfloor k/d \rfloor / 3}$ ). This extra term is carried until (B.34) therein, where it can be absorbed by the term  $U^4 2^k \log(Nd)/N$  therein. The rest of the proof remains unchanged.  $\square$

## B.2 Proofs of results in Section 3

Before we formally prove Theorem 9, we point out a key ingredient that distinguishes it from previous proofs where only a single decision tree is involved. Recall that  $n$  is the number of trees in the forest,  $\Sigma$  is the law of the splitting dimensions, and  $\mathbb{E}_n$  denotes the expectation with respect to the empirical measure on  $n$  samples from  $\Sigma$ . In Theorem 2, the cyclicity of the cyclic MinimaxSplit algorithm is essential to proving (54). However, a stronger upper bound for

$$\sum_{j \in J_k} \Delta g_j = \sum_{A \in \pi_k} \left( \sup_{\mathbf{x} \in A} g(\mathbf{x}) - \inf_{\mathbf{x} \in A} g(\mathbf{x}) \right)$$

exists by counting the (random) number of splits in each dimension, which is generally of the form

$$\sum_{A \in \pi_k} \left( \sup_{\mathbf{x} \in A} g(\mathbf{x}) - \inf_{\mathbf{x} \in A} g(\mathbf{x}) \right) \leq \sum_{i=1}^d \xi_{k,i} \|g_i\|_{\text{TV}}, \quad (57)$$

for some (random) positive integers  $\xi_{k,i}$ ,  $i \in [d]$  depending on the samples from  $\Sigma$ . See also (61) below. The intuition in proving Theorem 9 is that we keep (57) as an upper bound, instead of (54). Then, with enough randomness injected into the splitting dimensions (and hence the random variables  $\{\xi_{k,i}\}$ ), the right-hand side of (57) is small if averaged over all trees in the forest, as shown by the next lemma.

**Lemma B.2.** *Fix  $d \geq 2$ . Consider a stochastic recursion defined as follows. Let  $(\xi_{0,1}, \dots, \xi_{0,d}) = (1, \dots, 1)$  and for each  $k \geq 1$ , given  $(\xi_{k-1,1}, \dots, \xi_{k-1,d})$ , we define  $(\xi_{k,1}, \dots, \xi_{k,d})$  through the following procedure:*

- sample independent copies  $(\xi'_{k-1,1}, \dots, \xi'_{k-1,d})$  and  $(\xi''_{k-1,1}, \dots, \xi''_{k-1,d})$  of  $(\xi_{k-1,1}, \dots, \xi_{k-1,d})$ ;
- uniformly sample  $\zeta_k \in [d]$ ;
- define  $\xi_{k,\zeta_k} = \max\{\xi'_{k-1,\zeta_k}, \xi''_{k-1,\zeta_k}\}$ ;
- for  $j \in [d]$  and  $j \neq \zeta_k$ , define  $\xi_{k,j} = \xi'_{k-1,j} + \xi''_{k-1,j}$ .

Then  $\mathbb{E}[\xi_{k,j}] \leq 2^k e^{-k/(4d)}$  for all  $j \in [d]$ .

*Remark 22.* The rate  $e^{-1/(4d)}$  is not tight. Finding the tight exponent appears to be a non-trivial task, even for  $d = 2$ .

*Proof of Lemma B.2.* By construction, for each fixed  $k \geq 0$ , the law of each vector  $(\xi_{k,1}, \dots, \xi_{k,d})$  is exchangeable. As a consequence,  $\xi_{k,j} \stackrel{\text{law}}{=} W_k$  for all  $j \in [d]$ , where  $\{W_k\}_{k \geq 0}$  is defined as follows:  $W_0 = 1$ , and for each  $k \geq 1$ , we take independent copies  $W'_{k-1}, W''_{k-1}$  of  $W_{k-1}$  and define

$$W_k = \begin{cases} W'_{k-1} + W''_{k-1} & \text{with probability } 1 - 1/d; \\ \max\{W'_{k-1}, W''_{k-1}\} & \text{with probability } 1/d. \end{cases}$$

It remains to find  $\mathbb{E}[W_k]$ . It follows from construction that  $\mathbb{E}[(W_0)^2] = 1$  and for each  $k \geq 1$ ,

$$\begin{aligned}\mathbb{E}[(W_k)^2] &= (1 - \frac{1}{d})\mathbb{E}\left[\left(W'_{k-1} + W''_{k-1}\right)^2\right] + \frac{1}{d}\mathbb{E}\left[\left(\max\{W'_{k-1}, W''_{k-1}\}\right)^2\right] \\ &\leq 4(1 - \frac{1}{d})\mathbb{E}[(W_{k-1})^2] + \frac{2}{d}\mathbb{E}[(W_{k-1})^2] \\ &= (4 - \frac{2}{d})\mathbb{E}[(W_{k-1})^2].\end{aligned}$$

where we have used the inequality  $(a + b)^2 \leq 2(a^2 + b^2)$ . It follows that

$$\mathbb{E}[W_k] \leq \sqrt{\mathbb{E}[(W_k)^2]} \leq (4 - \frac{2}{d})^{k/2} \leq 2^k e^{-k/(4d)},$$

as desired.  $\square$

*Proof of Theorem 9.* In the following, we use  $S$  to denote a random variable with law  $\Sigma$ . We first establish an upper bound of

$$\mathbb{E}[(Y - \mathbb{E}_n[M_k^S])^2].$$

Since the randomness from  $\mathbb{E}_n$  is independent from that of  $(\mathbf{X}, Y)$ , we have by Jensen's inequality,

$$\mathbb{E}[(Y - \mathbb{E}_n[M_k^S])^2] \leq \mathbb{E}[\mathbb{E}_n[\mathbb{E}[(Y - M_k^S)^2]]]. \quad (58)$$

Here, the outer expectation is with respect to the randomness from the empirical measure  $\mathbb{E}_n$  (the law of  $(\mathbf{X}, Y)$  is fixed in the settings of Theorems 2 and 6), and the inner expectation is with respect to the joint law of  $(\mathbf{X}, Y, \{M_k^S\})$ . In other words, we trivially bound the risk of the average by the average of the risks among the  $n$  trees.

Denote the empirical samples from  $\Sigma$  by  $S_1, \dots, S_n$ . Our next goal is to control

$$\mathbb{E}_n[\mathbb{E}[(Y - M_k^S)^2]] = \frac{1}{n} \sum_{\ell=1}^n \mathbb{E}[(Y - M_k^{S_\ell})^2].$$

We apply the same decomposition as in step II of the proof of Theorem 2, with the specific choice of  $\delta = 1$ . For  $j \in J_k$ , we let  $g_j^\ell = g|_{I_j^\ell}$ , where  $\{I_j^\ell\}_{j \in J_k}$  is the partition at level  $k$  of a tree whose splitting rule is given by  $S_\ell$ . Then (53) now has the form

$$\sqrt{\frac{V_j^\ell}{p_j^\ell}} \leq 2^{3/2} \Delta g_j^\ell.$$

Proceeding as in step III of the proof of Theorem 2, (55) becomes

$$\sum_{j \in J_k^\ell} V_j^\ell \leq \left(2^{-k} \text{Var}(Y) 2^{3/2} \sum_{j \in J_k^\ell} \Delta g_j^\ell\right)^{2/3}, \quad (59)$$

and hence for all  $g \in \mathcal{G}$  with the representation  $g = g_1 + \dots + g_d$ ,

$$\mathbb{E}_n[\mathbb{E}[(Y - M_k^S)^2]] \leq 2\mathbb{E}[(Y - g(\mathbf{X}))^2] + 2\text{Var}(Y)^{2/3} 2^{-2k/3} \frac{1}{n} \sum_{\ell=1}^n \left( \sum_{j \in J_k^\ell} \Delta g_j^\ell \right)^{2/3}. \quad (60)$$

Next, we construct the (random) values  $\{\xi_{k,i}^\ell\}_{\ell \in [n], i \in [d]}$  such that for each  $k \in \mathbb{N}$  and  $\ell \in [n]$ ,

$$\sum_{j \in J_k^\ell} \Delta g_j^\ell \preceq_{\text{st}} \sum_{i=1}^d \xi_{k,i}^\ell \|g_i\|_{\text{TV}}, \quad (61)$$

where  $\preceq_{\text{st}}$  denotes stochastic dominance. Define  $\{\xi_{k,i}^\ell\}_{\ell \in [n], i \in [d]}$  as follows:

- $\{\xi_{k,i}^\ell\}_{i \in [d]}, \ell \in [n]$  are i.i.d. copies of  $\{\xi_{k,i}\}_{i \in [d]}$ .
- $\xi_{0,i} = 1$  for all  $i \in [d]$ .
- For  $k \geq 1$ , given the law of  $\{\xi_{k-1,i}\}_{i \in [d]}$ , generate two i.i.d. copies  $\{\xi'_{k-1,i}\}_{i \in [d]}$  and  $\{\xi''_{k-1,i}\}_{i \in [d]}$ , independently sample a uniform  $\zeta_k \in [d]$ , and define

$$\xi_{k,\zeta_k} = \max\{\xi'_{k-1,\zeta_k}, \xi''_{k-1,\zeta_k}\}; \quad \xi_{k,i} = \xi'_{k-1,i} + \xi''_{k-1,i}, \quad i \neq \zeta_k.$$

See Figure 11 for an illustration of the first few values of  $\{\xi_{k,i}\}$ .

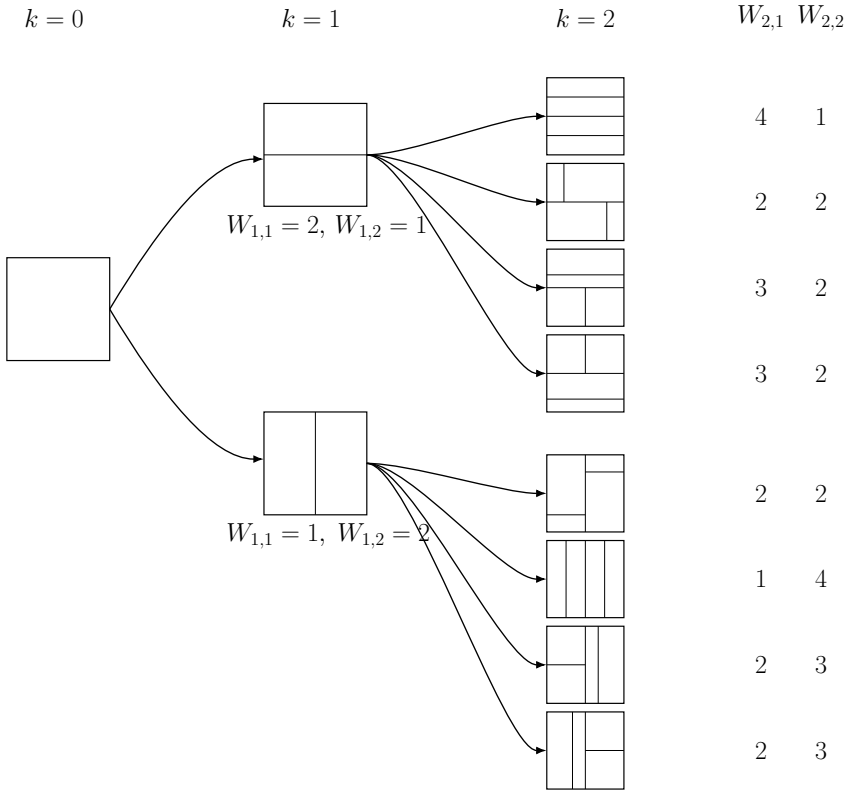


Figure 11: Showcasing the possibilities of the splits for levels  $k = 0, 1, 2$ , with  $d = 2$ .

To see that this definition yields (61), we apply induction. The base case  $k = 0$  is easy as  $\sup g - \inf g \leq \sum_{i=1}^d \|g_i\|_{\text{TV}}$ . Suppose that (61) holds with  $k - 1$ . Then given a tree of depth  $k$  (where we recall that the split dimensions of all nodes are i.i.d. uniform in  $[d]$ ), we condition on the split dimension at level zero (node  $\emptyset$ , say into child nodes  $u, v$ ), which we denote by  $\zeta_k$ . Next, we decompose each variation  $\Delta g_j^\ell$  in the  $d$  dimensions by  $\Delta g_j^\ell \leq \sum_{i=1}^d \Delta g_{j,i}^\ell$ , where  $\Delta g_{j,i}^\ell$  is the variation of the  $i$ -th coordinate of  $g$  in  $I_j$  for sample  $\ell$ .

- For a dimension  $i \neq \zeta_k$ , we apply the trivial bound that the variations over dimension  $i$  for  $j \in J_k^\ell$  is at most the sum of the variations among the descendants of  $u$  and of  $v$ . By induction hypothesis, we have

$$\begin{aligned} \sum_{j \in J_k} \Delta g_{j,i}^\ell &\leq \sum_{\substack{j \in J_k \\ j \succ u}} \Delta g_{j,i}^\ell + \sum_{\substack{j \in J_k \\ j \succ v}} \Delta g_{j,i}^\ell \\ &\preceq_{\text{st}} \xi'_{k-1,i} \|g_i\|_{\text{TV}} + \xi''_{k-1,i} \|g_i\|_{\text{TV}} = \xi_{k,i} \|g_i\|_{\text{TV}}, \end{aligned}$$

where  $j \succ u$  means that the set  $I_j$  is a descendant of  $u$  in the binary subtree representation.

- For dimension  $\zeta_k$ , we again use the fact that the variation  $\sum_{j \in J_k} \Delta g_{j,\zeta_k}^\ell$  is at most the sum of variations among the descendants of  $u, v$ , but the total variation  $\|g_{\zeta_k}\|_{\text{TV}}$  is already decomposed into two, say  $\|g_{\zeta_k}^{(i)}\|_{\text{TV}}$ ,  $i = 1, 2$ , corresponding to  $u, v$ . Therefore, by inductive hypothesis,

$$\begin{aligned} \sum_{j \in J_k} \Delta g_{j,\zeta_k}^\ell &\leq \sum_{\substack{j \in J_k \\ j \succ u}} \Delta g_{j,\zeta_k}^\ell + \sum_{\substack{j \in J_k \\ j \succ v}} \Delta g_{j,\zeta_k}^\ell \\ &\preceq_{\text{st}} \xi'_{k-1,\zeta_k} \|g_{\zeta_k}^{(1)}\|_{\text{TV}} + \xi''_{k-1,\zeta_k} \|g_{\zeta_k}^{(2)}\|_{\text{TV}} \\ &\leq \max\{\xi'_{k-1,\zeta_k}, \xi''_{k-1,\zeta_k}\} \|g_{\zeta_k}\|_{\text{TV}} \\ &= \xi_{k,\zeta_k} \|g_{\zeta_k}\|_{\text{TV}}. \end{aligned}$$

This proves (61).

Applying (61) and Hölder's inequality, we obtain

$$\begin{aligned} \frac{1}{n} \sum_{\ell=1}^n \left( \sum_{j \in J_k^\ell} \Delta g_j^\ell \right)^{2/3} &\preceq_{\text{st}} \frac{1}{n} \sum_{\ell=1}^n \left( \sum_{i=1}^d \xi_{k,i}^\ell \|g_i\|_{\text{TV}} \right)^{2/3} \\ &\leq 2^{2k/3} \left( \frac{1}{n} \sum_{\ell=1}^n \sum_{i=1}^d 2^{-k} \xi_{k,i}^\ell \|g_i\|_{\text{TV}} \right)^{2/3} \\ &\leq 2^{2k/3} \left( \frac{1}{n} \sum_{i=1}^d \|g_i\|_{\text{TV}} \max_{i \in [d]} \sum_{\ell=1}^n 2^{-k} \xi_{k,i}^\ell \right)^{2/3} \\ &\leq 2^{2k/3} \|g\|_{\text{TV}}^{2/3} \left( \frac{1}{n} \max_{i \in [d]} \sum_{\ell=1}^n 2^{-k} \xi_{k,i}^\ell \right)^{2/3}, \end{aligned}$$

where in the last step we recall that for  $g \in \mathcal{G}$ ,  $\|g\|_{\text{TV}} = \sum_{i=1}^d \|g_i\|_{\text{TV}}$ . The next step is to bound from above the inner maximum, where we recall that under the outer expectation (as  $S_1, \dots, S_n$  are i.i.d. sampled from  $\Sigma$ ), the random variables  $\{\xi_{k,i}^\ell\}_{\ell \in [n], i \in [d]}$  are i.i.d. in  $\ell$ . Employing Lemma B.2, we have for each  $i \in [d]$  that

$$\mathbb{E} \left[ \sum_{\ell=1}^n 2^{-k} \xi_{k,i}^\ell \right] = n 2^{-k} \mathbb{E}[\xi_{k,1}^\ell] \leq n e^{-\frac{k}{4d}}.$$

By the union bound and the Hoeffding inequality (note that  $2^{-k}\xi_{k,i}^\ell \in [0, 1]$ ), we have for  $u \geq 0$  that

$$\begin{aligned} \mathbb{P}\left(\max_{i \in [d]} \frac{1}{n} \sum_{\ell=1}^n 2^{-k} \xi_{k,i}^\ell \geq e^{-\frac{k}{4d}} + u\right) &\leq d \mathbb{P}\left(\frac{1}{n} \sum_{\ell=1}^n 2^{-k} \xi_{k,i}^\ell \geq e^{-\frac{k}{4d}} + u\right) \\ &\leq d \mathbb{P}\left(\sum_{\ell=1}^n 2^{-k} \xi_{k,i}^\ell \geq \mathbb{E}\left[\sum_{\ell=1}^n 2^{-k} \xi_{k,i}^\ell\right] + nu\right) \leq de^{-2nu^2}. \end{aligned}$$

Therefore, a standard computation yields

$$\mathbb{E}\left[\left(\max_{i \in [d]} \frac{1}{n} \sum_{\ell=1}^n 2^{-k} \xi_{k,i}^\ell\right)^{2/3}\right] \leq e^{-\frac{k}{6d}} + \frac{d}{n^{1/3}}.$$

Inserting into (60) and taking expectation, we see that for all  $g \in \mathcal{G}$ ,

$$\mathbb{E}[\mathbb{E}_n[\mathbb{E}[(Y - M_k^S)^2]]] \leq 2\mathbb{E}[(Y - g(\mathbf{X}))^2] + 2\text{Var}(Y)^{2/3} \|g\|_{\text{TV}}^{2/3} \left(e^{-\frac{k}{6d}} + \frac{d}{n^{1/3}}\right).$$

Using (58) and (47), we obtain that for all  $g \in \mathcal{G}$ ,

$$\mathbb{E}[(Y - \mathbb{E}_n[M_k^S])^2] \leq 2\mathbb{E}[(Y - g(\mathbf{X}))^2] + 2\left(\frac{4}{3}\mathbb{E}[(Y - g(\mathbf{X}))^2] + \|g\|_{\text{TV}}^2\right) \left(e^{-\frac{k}{6d}} + \frac{d}{n^{1/3}}\right).$$

Following the same lines as the proof of Theorem 6, we obtain that in the presence of marginal atoms of weights at most  $1/N$ , it holds for all  $g \in \mathcal{G}$ ,

$$\mathbb{E}[(Y - \mathbb{E}_n[M_k^S])^2] \leq 2\mathbb{E}[(Y - g(\mathbf{X}))^2] + \frac{8}{3}\left(\mathbb{E}[(Y - g(\mathbf{X}))^2] + \|g\|_{\text{TV}}^2 + \frac{2^k M^2}{N}\right) \left(e^{-\frac{k}{6d}} + \frac{d}{n^{1/3}}\right).$$

Finally, we proceed with the arguments in proving Theorem 7. Again we follow the arguments in the proof of Theorem 4.3 for CART of [Klusowski and Tian \(2024\)](#). By setting  $M = 2U$  where  $U = \max|Y_i|$ , the extra term of

$$\frac{8}{3} \frac{2^k M^2}{N} \left(e^{-\frac{k}{6d}} + \frac{d}{n^{1/3}}\right) \leq C \left(\frac{2^k U^2}{N} + \frac{2^k U^2 d}{N n^{1/3}}\right)$$

is carried until (B.34) of [Klusowski and Tian \(2024\)](#). The term  $2^k U^2/N$  is absorbed by the term  $U^4 2^k \log(Nd)/N$  therein. The other term  $2^k U^2 d/(N n^{1/3})$  is carried into (B.35), and is bounded by  $C 2^k (\log N) d/(N n^{1/3})$  under the choice of  $U = \|g^*\|_\infty + 2\sigma\sqrt{2\log N}$  at the end of that proof, where  $C > 0$  may depend on  $\|g^*\|_\infty$  and  $\sigma$ . This concludes (26).  $\square$

### B.3 Proofs of results in Section 4

The analysis in the classification setting also relies on two monotonicity envelopes for the conditional probability. Recall (27). Lemma B.3 provides left and right bounds for the probability of an order event inside a cell in terms of the functions

$$\begin{aligned} \varphi_L(x) &:= \mathbb{P}(\mathbf{X} \in A, X_j < x) h(\mathbb{P}(Y = 1 \mid \mathbf{X} \in A, X_j < x)); \\ \varphi_R(x) &:= \mathbb{P}(\mathbf{X} \in A, X_j \geq x) h(\mathbb{P}(Y = 1 \mid \mathbf{X} \in A, X_j \geq x)), \end{aligned}$$

which are nondecreasing and nonincreasing, respectively. Lemma B.4 further provides an information inequality that upper bounds the entropy. These two lemmas are the entropic analogues of the unconditional variance contraction used in the regression section; they are the technical bridges that allow us to carry over the exponential decay arguments from squared loss to cross-entropy.

**Lemma B.3.** *Suppose that  $\mathbf{X}$  is marginally atomless and  $j \in [d]$ . Then the function  $\varphi_L$  is non-decreasing and continuous, and  $\varphi_R$  is non-increasing and continuous. Moreover, under the (cyclic) MinimaxSplit construction,*

$$\max_{j \in J_k} \mathbb{E}[\log(1 + e^{-Y M_k}) \mathbb{1}_{\{\mathbf{X} \in I_j\}}] \leq 2^{-k} \mathbb{E}[\log(1 + e^{-Y M_0})] = 2^{-k} H(Y).$$

*Proof.* To see the monotonicity of  $\varphi_L$ , we take arbitrary  $a < b$ . Since the conditional entropy is bounded from above by the entropy, we have

$$h(\mathbb{P}(Y = 1 \mid \mathbf{X} \in A, X_j < b)) \geq \mathbb{P}(X_j < a \mid \mathbf{X} \in A, X_j < b) h(\mathbb{P}(Y = 1 \mid \mathbf{X} \in A, X_j < a)).$$

Rearranging yields that  $\varphi_L(a) \leq \varphi_L(b)$ . The continuity of  $\varphi_L$  and  $\varphi_R$  follows from the marginally atomless condition. The final claim follows in the same way as the derivation of (11).  $\square$

**Lemma B.4.** *Let  $Y$  be a  $\{\pm 1\}$ -valued random variable. For any joint distribution  $(X, Y)$ , it holds that*

$$H(Y) \leq \mathbb{E}[\log(1 + e^{-XY})] + \frac{1}{4} |\sup \text{supp } X - \inf \text{supp } X|. \quad (62)$$

*Proof.* We may assume that  $\sup \text{supp } X - \inf \text{supp } X$ , otherwise the claim is trivial. Given the marginal law of  $X$ , the right-hand side of (62) is minimized if  $X$  and  $Y$  are comonotonic. This is achieved by setting, with  $a = \inf \text{supp } X \leq \sup \text{supp } X = b$ , that  $p = \mathbb{P}(X = b, Y = 1) = 1 - \mathbb{P}(X = a, Y = -1)$ , for some  $p \in [0, 1]$ . It remains to show the deterministic inequality

$$\kappa_{a,b}(p) := h(p) + (p \log(1 + e^{-b}) + (1 - p) \log(1 + e^a)) + \frac{1}{4} |b - a| \geq 0.$$

Note that  $\kappa_{a,b}$  is convex in  $p$  and  $\kappa'_{a,b}(p) = 0$  if and only if

$$\log\left(\frac{1-p}{p}\right) = \log\left(\frac{1+e^{-b}}{1+e^a}\right),$$

or  $p = (1 + e^a)/((1 + e^a) + (1 + e^{-b}))$ . It remains to prove

$$\log\left(\frac{(1+e^a)(1+e^{-b})}{(1+e^a)+(1+e^{-b})}\right) \geq -\frac{1}{4} |b - a|,$$

or equivalently,

$$\log((1 + e^a)^{-1} + (1 + e^{-b})^{-1}) \leq \frac{1}{4} |b - a|. \quad (63)$$

With  $D := b - a > 0$  fixed, the left-hand side of (63) is maximized at  $a = -D/2$  and  $b = D/2$  by elementary calculus. On the other hand, it is easy to verify by elementary calculus that  $\log(2/(1 + e^{-D/2})) \leq D/4 = |b - a|/4$ . This proves (63) and hence completes the proof.  $\square$

*Proof of Theorem 10.* We first recall the notations from the proof of Theorem 2. Denote by  $\pi_k = \{I_j\}_{j \in J_k}$

the partition of  $\mathbb{R}^d$  formed at level  $k$  from the cyclic MinimaxSplit construction. Note that  $M_k \mathbb{1}_{\{\mathbf{X} \in I_j\}} = y_{k,j} \mathbb{1}_{\{\mathbf{X} \in I_j\}}$ , where  $y_{k,j} = \log(\mathbb{P}(Y = 1 \mid \mathbf{X} \in I_j)/\mathbb{P}(Y = -1 \mid \mathbf{X} \in I_j))$ . Define  $g_j = g|_{I_j}$ , so that  $\|g\|_{\text{TV}} = \sum_j \|g_j\|_{\text{TV}}$ . Recall that  $\Delta g_j = \sup g_j - \inf g_j \leq \|g_j\|_{\text{TV}}$ .

By applying Lemma B.4 to the joint distribution  $(g(\mathbf{X}), Y) \mid \mathbf{X} \in I_j$ , decompose

$$\mathbb{E}[\log(1 + e^{-Y M_k}) \mathbb{1}_{\{\mathbf{X} \in I_j\}}] = \mathbb{E}[\log(1 + e^{-Y y_{k,j}}) \mathbb{1}_{\{\mathbf{X} \in I_j\}}] \leq U_j + V_j, \quad (64)$$

where  $U_j = \mathbb{E}[\log(1 + e^{-Y g(\mathbf{X})}) \mathbb{1}_{\{\mathbf{X} \in I_j\}}]$  and

$$V_j = \min \left\{ \mathbb{E}[\log(1 + e^{-Y M_k}) \mathbb{1}_{\{\mathbf{X} \in I_j\}}], \frac{p_j \Delta g_j}{4} \right\}.$$

We have by construction and (64) that

$$\mathbb{E}[\log(1 + e^{-Y M_k})] = \sum_{j \in J_k} \mathbb{E}[\log(1 + e^{-Y M_k}) \mathbb{1}_{\{\mathbf{X} \in I_j\}}] \leq \sum_{j \in J_k} U_j + \sum_{j \in J_k} V_j. \quad (65)$$

The first term is easy to control by definition:

$$\sum_{j \in J_k} U_j \leq \sum_{j \in J_k} \mathbb{E}[\log(1 + e^{-Y g(\mathbf{X})}) \mathbb{1}_{\{\mathbf{X} \in I_j\}}] = \mathbb{E}[\log(1 + e^{-Y g(\mathbf{X})})]. \quad (66)$$

To control  $\sum_j V_j$ , we apply the same Hölder's inequality argument as in the proof of Theorem 16 in the regression setting. More precisely, we have

$$\begin{aligned} \sum_{j \in J_k} V_j &\leq \left( \sum_{j \in J_k} p_j \left( \frac{V_j}{p_j} \right)^2 \right)^{1/2} \left( \sum_{j \in J_k} p_j \right)^{1/2} \\ &\leq \left( \left( \max_{j \in J_k} V_j \right) \sum_{j \in J_k} \frac{V_j}{p_j} \right)^{1/2} \leq \left( \left( \max_{j \in J_k} \mathbb{E}[\log(1 + e^{-Y M_k}) \mathbb{1}_{\{\mathbf{X} \in I_j\}}] \right) \sum_{j \in J_k} \frac{V_j}{p_j} \right)^{1/2}. \end{aligned} \quad (67)$$

To further bound the right-hand side of (67), we recall from Lemma B.3 that as a consequence of the marginally atomless property,

$$\max_{j \in J_k} \mathbb{E}[\log(1 + e^{-Y M_k}) \mathbb{1}_{\{\mathbf{X} \in I_j\}}] \leq 2^{-k} \mathbb{E}[\log(1 + e^{-Y M_0})] = 2^{-k} H(Y). \quad (68)$$

Note that  $V_j/p_j \leq \Delta g_j/4$ . Following the proof of Theorem 16, we arrive at

$$\sum_{j \in J_k} \frac{V_j}{p_j} \leq 2^{-2+k-\lfloor k/d \rfloor} \|g\|_{\text{TV}}.$$

Inserting into (67) gives (using that  $H(Y) \leq \log 2$ )

$$\sum_{j \in J_k} V_j \leq (2^{k-2-\lfloor k/d \rfloor} \|g\|_{\text{TV}} 2^{-k} H(Y))^{1/2} \leq \sqrt{\frac{\log 2}{4}} 2^{-\lfloor k/d \rfloor/2} \|g\|_{\text{TV}}^{1/2}. \quad (69)$$

Finally, inserting (66) and (69) into (65) yields (29).  $\square$

*Proof of Theorem 11.* The only difference from the proof of Theorem 10 is (68). Denoting by  $\hat{x}_j$  the optimal

MinimaxSplit location on  $A$  in dimension  $j$ , we have

$$\max \left\{ \varphi_L(\hat{x}_j), \varphi_R(\hat{x}_j) \right\} \leq \frac{1}{2} \mathbb{P}(\mathbf{X} \in A) h(\mathbb{P}(Y = 1 \mid \mathbf{X} \in A)) + \frac{\log N}{N},$$

because adding an atom of weight  $\leq 1/N$  to a node increases the risk by at most  $\log N/N$  (which can be seen from the extreme case with a sample 1 added to samples of  $-1$ ). As a consequence, if we denote by

$$u_k := \max_{A \in \pi_k} \mathbb{P}(\mathbf{X} \in A) h(\mathbb{P}(Y = 1 \mid \mathbf{X} \in A)),$$

then  $u_k$  satisfies the recursive inequalities

$$u_{k+1} \leq \frac{u_k}{2} + \frac{\log N}{N}, \quad k \geq 0; \quad u_0 = H(Y).$$

Solving this yields

$$\max_{A \in \pi_k} \mathbb{P}(\mathbf{X} \in A) h(\mathbb{P}(Y = 1 \mid \mathbf{X} \in A)) = u_k \leq 2^{-k} H(Y) + \frac{2 \log N}{N}. \quad (70)$$

It is also easy to check that (70) is also satisfied for the case  $u_0 < 2 \log N/N$ , that is, (70) holds in general. Replacing (68) by (70) leads to

$$\mathbb{E}[(Y - M_k)^2] \leq \inf_{g \in \mathcal{G}} \left( \mathbb{E}[(Y - g(\mathbf{X}))^2] + \sqrt{\frac{\log 2}{4}} 2^{-\lfloor k/d \rfloor/2} \left( \|g\|_{\text{TV}} \left( 1 + 2^{k+1} \frac{\log N}{N} \right)^{1/2} \right) \right).$$

Applying concavity of the function  $x \mapsto x^{1/2}$  for  $x > 0$  and that

$$\|g\|_{\text{TV}}^{1/2} \left( 2^{k+1} \frac{\log N}{N} \right)^{1/2} \leq \frac{\|g\|_{\text{TV}}}{2} + \frac{2^k \log N}{N},$$

we obtain (31).  $\square$

## C Additional example for anti-symmetry-breaking preference

In this appendix, we provide an empirical version of Example 8, showing that the ASBP persists even when samples are involved and the symmetry is not perfect.

**Example 23.** Define  $f(\mathbf{x}) = x_1 + |x_2|$ ,  $\mathbf{x} = (x_1, x_2) \in [-1, 1]^2$ , which is Lipschitz and bounded. Let  $\mathbb{P}_*$  denote the law of  $\mathbf{X}$  in Example 8 and  $\mathbb{P}_n$  denote the empirical law of  $\{(\mathbf{X}_i, Y_i)\}_{1 \leq i \leq n}$ , where each  $\mathbf{X}_i$  is sampled from  $\mathbb{P}_*$  and  $Y_i = f(\mathbf{X}_i)$ . Denote by  $\mathcal{R}$  the set of all axis-aligned rectangles in  $[-1, 1]^2$ . It follows from standard arguments in [van der Vaart and Wellner \(2013\)](#) that the class  $\{f \mathbb{1}_R\}_{R \in \mathcal{R}}$  is a Donsker class, so with  $m_R = \mathbb{E}^{\mathbb{P}_*}[f(\mathbf{X}) \mid \mathbf{X} \in R]$ , we have  $\sup_{R \in \mathcal{R}} |\mathbb{E}^{\mathbb{P}_n}[f(\mathbf{X}) \mid \mathbf{X} \in R] - m_R| = O_{\mathbb{P}}(1/\sqrt{n})$ . Here, we use the notation  $\xi_n = O_{\mathbb{P}}(\alpha_n)$  if the sequence  $\{\xi_n/\alpha_n\}$  is tight. Let  $g_R(\mathbf{x}) = (f(\mathbf{x}) - m_R)^2$  for  $R \in \mathcal{R}$ . The class  $\{g_R \mathbb{1}_R\}_{R \in \mathcal{R}}$  is also Donsker. For  $R \in \mathcal{R}$ , let  $V_R$  denote the empirical risk on  $R$ , i.e.,

$$V_R = \frac{1}{n} \sum_{i=1}^n ((f(\mathbf{X}_i) - \mathbb{E}^{\mathbb{P}_n}[f(\mathbf{X}) \mid \mathbf{X} \in R])^2 \mathbb{1}_{\mathbf{X}_i \in R}).$$

It follows from the Donsker property and triangle inequality that

$$\sup_{R \in \mathcal{R}} |V_R - \mathbb{E}[V_R]| = O_{\mathbb{P}}\left(\frac{1}{\sqrt{n}}\right). \quad (71)$$

Next, we apply (71) to analyze the split dimensions and locations when applying MinimaxSplit to  $\mathbb{P}_n$ . For any  $\varepsilon > 0$ , there exists  $C = C(\varepsilon) > 0$  such that  $\mathbb{P}(\forall R \in \mathcal{R}, |V_R - \mathbb{E}[V_R]| < C/\sqrt{n}) > 1 - \varepsilon$ . Our goal is to show the deterministic fact that for some  $C_0 = C_0(\varepsilon) > 0$ , if  $n \geq C_0 64^K$ , on the event

$$\left\{ \forall R \in \mathcal{R}, |V_R - \mathbb{E}[V_R]| < \frac{C}{\sqrt{n}} \right\}, \quad (72)$$

the splits of the first  $K$  levels are all along the first coordinate  $x_1$ . Consider a rectangle  $R_{a,b} = [a, b] \times [-1, 1] \in \mathcal{R}$  where  $-1 \leq a < b \leq 1$ . Define

$$\begin{aligned} R_{a,b;u}^{\uparrow} &= [a, b] \times [u, 1], \quad R_{a,b;u}^{\downarrow} = [a, b] \times [-1, u], \quad u \in [-1, 1]; \\ R_{a,b;u}^{\leftarrow} &= [a, u] \times [-1, 1], \quad R_{a,b;u}^{\rightarrow} = [u, b] \times [-1, 1], \quad u \in [a, b]. \end{aligned}$$

Also denote by  $m(p) = \mathbb{E}[(M-1)\mathbb{1}_{\{M \geq 1\}}/M]$  where  $M \stackrel{\text{law}}{\sim} \text{Bin}(n, p)$ . A standard computation (by first conditioning on the number of samples in the rectangle) yields that

$$\begin{aligned} \mathbb{E}[V_{R_{a,b}}] &= m\left(\frac{b-a}{2}\right) \frac{b-a}{2} \frac{(b-a)^2 + 1}{12}; \\ \mathbb{E}[V_{R_{a,b;u}^{\uparrow}}] &= m\left(\frac{(1-u)(b-a)}{4}\right) \frac{(1-u)(b-a)}{4} \left(\frac{(b-a)^2}{12} + \phi(u)\right); \\ \mathbb{E}[V_{R_{a,b;u}^{\downarrow}}] &= m\left(\frac{(u+1)(b-a)}{4}\right) \frac{(u+1)(b-a)}{4} \left(\frac{(b-a)^2}{12} + \phi(-u)\right); \\ \mathbb{E}[V_{R_{a,b;u}^{\leftarrow}}] &= m\left(\frac{u-a}{2}\right) \frac{u-a}{2} \frac{(u-a)^2 + 1}{12}; \\ \mathbb{E}[V_{R_{a,b;u}^{\rightarrow}}] &= m\left(\frac{b-u}{2}\right) \frac{b-u}{2} \frac{(b-u)^2 + 1}{12}, \end{aligned} \quad (73)$$

where

$$\phi(u) = \begin{cases} \frac{(1-u)^2}{12} & \text{if } u \geq 0; \\ \frac{u^4 - 4u^3 - 6u^2 - 4u + 1}{12(1-u)^2} & \text{if } u < 0. \end{cases}$$

In the following, the constants  $C$  (depending on  $\varepsilon$  only) may vary from line to line. Note that  $m(p) = 1 - O(1/(np))$  jointly as  $np \rightarrow \infty$  (see e.g., Corollary 1 of [Wang et al. \(2008\)](#)). The following results hold if  $b-a \geq C/n^{1/6}$  for  $n$  large enough.

- Consider a split of  $R_{a,b}$  into  $R_{a,b;u}^{\leftarrow}$  and  $R_{a,b;u}^{\rightarrow}$ . The MinimaxSplit location satisfies  $|u - (a+b)/2| \leq C/\sqrt{n}$  by (72) and (73). The risk decay is at least

$$\mathbb{E}[V_{R_{a,b}}] - \mathbb{E}[V_{R_{a,b;u}^{\leftarrow}}] - \mathbb{E}[V_{R_{a,b;u}^{\rightarrow}}] - \frac{3C}{\sqrt{n}} \geq \frac{(b-a)^3}{32} - \frac{C}{\sqrt{n}}.$$

- Consider a split of  $R_{a,b}$  into  $R_{a,b;u}^{\uparrow}$  and  $R_{a,b;u}^{\downarrow}$ . The function  $u \mapsto (1-u)\phi(u)$  is decreasing and differentiable on  $[-1, 1]$  with a strictly negative derivative at  $u = 0$ . Therefore, the MinimaxSplit

location satisfies  $|u| \leq C/((b-a)\sqrt{n})$  by (72) and (73). The risk decay is at most

$$\mathbb{E} [V_{R_{a,b}}] - \mathbb{E} [V_{R_{a,b;u}^\downarrow}] - \mathbb{E} [V_{R_{a,b;u}^\uparrow}] + \frac{3C}{\sqrt{n}} \leq \frac{C}{\sqrt{n}}.$$

Therefore, if  $b-a \geq C/n^{1/6}$ , the MinimaxSplit dimension is always  $x_1$ . Next, we show that under our assumption  $n \geq C_0 64^K$ , we always have  $b-a \geq C/n^{1/6}$  for the first  $K$  levels of splits. The split at level  $k=0$  is obvious. Denote by  $a_k$  the smallest size (measured in dimension  $x_1$ ) of the rectangles at level  $k$ . It follows that  $a_0 = 2$  and for each  $k$ ,  $a_{k+1} \geq a_k/2 - C/\sqrt{n}$ . Solving this recursion yields  $a_k \geq 2^{1-k} - 2C/\sqrt{n}$  for all  $k$ . In particular,  $a_K \geq 2^{1-K} - 2C/\sqrt{n} \geq C/n^{1/6}$ .

In summary, we have shown that if  $n \geq C_0 64^K$ , with high probability, the MinimaxSplit dimension is always along the first dimension for the first  $K$  levels of the tree. As a consequence, the consistency of the MinimaxSplit algorithm is not always guaranteed in the large-sample regime, unlike VarianceSplit (Theorem 4.3 of [Klusowski and Tian \(2024\)](#)) and cyclic MinimaxSplit (Theorem 7).

## D Further numerics

### D.1 Performance metrics

**Mean Squared Error (MSE).** Given a matrix (or image)  $y \in \mathbb{R}^{H \times W}$  and an estimate  $\hat{y}$ , we define

$$\text{MSE}(y, \hat{y}) = \frac{1}{HW} \sum_{i=1}^H \sum_{j=1}^W (y_{ij} - \hat{y}_{ij})^2.$$

MSE emphasizes large errors (squaring) and is simple to optimize. We also define the Root Mean Squared Error (RMSE) as

$$\text{RMSE}(y, \hat{y}) = \sqrt{\text{MSE}(y, \hat{y})} = \sqrt{\frac{1}{HW} \sum_{i=1}^H \sum_{j=1}^W (y_{ij} - \hat{y}_{ij})^2}.$$

**Mean Absolute Error (MAE).** We define

$$\text{MAE}(y, \hat{y}) = \frac{1}{HW} \sum_{i=1}^H \sum_{j=1}^W |y_{ij} - \hat{y}_{ij}|.$$

MAE (an  $\ell_1$  criterion) is *more robust to outliers* than MSE and often produces sharper restorations with less over-smoothing in image restoration tasks; in practice, it can outperform  $\ell_2$  metrics on denoising and related problems ([Zhao et al., 2017; Jadon et al., 2024](#)).

**Coefficient of Determination ( $R^2$ ).** Let the spatial mean be

$$\bar{y} = \frac{1}{HW} \sum_{i=1}^H \sum_{j=1}^W y_{ij}.$$

Define the residual and total sums of squares

$$\text{SS}_{\text{res}} = \sum_{i=1}^H \sum_{j=1}^W (y_{ij} - \hat{y}_{ij})^2, \quad \text{SS}_{\text{tot}} = \sum_{i=1}^H \sum_{j=1}^W (y_{ij} - \bar{y})^2.$$

Then

$$R^2(y, \hat{y}) = 1 - \frac{\text{SS}_{\text{res}}}{\text{SS}_{\text{tot}}} = 1 - \frac{\text{MSE}(y, \hat{y})}{\text{Var}(y)}, \quad \text{where } \text{Var}(y) = \frac{1}{HW} \sum_{i=1}^H \sum_{j=1}^W (y_{ij} - \bar{y})^2.$$

**Structural Similarity (SSIM)** ([Wang et al., 2004](#)). For a window  $(\Omega \subset \{1, \dots, H\} \times \{1, \dots, W\})$  with non-negative weights  $(\{w_{uv}\}_{(u,v) \in \Omega})$  satisfying  $\sum_{(u,v) \in \Omega} w_{uv} = 1$ , define the local means, variances and covariance

$$\mu_y(\Omega) = \sum_{(u,v) \in \Omega} w_{uv} y_{uv}, \quad \mu_{\hat{y}}(\Omega) = \sum_{(u,v) \in \Omega} w_{uv} \hat{y}_{uv},$$

$$\sigma_y^2(\Omega) = \sum_{(u,v) \in \Omega} w_{uv} (y_{uv} - \mu_y(\Omega))^2, \quad \sigma_{\hat{y}}^2(\Omega) = \sum_{(u,v) \in \Omega} w_{uv} (\hat{y}_{uv} - \mu_{\hat{y}}(\Omega))^2,$$

$$\sigma_{y\hat{y}}(\Omega) = \sum_{(u,v) \in \Omega} w_{uv} (y_{uv} - \mu_y(\Omega)) (\hat{y}_{uv} - \mu_{\hat{y}}(\Omega)).$$

With stability constants  $C_1 = (K_1 L)^2$  and  $C_2 = (K_2 L)^2$  (dynamic range  $L$ ; typically  $K_1 = 0.01$ ,  $K_2 = 0.03$ ), the window-level structural similarity is

$$\text{SSIM}_{\Omega}(y, \hat{y}) = \frac{(2 \mu_y(\Omega) \mu_{\hat{y}}(\Omega) + C_1)(2 \sigma_{y\hat{y}}(\Omega) + C_2)}{(\mu_y(\Omega)^2 + \mu_{\hat{y}}(\Omega)^2 + C_1)(\sigma_y^2(\Omega) + \sigma_{\hat{y}}^2(\Omega) + C_2)}.$$

The image-level SSIM is the average over all window centers  $\{\Omega_m\}_{m=1}^M$ ,

$$\text{SSIM}(y, \hat{y}) = \frac{1}{M} \sum_{m=1}^M \text{SSIM}_{\Omega_m}(y, \hat{y}).$$

In our experiments the images are normalized to  $[0, 1]$ , hence  $L = 1$ , and we use Gaussian weights  $w_{uv}$  and mean aggregation as in `skimage.metrics.structural_similarity`.

## D.2 Higher-dimensional input domain

Consider a dimension  $d \geq 1$  that is a multiple of 4. The Powell function on  $[0, 1]^d$ ,

$$f(\mathbf{x}) = \sum_{i=1}^{d/4} [(x_{4i-3} + 10x_{4i-2})^2 + 5(x_{4i-1} - x_{4i})^2 + (x_{4i-2} - 2x_{4i-1})^4 + 10(x_{4i-3} - x_{4i})^4],$$

with uniformly random samples on  $[0, 1]^d$ , serves as an exemplary testbed for decision tree methods in high-dimensional regression problems due to its inherent non-linearity and intricate variable interactions. The

Sample Size	Dimension	Sklearn	VarianceSplit	MinimaxSplit
10	4	$4.48 \times 10^2$	$2.01 \times 10^2$	$2.57 \times 10^2$
10	16	$1.60 \times 10^4$	$1.52 \times 10^4$	$1.52 \times 10^4$
10	64	$3.70 \times 10^4$	$4.24 \times 10^4$	$3.79 \times 10^4$
10	256	$1.35 \times 10^5$	$1.24 \times 10^5$	$1.14 \times 10^5$
10	1024	$9.31 \times 10^5$	$8.04 \times 10^5$	$4.28 \times 10^5$
100	4	$5.49 \times 10^1$	$5.21 \times 10^1$	$5.31 \times 10^1$
100	16	$2.70 \times 10^3$	$2.67 \times 10^3$	$2.57 \times 10^3$
100	64	$1.99 \times 10^4$	$1.95 \times 10^4$	$2.20 \times 10^4$
100	256	$1.01 \times 10^5$	$1.02 \times 10^5$	$9.39 \times 10^4$
100	1024	$4.65 \times 10^5$	$4.29 \times 10^5$	$4.02 \times 10^5$
1000	4	$4.68 \times 10^1$	$4.65 \times 10^1$	$4.49 \times 10^1$
1000	16	$1.85 \times 10^3$	$1.85 \times 10^3$	$2.03 \times 10^3$
1000	64	$1.62 \times 10^4$	$1.62 \times 10^4$	$1.59 \times 10^4$
1000	256	$6.46 \times 10^4$	$6.47 \times 10^4$	$6.30 \times 10^4$
1000	1024	$2.94 \times 10^5$	$2.96 \times 10^5$	$2.88 \times 10^5$
10000	4	$4.61 \times 10^1$	$4.61 \times 10^1$	$4.63 \times 10^1$
10000	16	$1.87 \times 10^3$	$1.87 \times 10^3$	$1.97 \times 10^3$
10000	64	$1.36 \times 10^4$	$1.36 \times 10^4$	$1.43 \times 10^4$
10000	256	$6.22 \times 10^4$	$6.22 \times 10^4$	$6.11 \times 10^4$
10000	1024	$2.80 \times 10^5$	$2.80 \times 10^5$	$2.78 \times 10^5$

Table 1: Comparison of Decision Tree Methods (maximum depth = 3) using the Powell function without noise. Scikit-learn’s DecisionTreeRegressor uses MSE as its default splitting criterion, which is equivalent to minimizing the variance of the target variable within each split and serves as a baseline comparison here. The winner in each setting is boxed.

quartic terms in the function introduce sharp curvatures in the response surface, necessitating sophisticated splitting strategies to approximate these non-linear relationships accurately.

Table 1 compares three decision tree methods—scikit-learn’s standard implementation, VarianceSplit and MinimaxSplit—across various sample sizes  $n$  and dimensions  $d$  for the Powell function. In the dense design regime ( $n > d$ ), we observe relatively consistent performance across all three methods. However, as we transition into sparse designs ( $d > n$ ), more pronounced differences emerge. The MinimaxSplit method often demonstrates superior performance in these high-dimensional, data-scarce scenarios. For instance, with 10 samples and 256 dimensions, the MinimaxSplit approach achieves an MSE of  $8.91 \times 10^4$ , outperforming both scikit-learn ( $1.07 \times 10^5$ ) and the VarianceSplit method ( $9.58 \times 10^4$ ).

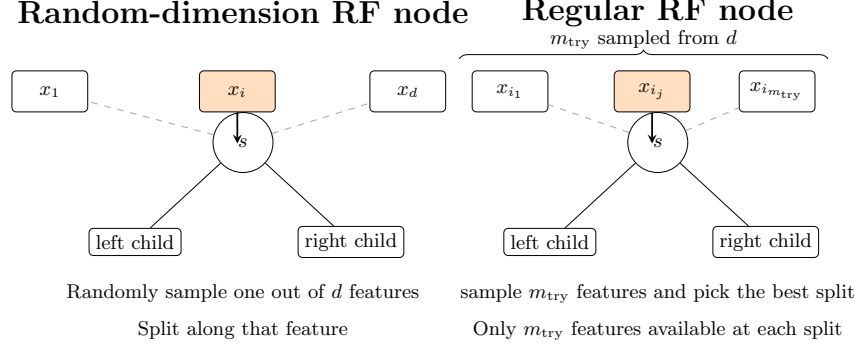


Figure 12: Comparison of node-level split selection in two random forest variants. Left: a random-dimension random forest selects a random feature uniformly for each node and choose the best split over the chosen feature. Right: a regular RF node samples  $m_{try}$  coordinates uniformly from the  $d$  features and chooses the best split over all features according to the chosen impurity/criterion (the highlighted feature illustrates the winner).

## E Pseudocode for algorithms

---

### Algorithm 1: Node-level splitting rules in the notation of Section 2

---

**Input:** Node  $A_t$  at depth  $k$  with sample  $D_t = \{(x_i, y_i) : x_i \in A_t\}$ ; feature set  $[d] = \{1, \dots, d\}$  and  $m_{try} = d$  by default

**Output:**  $S_j(A_t)$ : candidate thresholds for feature  $j$  at  $A_t$ ;  $A_{j,s}^L = A_t \cap \{x_j \leq s\}$ ,  $A_{j,s}^R = A_t \cap \{x_j > s\}$ ;  $P_t(B) = \Pr(X \in B \mid X \in A_t) \approx n(B)/n(A_t)$

**1** **VarianceSplit (CART)** *// cf. Fig. 2, left*

**2** **for**  $(j, s) \in \{(j, s) : j \in [d], s \in S_j(A_t)\}$  **do**

**3**    $\text{Crit}(j, s) \leftarrow P_t(A_{j,s}^L) \text{Var}(Y \mid A_{j,s}^L) + P_t(A_{j,s}^R) \text{Var}(Y \mid A_{j,s}^R)$

**4**    $(j^*, s^*) \leftarrow \arg \min_{(j,s)} \text{Crit}(j, s)$ ;   **split**  $A_t \rightarrow A_{j^*,s^*}^L, A_{j^*,s^*}^R$ .

**5** **MinimaxSplit** *// cf. Fig. 2, middle*

**6** **for**  $(j, s) \in \{(j, s) : j \in [d], s \in S_j(A_t)\}$  **do**

**7**    $\text{Crit}(j, s) \leftarrow \max \{P_t(A_{j,s}^L) \text{Var}(Y \mid A_{j,s}^L), P_t(A_{j,s}^R) \text{Var}(Y \mid A_{j,s}^R)\}$

**8**    $(j^*, s^*) \leftarrow \arg \min_{(j,s)} \text{Crit}(j, s)$ ;   **split**  $A_t \rightarrow A_{j^*,s^*}^L, A_{j^*,s^*}^R$ .

**9** **Cyclic MinimaxSplit** *// cf. Fig. 2, right*

**10**  $j_k \leftarrow 1 + (k \bmod d)$  *// cyclic feature at depth k*

**11** **for**  $s \in S_{j_k}(A_t)$  **do**

**12**    $\text{Crit}(j_k, s) \leftarrow \max \{P_t(A_{j_k,s}^L) \text{Var}(Y \mid A_{j_k,s}^L), P_t(A_{j_k,s}^R) \text{Var}(Y \mid A_{j_k,s}^R)\}$

**13**    $s^* \leftarrow \arg \min_{s \in S_{j_k}(A_t)} \text{Crit}(j_k, s)$ ;   **split**  $A_t \rightarrow A_{j_k,s^*}^L, A_{j_k,s^*}^R$ .

---

---

**Algorithm 2:** Random Forest with generic split rule

---

**Input:** Sample  $\mathcal{D} = \{(X_i, Y_i)\}_{i=1}^N$ , number of trees  $B \in \mathbb{N}$ , maximum depth  $K \in \mathbb{N}$ , minimum leaf size  $n_{\min} \in \mathbb{N}$ , per-node feature budget  $m_{\text{try}}$ , split rule `SplitRule`.

**Output:** Ensemble predictor  $\hat{f}_B(x) = \frac{1}{B} \sum_{b=1}^B \hat{f}^{(b)}(x)$ .

```

1 for  $b \leftarrow 1$  to  $B$  do
2   // Bootstrap sample
3   Draw  $N$  indices  $I^{(b)} = (i_1, \dots, i_N)$  uniformly with replacement from  $[N]$  and set
4    $\mathcal{D}^{(b)} = \{(X_{i_\ell}, Y_{i_\ell})\}_{\ell=1}^N$ .
5   // Grow a full tree on  $\mathcal{D}^{(b)}$ 
6   Initialize root node with index set  $S_{\text{root}} = [N]$  and depth 0.
7   while there exists a node  $(S, \text{depth})$  with  $|S| > n_{\min}$  and  $\text{depth} < K$  do
8     // Sample a random subset of coordinates at this node
9     Draw without replacement a subset  $\mathcal{J} \subseteq [d]$  with  $|\mathcal{J}| = m_{\text{try}} \in [d]$ .
10    // Choose best coordinate/threshold according to the chosen impurity
11    criterion
12     $(j^*, t^*) \leftarrow \text{SplitRule}(S, \mathcal{J}, \mathcal{D}^{(b)})$ .
13    // Partition the node
14     $S_L \leftarrow \{i \in S : X_{ij^*} \leq t^*\}, \quad S_R \leftarrow \{i \in S : X_{ij^*} > t^*\}$ .
15    // Create children; stop if a child is too small
16    if  $|S_L| \leq n_{\min}$  or  $\text{depth} + 1 = K$  then
17      | mark left child as a leaf with prediction  $\hat{\mu}_{S_L} = \frac{1}{|S_L|} \sum_{i \in S_L} Y_i$ ;
18    else
19      | push  $(S_L, \text{depth} + 1)$  to the queue;
20    if  $|S_R| \leq n_{\min}$  or  $\text{depth} + 1 = K$  then
21      | mark right child as a leaf with prediction  $\hat{\mu}_{S_R} = \frac{1}{|S_R|} \sum_{i \in S_R} Y_i$ ;
22    else
23      | push  $(S_R, \text{depth} + 1)$  to the queue;
24
25    // Define the tree predictor by leaf means
26    For any  $x \in \mathbb{R}^d$ , let  $\hat{f}^{(b)}(x)$  be the mean  $\hat{\mu}_S$  of the leaf whose cell contains  $x$ .

```

---

---

**Algorithm 3:** Random-Dimension Random Forest (feature subsampling at each node)

---

**Input:** Sample  $\mathcal{D} = \{(X_i, Y_i)\}_{i=1}^N$ , number of trees  $B$ , maximum depth  $K$ , minimum leaf size  $n_{\min}$ , per-node feature budget  $m_{\text{try}} = 1$ , split rule `SplitRule`.

**Output:** Ensemble predictor  $\hat{f}_B(x) = \frac{1}{B} \sum_{b=1}^B \hat{f}^{(b)}(x)$ .

```

1 for  $b \leftarrow 1$  to  $B$  do
2   Draw a bootstrap sample  $\mathcal{D}^{(b)}$  of size  $N$  from  $\mathcal{D}$ .
3   Initialize the root node with index set  $S_{\text{root}} = [N]$  and depth 0.
4   while there exists a node  $(S, \text{depth})$  with  $|S| > n_{\min}$  and  $\text{depth} < K$  do
5     // Sample a random subset of coordinates at this node
6     Draw without replacement a subset  $\mathcal{J} \subseteq [d]$  with  $|\mathcal{J}| = m_{\text{try}}$ , where we set  $m_{\text{try}} = 1$ .
7     // Choose best coordinate/threshold using only  $\mathcal{J}$ 
8      $(j^*, t^*) \leftarrow \text{SplitRule}(S, \mathcal{J}, \mathcal{D}^{(b)})$ .
9     // Partition and create children
10     $S_L \leftarrow \{i \in S : X_{ij^*} \leq t^*\}, \quad S_R \leftarrow \{i \in S : X_{ij^*} > t^*\}$ .
11    if  $|S_L| \leq n_{\min}$  or  $\text{depth} + 1 = K$  then
12      | make left child a leaf with prediction  $\hat{\mu}_{S_L}$ ;
13    else
14      | push  $(S_L, \text{depth} + 1)$ ;
15    if  $|S_R| \leq n_{\min}$  or  $\text{depth} + 1 = K$  then
16      | make right child a leaf with prediction  $\hat{\mu}_{S_R}$ ;
17    else
18      | push  $(S_R, \text{depth} + 1)$ ;
19
20  Define  $\hat{f}^{(b)}(x)$  by the mean of the leaf containing  $x$ .

```

---